School of Electrical and Computer Engineering
CHALMERS UNIVERSITY OF TECHNOLOGY
Göteborg, Sweden.

Technical Report No. 292

Design of Direct-driven Permanent-magnet Generators for Wind Turbines

by

Anders Grauers

Submitted to the School of Electrical and Computer Engineering, Chalmers University of Technology, in partial fulfillment of the requirements for the degree of Doctor of Philosophy.

Department of Electric Power Engineering

Göteborg, October 1996.

CHALMERS UNIVERSITY OF TECHNOLOGY
Department of Electric Power Engineering
S - 412 96 GÖTEBORG, SWEDEN

ISBN 91-7197-373-7

ISSN 0346-718X

Chalmers Bibliotek, Reproservice

Göteborg, 1996

Abstract

This thesis presents an investigation of how a direct-driven wind turbine generator should be designed and how small and efficient such a generator will be. Advantages and disadvantages of various types of direct-driven wind turbine generators are discussed, and a radial-flux permanent-magnet generator connected to a forced-commutated rectifier is chosen for a detailed theoretical investigation. Further, a design method is developed for the electromagnetic part of the chosen generator type. The generator is optimized with a simplified cost function which, besides including the cost of the active generator parts and the cost of the structure, also includes the cost of the average losses. Therefore, a method to calculate the average losses is derived. The design method is used to investigate the optimization of a 500 kW generator, and the size, efficiency and active weight of optimized generators from 30 kW to 3 MW are presented. A result of the investigation is that the outer diameters of the direct-driven generators are only slightly larger than the width of conventional wind energy converter nacelles. A comparison of average efficiency shows that direct-driven generators, including the losses in the frequency converters, are more efficient than conventional wind energy converter drive trains. Compared with other direct-driven generators, the proposed generator type is small, mainly because of the forced-commutated rectifier and because the generator is not required to produce a pull-out torque higher than the rated torque.

Preface

The work presented in this thesis was carried out at the Department of Electrical Power Engineering at Chalmers University of Technology. The work was financed by NUTEK, partly under the Swedish wind energy research program, partly as an EU Joule II project. The financial support is gratefully acknowledged.

I would like to thank Dr Ola Carlson for interesting discussions about the application of the low-speed generator in wind energy converters. Deborah Fronko and Margot Bolinder both made an important contribution by revizing my English. Finally, I wish to express my gratitude to Professor Jorma Luomi for valuable help with the generator design and for discussions on how to present the results from my project.

Table of Contents

List of Symbols

Symbol	Unit	Description
a	–	Exponent for the structure cost
A	–	Parameter for wind speed probability density function
b_{Cu}	m	Conductor width
b_d	m	Tooth width
b_m	m	Magnet width
b_s	m	Slot width
b_{s1}	m	Slot opening
$\hat{B}_{d0}$	T	Maximum flux density in the teeth at no-load
B_{min}	T	Min. flux density allowed in the permanent-magnets
$\hat{B}_s$	T	Peak air gap flux density generated by the stator at rated current
$\hat{B}_{yr}$	T	Maximum flux density in the rotor yoke
$\hat{B}_{ys}$	T	Maximum flux density in the stator yoke
$\hat{B}_{\delta 0}$	T	Peak air gap flux density at no-load
$B_{\delta(1)}$	T	Fundamental air gap flux density (RMS value)
c	–	Parameter for wind speed probability density function
c_{Cu}	ECU/kg	Specific cost of the copper
c_d	ECU/kW	Specific cost of average losses
c_{el}	ECU/kWh	Specific cost of electric energy
c_{Fe}	ECU/kg	Specific cost of the active iron
c_m	ECU/kg	Specific cost of the permanent magnets
c_{str}	ECU	Cost of a reference structure
C_{act}	ECU	Cost of the active parts of the generator
C_d	ECU	Cost of the losses of the generator
C_{str}	ECU	Cost of the generator structure
C_{tot}	ECU	Total cost function for generator optimization
d	m	Air gap diameter
d_{ref}	m	Diameter of the reference structure
d_{se}	m	Outer diameter of the stator
E	V	Internal line-to-line emf
E_p	V	Internal phase emf
E_{pN}	V	Internal phase emf at rated speed

f	Hz	Frequency
f_{N}	Hz	Rated frequency
g_{ad}	–	Factor for the additional losses
g_{Cu}	–	Factor for the copper losses
g_{Ft}	–	Factor for the eddy current losses
g_{Hy}	–	Factor for the hysteresis losses
g_{t}	–	Factor for the turbine power
g_{μ}	–	Factor for the windage and friction losses
h_{Cu}	m	Conductor height
h_{i}	m	Insulation height (in the slots)
h_{m}	m	Magnet height
h_{s}	m	Stator slot height
h_{s1}	m	Tooth tip height 1
h_{s2}	m	Tooth tip height 2
h_{s3}	m	Slot height, excluding tooth tips
h_{yr}	m	Rotor yoke height
h_{ys}	m	Stator yoke height
H_{c}	A/m	Coercivity of the magnets
i	–	Real interest rate
I_{a}	A	Armature current
I_{aN}	A	Rated armature current
$I_{(1)}$	A	Fundamental armature current
J_{s}	$\mathrm{A/m^2}$	Current density in the armature winding
k_{Cu}	—	Copper fill factor of the stranded wire
k_{dad}	—	Average loss factor for additional losses
k_{dCu}	—	Average loss factor for copper losses
k_{dFt}	—	Average loss factor for eddy current losses
k_{dHy}	—	Average loss factor for hysteresis losses
$k_{\mathrm{d}\mu}$	—	Average loss factor for windage and friction losses
k_{Fes}	—	Fill factor for the stator iron
k_{Ftd}	—	Empirical eddy current loss factor for the teeth
k_{Ftys}	—	Empirical eddy current loss factor for the stator yoke
k_{Hyd}	—	Empirical hysteresis loss factor for the teeth
k_{Hyys}	—	Empirical hysteresis loss factor for the stator yoke
k_{N}	—	Factor for the present value of future costs
k_{t}	—	Average factor for the turbine power (capacity factor)

$k_{w(1)}$	—	Winding factor for the fundamental voltage
l	m	Active length of the generator
l_b	m	End winding length
l_e	m	Equivalent core length
l_{ref}	m	Length of the reference structure
l_{tot}	m	Total length of the stator and end windings
l_u	m	Useful length of the stator core
L_a	H	Total armature inductance per phase
L_b	H	End winding leakage inductance
L_m	H	Magnetizing inductance per phase
L_{sl}	H	Slot leakage inductance
L_{tl}	H	Tooth tip leakage inductance
L_σ	H	Total leakage inductance
m	—	Number of phases
m_{Cu}	kg	Copper weight
m_{Fe}	kg	Iron weight of the active parts of the generator
m_{Fed}	kg	Teeth weight
m_{Feyr}	kg	Rotor yoke weight
m_{Feys}	kg	Stator yoke weight
m_m	kg	Weight of the magnets
m_{tot}	kg	Total active weight of the generator
n	rpm	Generator speed
n_N	rpm	Rated speed of the generator
N_{WEC}	—	Number of years of the assumed wind energy converter life time
N_y	—	Number of hours per year
p	—	Number of pole pairs
p_{Ft}	W/kg	Eddy current loss density at 50 Hz and 1.5 T
p_{Ftm}	W/m^2	Eddy current loss density of the magnet surface
p_{Hy}	W/kg	Hysteresis loss density at 50 Hz and 1.5 T
P_a	W	Armature output power
P_{ad}	W	Additional losses
P_{adN}	W	Additional losses at rated load
P_{aN}	W	Rated electrical power
P_{Av}	W	Average turbine power
P_{Cu}	W	Copper losses

P_{CuAv}	W	Copper losses at average ambient tempearture
P_{CuMax}	W	Copper losses at maximum ambient tempearture
P_{CuN}	W	Copper losses at rated load (only in Chapter 3)
P_{d}	W	Total generator losses
P_{dAv}	W	Average losses
P_{Ft}	W	Total eddy current losses
P_{Ftd}	W	Eddy current losses in the teeth
P_{Ftm}	W	Eddy current losses in the magnets
P_{FtN}	W	Total eddy current losses at rated load
P_{Ftys}	W	Eddy current losses in the stator yoke
P_{Hy}	W	Total hysteresis losses
P_{Hyd}	W	Hysteresis losses in the teeth
P_{HyN}	W	Total hysteresis losses at rated load
P_{Hyys}	W	Hysteresis losses in the stator yoke
P_{lossAv}	W	Total average losses
P_{lossMax}	W	Total losses at maximum ambient temperature
P_{N}	W	Rated mechanical input power of the generator
P_{t}	W	Active power from the turbine
P_{μ}	W	Friction and windage losses
$P_{\mu\mathrm{N}}$	W	Friction and windage losses at rated load
Q	—	Number of slots
q	—	Number of slots per pole and phase
R_{a}	Ω	Armature resistance
T_{Max}	N m	Pull-out torque
T_{N}	N m	Rated torque of the generator
U_{a}	V	Armature voltage
U_{ap}	V	Armature phase voltage
U_{apN}	V	Rated armature phase voltage
v	m/s	Wind speed
v_{in}	m/s	Cut-in wind speed
v_{N}	m/s	Wind speed at which the rated power is reached
v_{nN}	m/s	Wind speed at which the rated speed is reached
v_{out}	m/s	Cut-out wind speed
$\hat{V}_{\mathrm{d}}$	A	Mmf drop of the teeth
$\hat{V}_{\mathrm{m}}$	A	Mmf drop of the magnets
$\hat{V}_{\mathrm{yr}}$	A	Mmf drop of the rotor yoke

$\hat{v}_{ys}$	A	Mmf drop of the stator yoke
$\hat{v}_{\delta}$	A	Mmf drop of the air gap
V_{Cu}	m^3	Copper volume
V_{Fed}	m^3	Stator teeth volume
V_{Feyr}	m^3	Rotor yoke volume
V_{Feys}	m^3	Stator yoke volume
V_M	m^3	Magnet volume
w	s/m	Weibull distributed probabillity density of wind speeds
W	m	Winding pitch
x_a	m	Per unit armature reactance
X_a	m	Armature reactance

φ	Rad	Terminal phase angle
φ_N	Rad	Terminal phase angle at rated load
δ	m	Mechanical air gap
δ_{ef}	m	Effective air gap
θ_{Cu}	K	Temperature of the winding
θ_{CuAv}	K	Temp. of the winding at average ambient temp.
θ_{CuN}	K	Maximum temperature of the winding
θ_m	K	Temperature of the magnets
τ	m	Slot pitch
τ_p	m	Pole pitch
μ_0	—	Permeabillity of air
μ_m	—	Relative permeabillity of the magnet material
η_{av}	—	Average efficiency
η_N	—	Efficiency at rated load
Ψ	Vs	Flux linkage of the stator winding
Ψ_N	Vs	Flux linkage at rated load

1 Introduction

1.1 Why Use Direct-driven Wind-turbine Generators

Today almost all wind energy converters of a rated power of a few kilowatts or more use standard generators for speeds between 750 and 1800 rpm. The turbine speed is much lower than the generator speed; typically between 20 and 60 rpm. Therefore, in a conventional wind energy converter a gear is used between the turbine and the generator. An alternative is to use a generator for very low speed. The generator can then be directly connected to the turbine shaft. Direct-driven generators are already in use in at least two large commercial wind energy converters of 230 and 500 kW. The drive trains of a conventional 500 kW wind energy converter and a wind energy converter with a direct-driven generator are shown in Figure 1.1.

There are two main reasons for using direct-driven generators in wind energy converters. The cost of the produced electricity and the noise of the wind energy converter can both be reduced. Reducing the noise can be important when applying for permission to erect wind energy converters close to dwelling places. The reasons why direct-driven generators can decrease the cost of the produced electricity are as follows:

- they can decrease the cost of the drive train;
- they can decrease the losses of the energy conversion;
- they can improve the availability of the wind energy converter.

Nevertheless, to achieve all of these advantages simultaneously, an efficient generator type, which is well optimized and rationally manufactured, is required.

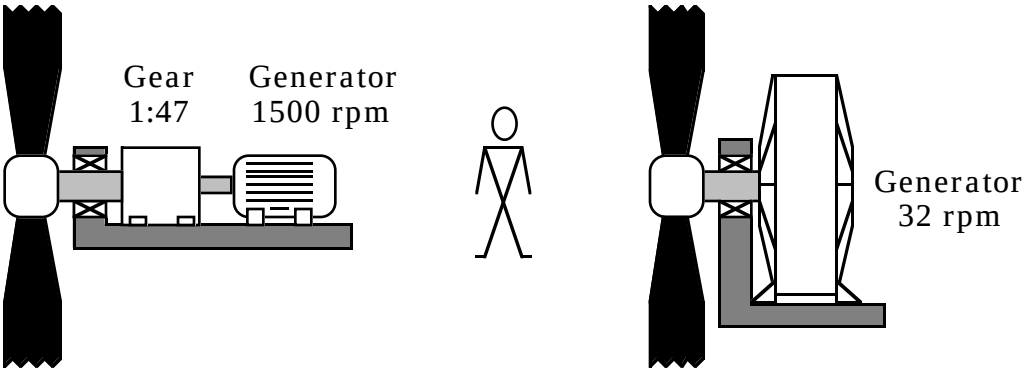

Figure 1.1 500 kW drive trains of one conventional wind energy converter (left) and one with a direct-driven generator (right).

1.2 Differences Compared with Conventional Generators

Theoretically, direct-driven wind turbine generators do not differ much from other generator types. They can be designed and built in the same way as other generators. The most important difference between conventional and direct-driven wind turbine generators is that the low speed of the direct-driven generator makes a very high rated torque necessary. This is an important difference, since the size and the losses of a low-speed generator depend on the rated torque rather than on the rated power. A direct-driven generator for a 500 kW, 30 rpm wind turbine has the same rated torque as a 50 MW, 3000 rpm steam-turbine generator.

Because of the high rated torque, direct-driven generators are usually heavier and less efficient than conventional generators. To increase the efficiency and reduce the weight of the active parts, direct-driven generators are usually designed with a large diameter. To decrease the weight of the rotor and stator yokes and to keep the end winding losses small, direct-driven generators are also usually designed with a small pole pitch.

1.3 Proposed Generator Types

Many different generators have been proposed as direct-driven wind-turbine generators. This section describes some of them and presents some results from the research on these generators. The generators described below are either direct grid-connected generators or variable-speed generators connected to the grid via a frequency converter.

The generators can be divided into electrically excited generators and permanent-magnet-excited generators. The electrically excited generators presented are:

- sector induction generator;
- electrically excited synchronous generator;
- switched reluctance generator.

The permanent-magnet generators presented are:

- radial-flux synchronous generator;
- axial-flux synchronous generator with toroidal stator or double-sided stator ;
- transversal-flux generator.

1.3.1 Sector Induction Generator

Gribnau and Kursten (1991) and Deleroi (1992) have presented a direct-driven sector induction generator for direct grid connection, shown in Figure 1.2. The generator is an axial-flux generator with a stator only on a

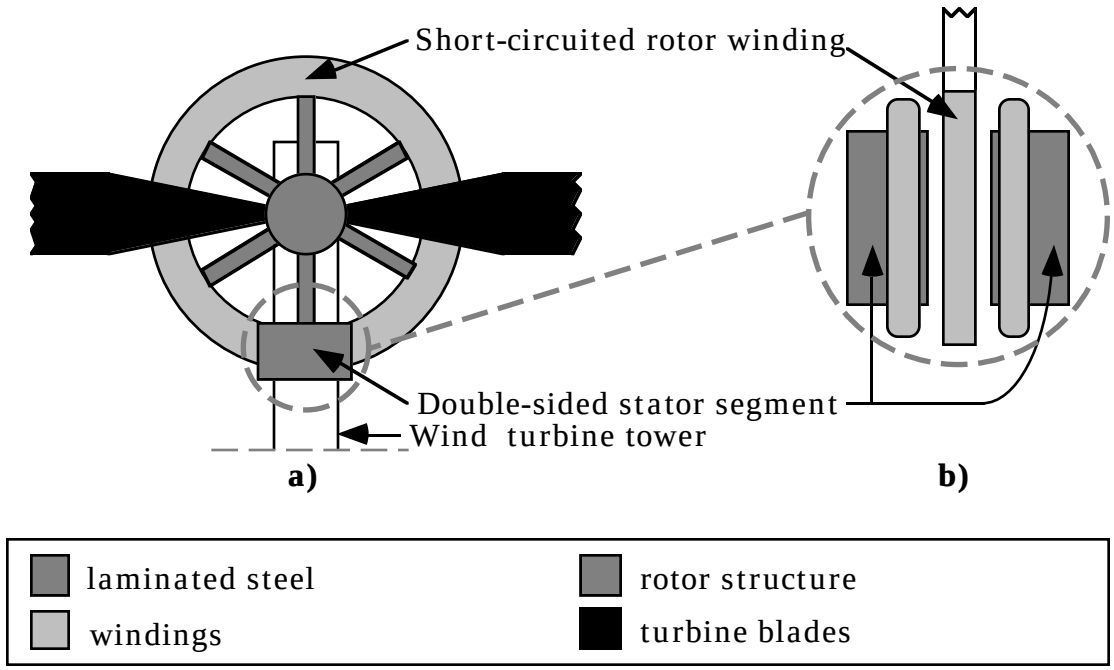

Figure 1.2 Axial-flux sector induction generator. a) Complete generator, axial view, and b) Active part, tangential view.

segment of the circumference. It has a large diameter in order to achieve a high air-gap speed, but since the stator segment is fixed to the tower of the wind energy converter, the structure is simple. Since it is an induction generator with a high slip, the damping of the generator is no problem for the design, even though it is direct grid-connected. The generator is developed by a Dutch company and only very little data is available on it. A 500 kW version with a diameter of about 9 m and a speed of about 40 rpm is presented (Gribnau and Kursten, 1991). The efficiency is estimated to be about 80 to 85 % with a rated slip of about 10 to 15 %. A 150 kW prototype has been built and tested. The efficiency of the prototype is much lower than the goal for the 500 kW version, only 65 % at a rated slip of about 20 %.

1.3.2 Electrically Excited Synchronous Generator

The two commercial direct-driven wind energy converters both use electrically excited synchronous generators with frequency converters. The generators are of the same principal design as hydropower generators. Very little information is available on these generators. One of them is a 500 kW generator and has a rated speed of 40 rpm (Anon. 1994a). The air gap diameter is about 4 m and the generator frequency is lower than 50 Hz. This generator is in 1996 used in more than 600 wind energy converters.

1.3.3 Switched Reluctance Generator

de Haan et al. (1994) present a switched reluctance generator which produces 20 kW at 120 rpm. The generator has been optimized using an analytical design method. Finite element calculations are carried out for the chosen design, but the finite element calculations predict a much higher torque than the analytical model. The active part of the generator is shown in Figure 1.3.

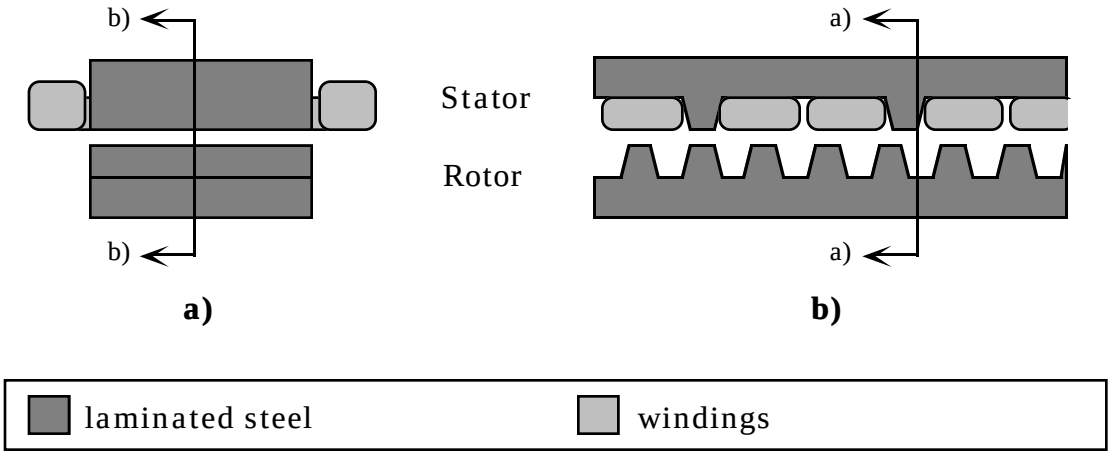

Figure 1.3 A switched reluctance generator. a) Tangential view and b) Axial view.

1.3.4 Permanent-magnet Radial-flux Synchronous Generator

Spooner and Williamson (1992a,1992b,1992c) have discussed the feasibility of direct grid-connected, direct-driven wind-turbine generators. The proposed generators are permanent-magnet synchronous generators, and when connected directly to the grid, they operate at a constant speed. Rotors with surface-mounted high-energy magnets have been investigated, as well as rotors with ferrite magnets and flux concentration. The two versions of the generator are shown in Figures 1.4 and 1.5. The stator is of a conventional design, but with a very small pole pitch, approximately 40 mm, in order to generate 50 Hz frequency without having a large generator diameter. The winding is a three-phase, fractional-slot winding with less than 1 slot per pole and phase. Spooner and Williamson show that direct-driven, direct grid-connected generators can be designed with a small diameter if permanent-magnet excitation is used. Both the rotor types have been found to be feasible. The main difference between them is that the generator with ferrite-magnet, flux-concentrating rotor is heavier and more complicated but leads to a shorter generator with higher efficiency at rated load. A radial-flux, permanent-magnet generator with a modular stator design, was also presented by Spooner et al. (1994).

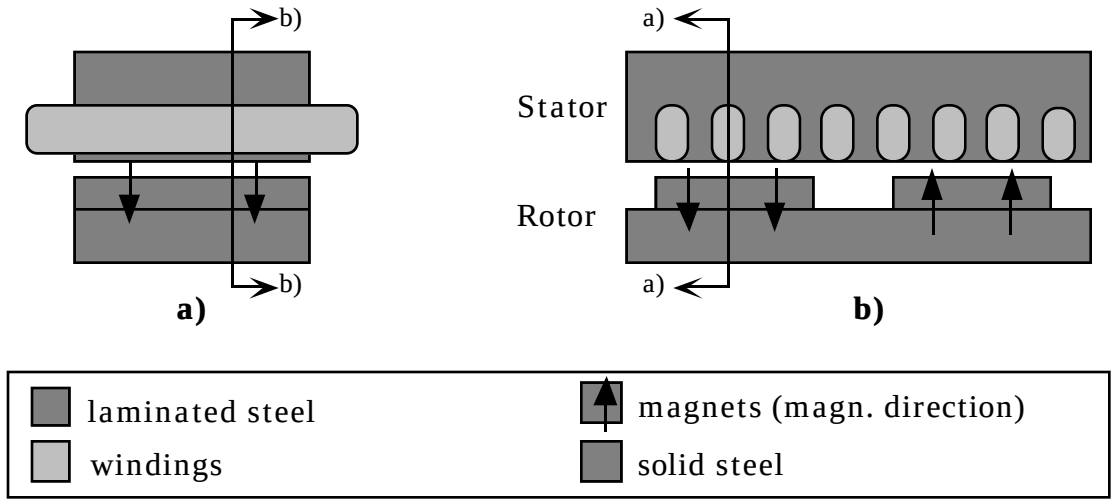

Figure 1.4 The radial-flux generator with surface-mounted magnets. a) Tangential view and b) Axial view.

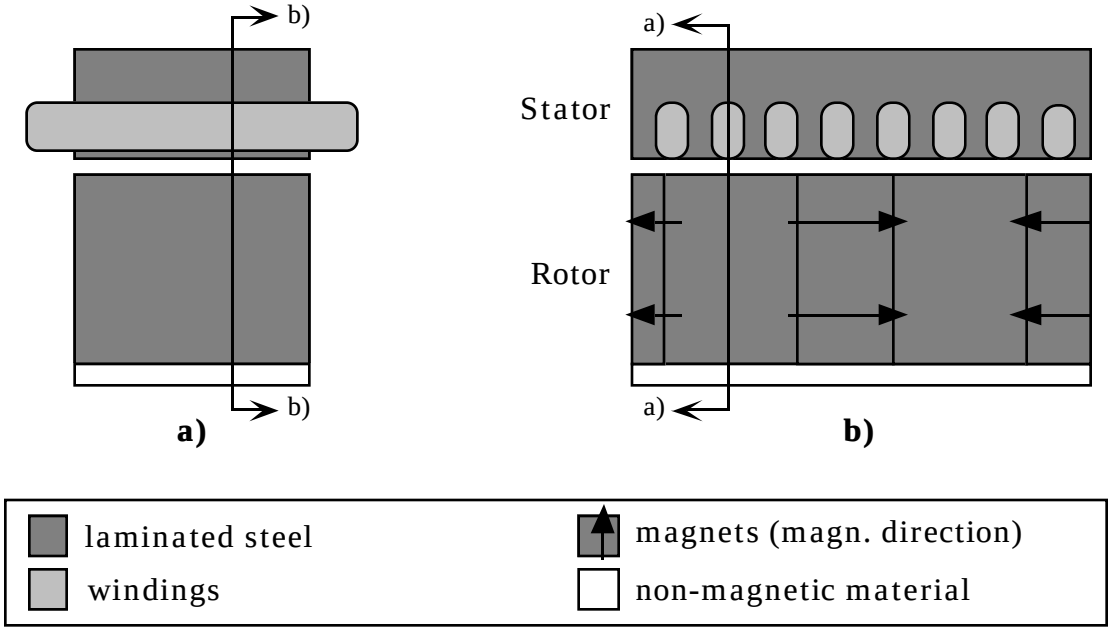

Figure 1.5 The radial-flux generator with flux concentration and ferrite magnets. a) Tangential view and b) Axial view.

Two problems of the proposed design are mentioned in the papers. First, the sub-harmonic flux waves from the fractional-slot winding are considered a problem, because they may lead to additional losses. Second, parallel paths in the winding should be avoided. The reason for this is that the poles may generate unequal voltages leading to circulating currents between the parallel coils.

Two small generator prototypes have been made. They showed that a fractional-slot winding with only 0.75 slots per pole and phase can generate an almost sinusoidal voltage from a very non-sinusoidal flux

wave form, and that the flux-concentration method can be used to achieve high flux densities from low-energy magnets.

A mechanical damping system for the direct grid-connected generator is discussed by Westlake et al. (1996). In conventional synchronous generators, the damping is provided by damper windings in the rotor. The direct-driven direct grid-connected wind turbine generator must have a very small pole pitch if the diameter is not very large. The small pole pitch makes the damper windings insufficient. Instead, a mechanical damping of the stator, by means of a spring and a damper, can be used. The mechanical damping system is shown to be sufficient, but it may be difficult and expensive to construct for large generators.

Lampola et al. (1995a) present a 500 kW radial-flux permanent-magnet generator. The generator is of the same design as the one in Figure 1.4 but it is not designed for direct grid-connection. The generator has been calculated in detail using the finite element method and time stepping. The torque ripple, cogging torque and rotor losses are kept minor by using 1.5 slots per pole and phase. The permanent-magnet generator is compared with a direct-driven induction generator by Lampola (1995b). The induction generator is found to be larger, heavier and less efficient than the permanent-magnet generator. In another paper (Lampola et al. 1996b) the influence of the rectifier on the generator rated power and efficiency is investigated. It is shown that the rated power and efficiency are lower if the generator is connected to a diode rectifier than if it is supplied with sinusoidal voltages.

1.3.5 Axial-flux Generators

Honorati et al. (1991), Di Napoli et al. (1991) and Carrichi et al. (1992) have proposed a permanent-magnet axial-flux synchronous generator. The generator design is shown in Figure 1.6. It is a generator with a toroidal stator, air gap winding and two rotor discs.

Two prototypes of approximately 1 kW have been built. A 1 MW generator design is presented, but it has a rated speed of 100 rpm, too high for a 1 MW wind energy converter. Because of the high speed, the generator has high efficiency and low weight.

Alatalo and Svensson (1993) have proposed an axial-flux permanent-magnet synchronous generator with a double-sided stator and air gap windings. The generator design is shown in Figure 1.7. A 5 kW prototype is presented by Alatalo (1991). The generator type has low iron weight because there is no rotor yoke but the magnet weight is high since an air gap winding is used.

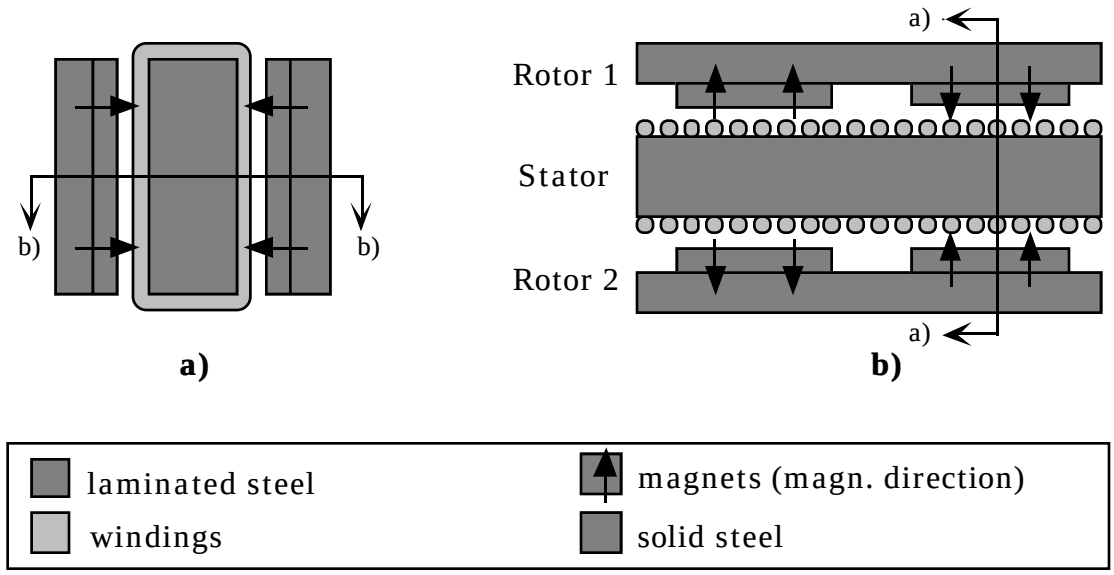

Figure 1.6 An axial-flux generator with a toroidal stator winding and surface-mounted magnets on two rotor discs. a) Tangential view b) Radial view.

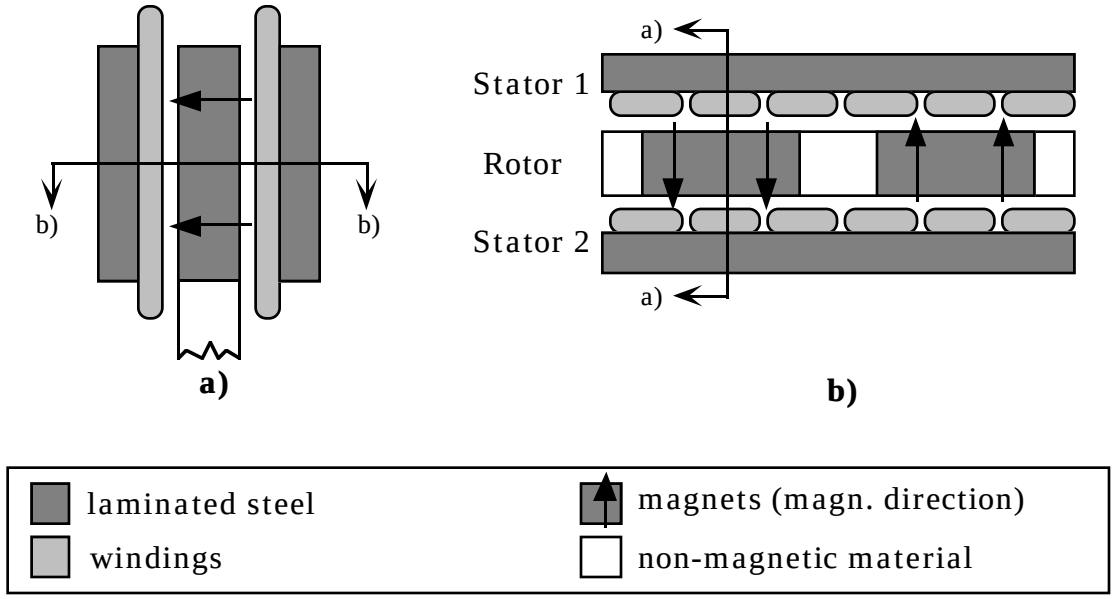

Figure 1.7 An axial-flux generator with double-sided stator and air gap windings. a) Tangential view b) Radial view.

1.3.6 Transversal-flux Variable-speed Generator

Weh et al. (1988) have proposed a direct-driven transversal-flux generator for wind turbines. The generator is a two-phase generator and is magnetized by permanent magnets with flux concentration. Since the

generator is a two-phase machine, it cannot be direct grid-connected. Instead, it is connected to two single-phase rectifiers feeding one three-phase inverter. This generator type is designed for a frequency in the range of 100 to 200 Hz to get a high force-to-weight ratio. The transversal-flux generator has a very high force per weight ratio but one disadvantage is its complex structure. If the generator is connected to a diode rectifier, the force density is lower than what would be possible to achieve with a sinusoidal supply voltage because of high inductance. If connected to a forced-commutated rectifier, the transversal-flux generator is capable of producing higher force densities than conventional generator designs. One phase of the transversal-flux generator is shown in Figure 1.8. Each phase has a double-sided stator with two cylindrical windings around the generator circumference.

A number of transversal-flux machine-prototypes have been built, one example of which is a wind-turbine generator. It is a 5.8 kW generator for 195 rpm (Weh et al. 1988). A 55 kW generator design for 78 rpm is also presented and compared with a conventional drive train consisting of a gear and a four-pole generator (Weh et al. 1988). It is shown that the weight of a 55 kW drive train is approximately halved by using the direct-driven transversal-flux generator instead of a gear and an induction generator.

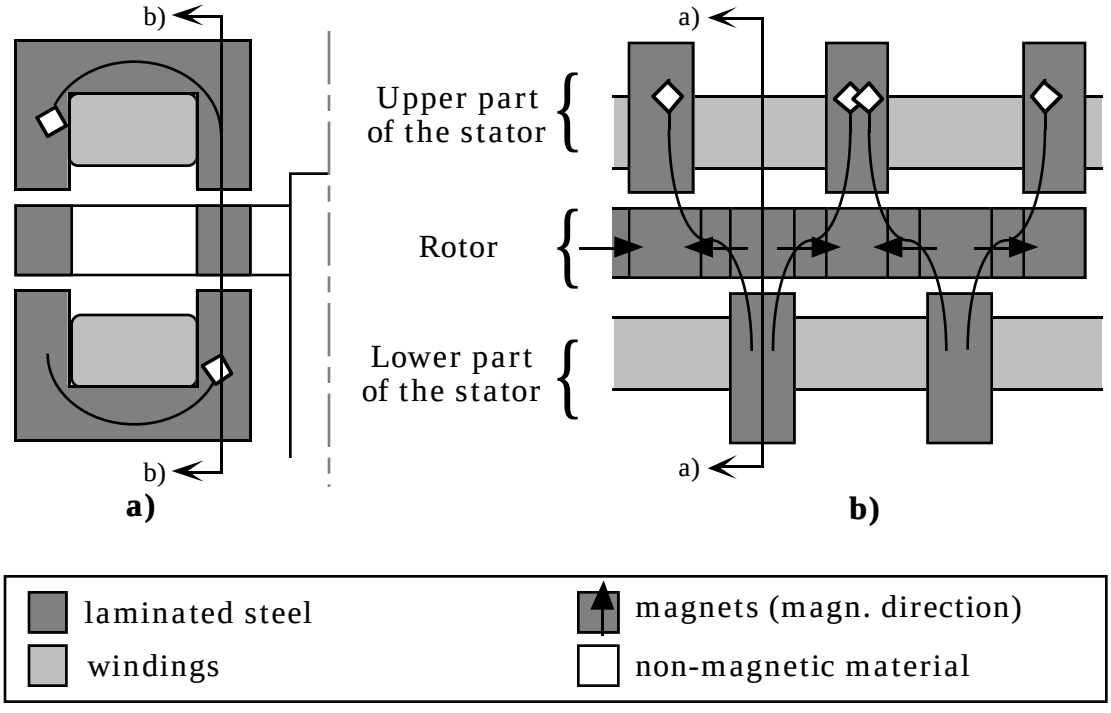

Figure 1.8 One phase of the two-phase transversal-flux generator with double-sided stator. The flux paths are shown. a) Tangential view and b) Axial view.

1.4 Discussion of Earlier Research

It is clear, from the papers mentioned above, that many generator types can be used as direct-driven wind-turbine generators. It is, however, difficult to compare the generator types based on data given in the papers since the generators are designed for different specifications, using different methods and since all data is not presented.

An investigation of direct-driven generators in general, including a comparison with conventional generators and gears, was made by Bindner et al. (1995). In the report, the switched reluctance generator, the induction generator, the electrically excited synchronous generator and the permanent-magnet synchronous generator were discussed briefly. Switched reluctance generators and induction generators have a low power factor leading to a large stator, and electrically-excited synchronous generators are larger and less efficient than permanent-magnet synchronous generators. Consequently, the permanent-magnet synchronous generator was found to be the best suited for a direct-driven wind-turbine generator.

Generators of up to 1500 kW were designed and the size, the weight and the efficiency were discussed by Søndergaard and Bindner (1995). In comparison with conventional generators and gears, direct-driven generators were found to have a much larger diameter, about the same efficiency, about the same total weight and, at present, a slightly higher price. The authors expect that there will be an upper power limit of about 500 to 1000 kW for direct-driven generators. The rated power is limited mainly because the outer diameter becomes too large as the rated power increases.

Since the size of the generator is very important for transportation and manufacturing, it is important to further investigate how small the diameter can be made. Also generator efficiency has to be investigated more thoroughly to evaluate the cost of the losses. Since the losses change with load, the cost of the losses cannot be calculated from the losses at rated load. Instead, the average losses have to be evaluated based on a typical wind speed distribution. The average losses of the generator system have not been calculated in any of the papers mentioned above.

1.5 Goal and Outline of the Thesis

The goal of this thesis is to investigate how to design a permanent-magnet generator in order to be suitable for application as a direct-driven wind-turbine generator, and what can be expected of size and performance of such a generator. The optimum generator diameter and length, and the average efficiency are investigated in particular. The goal is also to reduce the size of the generator in comparison with the generators presented in

Section 1.3. The investigation is theoretical and limited to the electromagnetic part of a permanent-magnet generator, but the influence of the generator structure on the electromagnetic optimization is also included.

A specification and a cost function for the design and optimization of direct-driven generators are defined. To calculate the cost of the losses, a method to estimate the average losses of a wind turbine generator is developed. Advantages and disadvantages of various generator types are discussed, and a radial-flux permanent-magnet generator with a frequency converter is chosen for further investigation.

A detailed design method is developed for the active parts of the chosen generator type. The design method is based on well-known analytical methods and a lumped-parameter thermal model. This design method is used together with numerical optimization to find a design suitable for use as a direct-driven wind turbine generator.

The influence of different parameters on the generator design is investigated in detail for a 500 kW generator. Generators from 30 kW to 3 MW are then designed and their data are discussed. Some of these generators are compared with conventional generators and gears and the proposed generator type is also compared with direct-driven generators proposed by other authors.

2 Generator Specification and Cost Function

This chapter presents a specification for direct-driven wind-turbine generators of different rated powers. A method to estimate the total cost of generators is also presented. The total cost includes the cost of the active parts, the cost of the average losses and the cost of the generator structure.

2.1 Specification

Only the quantities which significantly affect the generator performance are included in the specification. A complete specification for the final design of a generator will include many more detailed requirements. The rated power used here is the mechanical power from the turbine, not the electrical power to the grid. The reason for using mechanical power is that generators designed for the same turbine should be compared with each other, not with generators of the same output power at rated load. The difference in generator efficiency is included as a cost of the losses.

The size of a generator depends to a very large extent on the required rated torque. Consequently, the rated torque is one of the most important parts of the specification. The rated torque differs for different wind turbines of the same rated power, because of different turbine speeds. Data from 25 wind energy converters from Bindner et al. (1995) and Anon. (1994b) were used to find the typical values of the rated torque for different sizes of wind energy converters. A curve fit to the data was made to find an analytical expression of the rated torque. The rated torque can be approximated as

$$T_{\mathrm{N}} = 71.1\ \mathrm{Nm}\left(\frac{P_{\mathrm{N}}}{1\ \mathrm{kW}}\right)^{1.23} \tag{2.1}$$

The rated torque determines the rated speed, which can be expressed as

$$n_{\mathrm{N}} = 134\ \mathrm{rpm}\left(\frac{P_{\mathrm{N}}}{1\ \mathrm{kW}}\right)^{-0.23} \tag{2.2}$$

The empirical function (2.1) for the rated torque can be compared with the one used by Veltman et al. (1994) and Søndergaard & Bindner (1995)

$$T_{\mathrm{N}} = k\ \left(\frac{P_{\mathrm{N}}}{1\ \mathrm{kW}}\right)^{1.5} \tag{2.3}$$

where k is approximately 13 Nm for a 500 kW turbine. Equation (2.3) predicts a faster increase in rated torque as the turbine power increases than Equation (2.1) does. The difference depends on the assumption that k is a constant. In order for k to be a constant, the tip speed of the turbine and the rated power per swept area has to be independent of the rated power. However, the tip speed increases slightly and the rated power per

swept area also increases as the turbine power increases. In Figure 2.1 the rated torques for the 25 wind energy converters are plotted in a log-log diagram together with the torque according to Equations (2.1) and (2.3). It is obvious that Equation (2.3) can only be used to predict the rated torque for generators with a rated power similar to the rated power for which k has been determined.

Since the winding temperature is a limiting factor for the rated current, the maximum allowed winding temperature is also vital to generator performance. The generators designed in this thesis are made for class F winding insulation. According to *Det Norske Veritas* wind energy converter standard (Anon. 1992, Section 8, p. 11) the allowed temperature rise for class F insulation is 90˚C and the thermal calculations are to be made for an ambient temperature of 40˚C. Consequently, the maximum temperature for the winding is 130˚C.

There are often technical demands that vary between different wind energy converters. In some wind energy converters, the generator has to be used as a start motor for the turbine, usually for stall-controlled turbines. The required peak torque differs between turbines with different control principles. Stall-controlled turbines need a high peak torque to limit the turbine speed during wind gusts, while pitch-controlled turbines do not have to use the generator to limit the speed and, therefore, do not

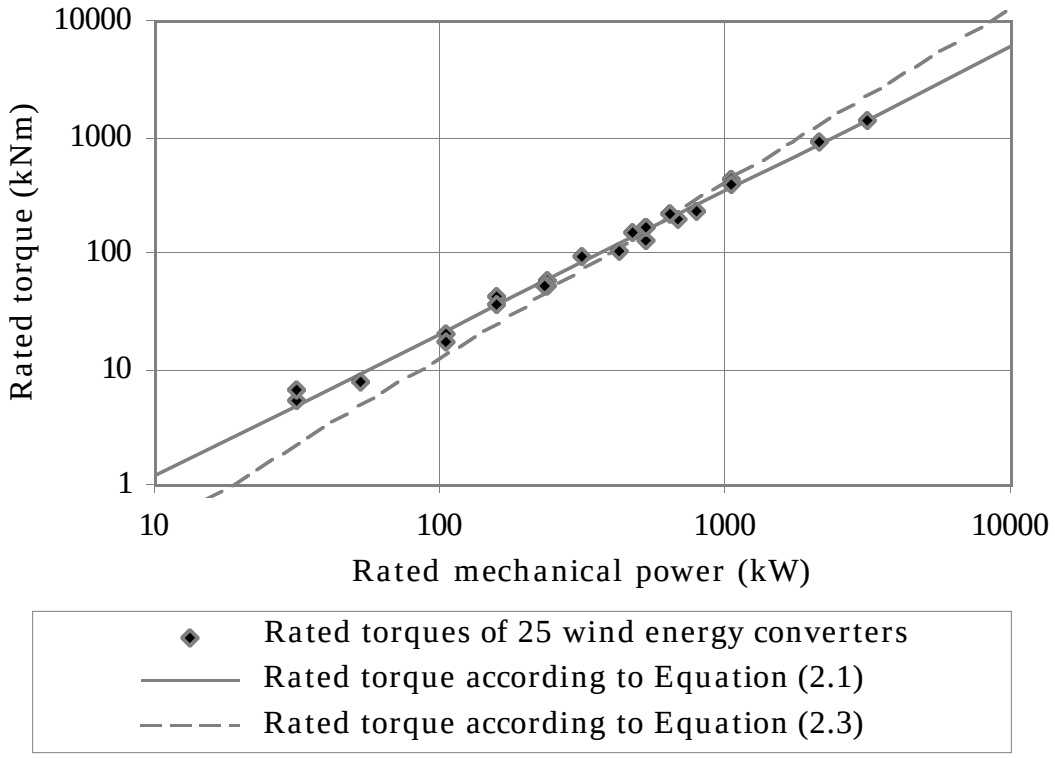

Figure 2.1 The rated torque as a function of mechanical power.

need over-torque capacity. If the generator is used for electrical emergency braking, a high peak torque is also needed. The generators in this thesis are assumed to be used in a pitch-controlled wind energy converter and are not required to produce a torque higher than the rated one. The specification used in this thesis is summarized in Table 2.1.

Table 2.1 The specification used in this thesis for a direct-driven generator of a rated power of P_N.

Rated torque	$T_N = 71.1\ \text{Nm}\left(\frac{P_N}{1\ \text{kW}}\right)^{1.23}$
Rated speed	$n_N = 134\ \text{rpm}\left(\frac{P_N}{1\ \text{kW}}\right)^{-0.23}$
Winding temperature	$\theta_{CuN} \leq 130^{\circ}\text{C}$
Peak torque	$T_{Max} \geq T_N$

2.2 Generator Cost Function

The generator system for a wind energy converter can be chosen by comparing the total cost of the different alternatives. The total cost includes more than the cost of purchasing or manufacturing the generator. It includes both direct costs and indirect costs. Some of the costs are:

- material costs (direct);
- manufacturing costs (direct);
- cost of losses (indirect);
- cost of maintenance (indirect);
- cost of availability (indirect).

The material and manufacturing cost of the active part of the generator is estimated from the weights of the active materials. The cost of the supporting structure is determined from the diameter and length of the generator structure and the cost of the losses is calculated from the average losses of the system. Because the maintenance required for a generator and a gear is very limited, the cost of maintenance is neglected. Moreover, the cost of the availability is neglected since the availability is assumed to be very close to 100 % for all generator systems.

Apart from the total cost of the generator system, a comparison can include other aspects that cannot easily be economically evaluated. For instance, the noise of the generator can be crucial to the acceptance of the wind energy converter. Such aspects have not been included here.

2.2.1 Cost of Active Parts

The cost of the active parts of the generator is based on the assumption that the cost, of both the material and the manufacturing, can be expressed as a specific cost per weight of the different materials. The cost of the active parts is, thus, expressed as

$$C_{\mathrm{act}} = c_{\mathrm{Cu}}\ m_{\mathrm{Cu}} + c_{\mathrm{Fe}}\ m_{\mathrm{Fe}} + c_{\mathrm{m}}\ m_{\mathrm{m}} \tag{2.4}$$

where m_{Cu}, m_{Fe} and m_{m} are the weight of the copper, the active iron and the permanent magnets, respectively. The used values of the specific costs of the different materials c_{Cu}, c_{Fe} and c_{m} are given in Section 2.2.4.

2.2.2 Cost of Structure

The cost of the structure has not been analyzed thoroughly. Only an approximate model is used. Without going into mechanical details, it is clear that the amount of material used and the difficulty in manufacturing the structure increase as the diameter and length increase. Thus, the structural cost is a function of the stator outer diameter d_{se} and stator length including end windings l_{tot}. In this thesis, the cost of the structure is approximated as

$$C_{\mathrm{str}} = c_{\mathrm{str}}\ \frac{1}{2}\left[\left(\frac{d_{\mathrm{se}}}{d_{\mathrm{ref}}}\right)^{a} + \left(\frac{l_{\mathrm{tot}}}{l_{\mathrm{ref}}}\right)^{a}\right] \tag{2.5}$$

where the constant c_{str} is the cost of a reference structure with the diameter d_{ref} and the length l_{ref}. The exponent a describes how fast the cost increases with increasing diameter and length. The cost of a structure of 2 m diameter and 1 m length is assumed to be 20000 ECU (i.e., d_{ref} = 2 m, l_{ref} = 1 m and c_{str}=20000). For small generators, the cost of a structure of 1 m diameter and 0.5 m length is estimated to be 2500 ECU. The exponent a is then 3.

Of course, this model is only approximate. The real cost function will be much more complicated and include terms which depend on both diameter and length as well as terms which are functions of other variables than the outer dimensions. The real cost function will also be discontinuous, for instance at the diameter above which the generator can no longer be transported in one piece, but instead has to be mounted at the wind energy converter site. Nevertheless, it will be shown in Section 6.3 that the exact shape of the cost function for the structure is not very important for the optimization of the generator diameter and length.

2.2.3 Cost of Average Losses

The losses decrease the energy production of the wind energy converter and reduce the income from the sold electric energy. Being proportional to

the reduction of the energy production, the cost of losses is proportional to the average losses, not proportional to the losses at rated load. The cost of losses can be expressed as average losses P_{dAv} times the specific cost per kilowatt of average losses c_d, i.e.

$$C_d = P_{dAv}\ c_d \tag{2.6}$$

The specific cost per kilowatt of average losses is the present value of all the annual costs of one kilowatt losses during the economical lifetime of a wind energy converter. The value of this specific cost of average losses depends on several variables which are difficult to estimate, such as the future price of electricity, the real interest rate, and the lifetime of the wind energy converter. However, these problems are the same for any type of long-term investment calculation. The specific cost of average losses can be calculated as

$$c_d = c_{el}\ N_y\ k_N \tag{2.7}$$

where c_{el} is the specific cost of electric energy (ECU/kWh), N_y the number of hours per year and k_N is the factor for the present value of N_{WEC} years of losses. With the real interest rate i the factor for the present value is

$$k_N = \frac{(1+i)^{N_{WEC}} - 1}{i\ (1+i)^{N_{WEC}}} \tag{2.8}$$

In Table 2.2, examples of the specific cost of average losses are shown, with various real-interest rates and electricity prices. The number of years N_{WEC} is assumed to be 20. Electricity produced in modern wind turbines on good sites costs about 0.04 to 0.06 ECU/kWh. The real interest rate is usually about 2-4 % for infrastructure investments, but private companies often use higher rates. It can be seen that the variation in the cost of losses is large, from 4000 to 8600 ECU. For the optimization, a specific cost of average losses of 6000 ECU/kW is used.

Table 2.2 Examples of the specific cost of average losses c_d for a wind energy converter lifetime of 20 years.

Electricity price	Real interest rate, i		
c_{el}	2 %	4 %	6 %
0.04 ECU/kWh	5700 ECU/kW	4800 ECU/kW	4000 ECU/kW
0.06 ECU/kWh	8600 ECU/kW	7100 ECU/kW	6000 ECU/kW

2.2.4 Total Cost Function

The total cost function used in this thesis includes the cost of the active parts, the cost of the structure and the cost of average losses, i.e.

$$C_{\mathrm{tot}} = C_{\mathrm{act}} + C_{\mathrm{str}} + C_{\mathrm{d}} \tag{2.9}$$

This cost function is intended for approximate optimization of the generator and should not be used to estimate the manufacturing cost of a generator. The parameters for the different parts of the cost function are presented in Table 2.3.

Table 2.3 The cost function parameters and their nominal values.

Cost parameter		Nominal value
Cost of copper	c_{Cu}	6 ECU/kg
Cost of iron	c_{Fe}	4 ECU/kg
Cost of NdFeB magnets	c_{m}	100 ECU/kg
Cost of reference structure	c_{str}	20 000 ECU
Reference diameter	d_{ref}	2 m
Reference length	l_{ref}	1 m
Structure exponent	a	3
Cost of average losses	c_{d}	6000 ECU/kW

3 Calculation Method for the Average Losses

In this Chapter, a method to calculate the average losses and average efficiency is derived. The average losses are calculated from the different types of losses by multiplying each type of loss at rated load with an average loss factor for that type of loss. The average loss factors need be calculated only once for a generator type. Consequently, the average losses are easy to include in the cost function for the optimization of the generator. The calculations are made for a permanent-magnet generator, but they can be made in a similar way also for other types of generators.

3.1 Average Losses

To find the average losses P_{dAv} the probability density function $w(v)$ is used as a weighting function for the losses $P_{\mathrm{d}}(v)$ at different wind speeds. The average losses can be calculated as

$$P_{\mathrm{dAv}} = \int_{v_{\mathrm{in}}}^{v_{\mathrm{out}}} P_{\mathrm{d}}(v)\ w(v)\,\mathrm{d}v \tag{3.1}$$

where v is the wind speed and v_{in} and v_{out} the cut-in and cut-out wind speed of the turbine. The cut-in wind speed used in the calculation of the average loss factors is 3 m/s and the cut-out wind speed is 24 m/s.

The probability density of wind speeds is approximated with high accuracy by a Weibull distribution

$$w = \frac{c}{v}\left(\frac{v}{A}\right)^{c} \mathrm{e}^{-\left(\frac{v}{A}\right)^{c}} \tag{3.2}$$

where c is a shape parameter which varies a little, but is close to 2 for normal sites. The parameter A is determined by the average wind speed of the site. By definition the integral of the wind speed probability density function over wind speeds from zero to infinity is exactly one. Three typical wind speed probability density distributions are shown in Figure 3.1.

The average losses of the generator depend on which site the wind energy converter is placed on. Therefore, the average losses must be calculated for a site with wind conditions similar to the ones at the site on which the wind energy converter will be used. In Section 3.3 the average losses are calculated for three different sites.

To use Equation (3.1) to calculate the average losses, the losses must be expressed as a function of wind speed. The main types of losses for a permanent-magnet generator are: stator copper losses P_{Cu} which are a

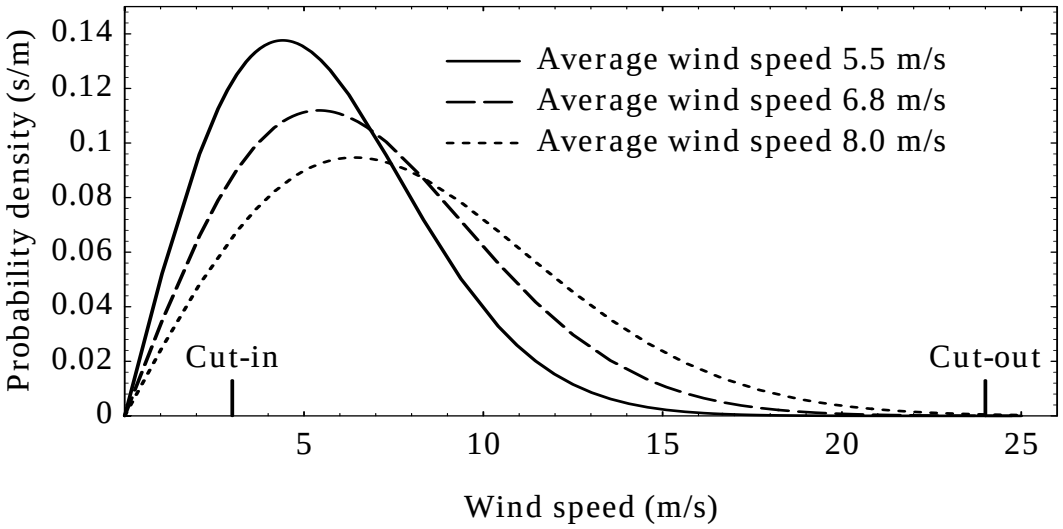

Figure 3.1 Weibull probability density distributions for sites with different average wind speeds.

function of armature current; stator core hysteresis and eddy current losses, P_{Hy} and P_{Ft}, which are functions of flux linkage and frequency; and friction and windage losses P_{μ} which are a function of the rotational speed of the generator. The additional losses P_{ad} are mainly a function of the armature current. By defining the armature current, flux linkage, frequency and rotational speed as functions of wind speed, the different losses can be expressed as functions of wind speed. The total losses can then be expressed as

$$P_d(v) = P_{Cu}(v) + P_{Hy}(v) + P_{Ft}(v) + P_{\mu}(v) + P_{ad}(v) \qquad (3.3)$$

One way to calculate the average losses is to use $P_d(v)$ from Equation (3.3) directly in (3.1). But when the average losses are to be included in the optimization of a generator design, this method is inefficient. The average losses must be calculated by an integral for each new set of generator variables that is used in the optimization procedure. To simplify the generator optimization, the average losses can instead be calculated from the different types of losses at rated load using average loss factors:

$$P_{dAv} = P_{CuN}\, k_{dCu} + P_{HyN}\, k_{dHy} + P_{FtN}\, k_{dFt} + P_{\mu N}\, k_{d\mu} + P_{adN}\, k_{dad} \qquad (3.4)$$

where k_{dCu}, k_{dHy}, k_{dFt}, $k_{d\mu}$ and k_{dad} are the average loss factors for the different types of losses. P_{CuN}, P_{HyN}, P_{FtN}, $P_{\mu N}$ and P_{adN} are the losses at rated load.

The average loss factors are independent of how high the losses are at rated load. If the losses at different wind speeds are expressed as the losses at rated load multiplied by functions representing the dependence

on the wind speed, the average loss factors can be derived from Equation (3.1). The different losses are then expressed as

$$P_{\mathrm{Cu}}(v) = P_{\mathrm{CuN}}\ g_{\mathrm{Cu}}(v) \tag{3.5}$$

$$P_{\mathrm{Hy}}(v) = P_{\mathrm{HyN}}\ g_{\mathrm{Hy}}(v) \tag{3.6}$$

$$P_{\mathrm{Ft}}(v) = P_{\mathrm{FtN}}\ g_{\mathrm{Ft}}(v) \tag{3.7}$$

$$P_{\mu}(v) = P_{\mu\mathrm{N}}\ g_{\mu}(v) \tag{3.8}$$

$$P_{\mathrm{ad}}(v) = P_{\mathrm{adN}}\ g_{\mathrm{ad}}(v) \tag{3.9}$$

By substituting the total losses in (3.1) according to Equations (3.3) and (3.5)–(3.9), the average power losses can be calculated as a few integrals representing the different types of average losses. Since the losses at rated load are constant, irrespective of the wind speed, the average losses can be expressed

$$\begin{aligned} P_{\mathrm{dAv}} = {} & P_{\mathrm{CuN}} \int_{v_{\mathrm{in}}}^{v_{\mathrm{out}}} w(v)\, g_{\mathrm{Cu}}(v)\, \mathrm{d}v + \\ & + P_{\mathrm{HyN}} \int_{v_{\mathrm{in}}}^{v_{\mathrm{out}}} w(v)\, g_{\mathrm{Hy}}(v)\, \mathrm{d}v + P_{\mathrm{FtN}} \int_{v_{\mathrm{in}}}^{v_{\mathrm{out}}} w(v)\, g_{\mathrm{Ft}}(v)\, \mathrm{d}v + \\ & + P_{\mu\mathrm{N}} \int_{v_{\mathrm{in}}}^{v_{\mathrm{out}}} w(v)\, g_{\mu}(v)\, \mathrm{d}v + P_{\mathrm{adN}} \int_{v_{\mathrm{in}}}^{v_{\mathrm{out}}} w(v)\, g_{\mathrm{ad}}(v)\, \mathrm{d}v \end{aligned} \tag{3.10}$$

By making a comparison with Equation (3.4) the average loss factors can be identified. For instance, the average loss factor of the copper losses is

$$k_{\mathrm{dCu}} = \int_{v_{\mathrm{in}}}^{v_{\mathrm{out}}} w(v)\, g_{\mathrm{Cu}}(v)\, \mathrm{d}v \tag{3.11}$$

It remains to define the functions $g_{\mathrm{Cu}}(v)$, $g_{\mathrm{Hy}}(v)$, $g_{\mathrm{Ft}}(v)$, $g_{\mu}(v)$ and $g_{\mathrm{ad}}(v)$ in order to calculate values of the average loss factors. These functions will be different for different wind energy converters since they depend on how the turbine and the generator are controlled. In Section 3.3 the average loss factors are derived for one permanent-magnet generator type.

3.2 Average Efficiency and Average Power

The average efficiency of a generator expresses the percentage of the mechanical input energy which is converted into electrical energy. The average efficiency can be calculated from the average input power P_{Av} and the average losses

$$\eta_{\mathrm{Av}} = 1 - \frac{P_{\mathrm{dAv}}}{P_{\mathrm{Av}}} \tag{3.12}$$

The average input power can be calculated in the same way as the average losses

$$P_{Av} = k_t \; P_N \tag{3.13}$$

where P_N is the rated mechanical power of the turbine and k_t the average factor for the turbine power. The average factor can be calculated by expressing the turbine power as the power at rated load times a function g_t representing the wind speed dependence, i.e.,

$$P_t(v) = P_N \; g_t(v) \tag{3.14}$$

The average factor for the turbine power is then

$$k_t = \int_{v_{in}}^{v_{out}} w(v)\, g_t(v)\, \mathrm{d}v \tag{3.15}$$

The value of the average factor for the turbine power is almost the same as the value of the often used capacity factor for the wind energy converter. The capacity factor expresses the relation between average power to the grid divided by rated power to the grid.

3.3 Determining Average Loss Factors

In this section, the average loss factors will be calculated for the different loss components. To calculate these factors, the *g*-functions, representing the dependence of the different loss components on the wind speed, are derived. Finally, the average loss factors are calculated and discussed.

The *g*-functions can be derived from a loss model for electrical machines. An approximate model, for how the losses change with armature current I_a, flux linkage Ψ, frequency f and speed n, is used. The model has been verified for a wide range of generator speeds, voltages and currents by measurements on a four-pole synchronous generator (Grauers, 1994, p. 70-86). The *g*-function of the copper losses can be expressed as

$$g_{Cu}(v) = \frac{I_a(v)^2}{I_{aN}{}^2} \tag{3.16}$$

where I_{aN} is the armature current at rated load. Additional losses can be approximated as proportional to the armature current squared, just like the copper losses (Adkins & Harley, 1975). Therefore, there is no need for a special *g*-function for the additional losses since they can be included in the copper losses.

The *g*-function of the eddy current losses in the iron core can be expressed approximately as

$$g_{Ft}(v) = \left(\frac{f \; \Psi}{f_N \; \Psi_N} \right)^2 \tag{3.17}$$

where f_N and Ψ_N are the frequency at rated load and the flux linkage at rated load, respectively. The g-function of the hysteresis loss function is approximated as

$$g_{Hy}(v) = \frac{f}{f_N}\left(\frac{\Psi}{\Psi_N}\right)^2 \tag{3.18}$$

The friction and windage losses are bearing friction losses, approximately proportional to the rotational speed, and fan and windage losses, approximately proportional to the cube of the rotational speed. The g-function, therefore, can be expressed as

$$g_\mu(v) = C_{\mu 1}\ \frac{n}{n_N}\ +\ C_{\mu 2}\ \left(\frac{n}{n_N}\right)^3 \tag{3.19}$$

where $C_{\mu 1} + C_{\mu 2} = 1$ and n_N is the speed at rated load. The parameter $C_{\mu 1}$ represents friction that is proportional to the speed and $C_{\mu 2}$ represents losses that are proportional to the cube of the speed. Here it is assumed that $C_{\mu 1} = C_{\mu 2} = 0.5$. For a 50 kVA, four-pole, electrically excited synchronous generator $C_{\mu 1}$ is 0.28 and $C_{\mu 2}$ is 0.72 (Grauers, 1994, p. 74). The lower the generator speed is, the larger $C_{\mu 1}$ is and the lower $C_{\mu 2}$ is.

The g-functions above have to be defined with the wind speed as a parameter. Consequently, the generator speed, frequency, current and flux linkage have to be expressed as functions of the wind speed. In a variable speed wind energy converter, the speed of the turbine is usually controlled to maximize turbine efficiency. The turbine speed is increased linearly with the wind speed until the rated speed n_N is reached. The rated speed is reached at a wind speed v_{nN}, which is lower than the rated wind speed. (v_{nN} = 10 m/s in this thesis.) Thus, the speed can be defined as

$$n(v) = \begin{cases} \left(\dfrac{v}{v_{nN}}\right) n_N & \text{if} \quad v \le v_{nN} \\ n_N & \text{if} \quad v > v_{nN} \end{cases} \tag{3.20}$$

The frequency varies in the same way as the turbine speed, i.e.,

$$f(v) = \begin{cases} \left(\dfrac{v}{v_{nN}}\right) f_N & \text{if} \quad v \le v_{nN} \\ f_N & \text{if} \quad v > v_{nN} \end{cases} \tag{3.21}$$

The core losses of the generator are determined by the flux linkage of the generator armature. The rectifier is assumed to control the armature voltage to keep the flux linkage constant

$$\Psi(v) = \Psi_N \tag{3.22}$$

The current as a function of wind speed can be calculated from the equation for the generator output power

$$P_a(v) = 3\, U_{ap}(v)\; I_a(v)\; \cos(\varphi) \tag{3.23}$$

where U_{ap} is the armature phase voltage and $\cos(\varphi)$ the terminal power factor. The terminal voltage is kept at the same level by the rectifier control as the internal emf E_p and the emf is proportional to the frequency

$$U_{ap}(v) = E_{pN} \left(\frac{f}{f_N} \right) \tag{3.24}$$

where E_{pN} is the internal emf at rated speed. The reactance X_a of the generator ($= 2\,\pi\, f\,(v)\, L_a$) makes the power factor current-dependent

$$\cos(\varphi) = \sqrt{1 - \left(\frac{0.5\, I_a(v)\; 2\,\pi\, f\,(v)\, L_a}{U_{ap}(v)} \right)^2} \tag{3.25}$$

In calculating the current as a function of wind speed, generator efficiency is approximated as being constant. The electric power is consequently proportional to the turbine power

$$P_a(v) \sim P_t(v) \tag{3.26}$$

The losses in the generator are not neglected, it is only assumed that the armature power can be scaled in proportion to the turbine power. The armature power, then, can be expressed as

$$P_a(v) = \frac{P_t(v)}{P_t(v_N)}\; P_{aN} \tag{3.27}$$

where P_{aN} is the armature power at rated load and v_N is the rated wind speed, here assumed to be 13 m/s. The power from the turbine $P_t(v)$ is

$$P_t(v) = C_P(v, n)\; \tfrac{1}{2}\; \rho_a\; A_t\; v^3 \tag{3.28}$$

where C_P is the power coefficient of the turbine, ρ_a is the density of the air and A_t is the area swept by the turbine. Equations (3.27) and (3.28) can be used to express the armature power as

$$P_a(v) = \frac{C_P(v, n(v))}{C_P(v_N, n_N)} \left(\frac{v}{v_N} \right)^3 P_{aN} \tag{3.29}$$

From (3.23) and (3.25) the current as a function of electrical power and voltage can be found

$$I_a(v) = \sqrt{\frac{2 \left\{ U_{ap}(v)^2 - \sqrt{U_{ap}(v)^4 - 1/9\, [P_a(v)\, 2\,\pi\, f(v)\, L_a]^2} \right\}}{[\, 2\,\pi\, f(v)\, L_a\,]^2}} \tag{3.30}$$

The way in which armature current changes with wind speed depends on the generator design, since the armature inductance L_a is not constant. Therefore, the average loss factor for the copper losses will vary during

the optimization of a generator. If the variation of the average loss factor is large, the loss factor has to be calculated for each new set of generator variables used in the optimization. It will later be shown that the variation in the average loss factor is small enough to be neglected.

The *g*-functions for the different types of losses can be calculated by means of the above functions for the current, rotational speed and flux linkage as functions of wind speed. In Figure 3.2 the *g*-functions for different types of losses are plotted. It can be seen that all types of losses decrease from their rated values when the wind speed decreases. The copper losses decrease rapidly as the wind speed decreases because the current is almost proportional to the power. The hysteresis losses are reduced because of the reduced speed but the reduction is much smaller than for the copper losses, since the flux of the generator remains constant. The eddy current losses are reduced more than the hysteresis losses because they decrease as the square of the frequency. The reduction of the friction and windage losses is similar to that of the eddy current losses.

The average loss factors are calculated for three different sites with the wind speed probability density approximated as a Weibull distribution. The first site is a high wind speed site, the second site is a typical wind energy converter site, and the third site is a low wind speed site. The average factors for the turbine power are 0.35, 0.25 and 0.15 on the three sites. The average loss factors for the different sites and the different types

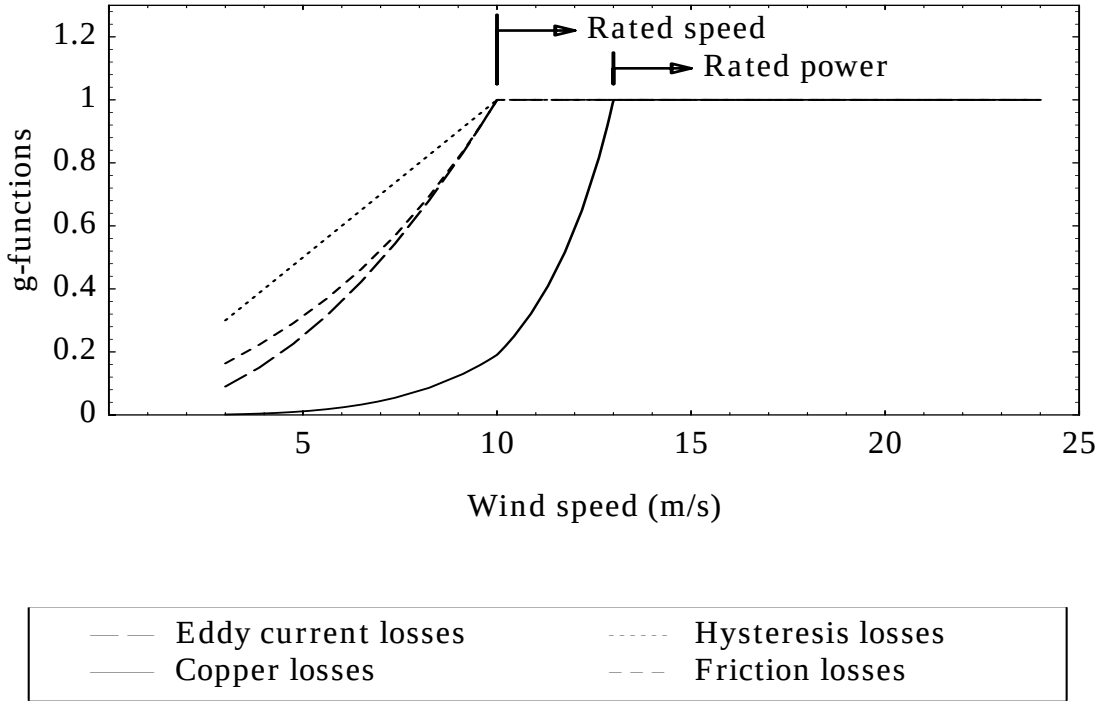

Figure 3.2 The g-functions for different types of losses from the cut-in to the cut-out wind speed.

of losses are shown in Table 3.1. An armature reactance x_a of 1 p.u. has been used.

It is clear that copper losses cause rather low average losses. When the generator is optimized for a wind energy converter, it will be more important to keep the core losses low than to keep the copper losses low. The average loss factors must be calculated for each new type of generator and drive train because they can differ between different generator designs and also the control of the generator affects the loss constants.

The average loss factor for the copper losses depends on the armature reactance. In Figure 3.3 the value of the average loss factor for the copper

Table 3.1 The average loss factors for different types of losses at different sites.

Average wind speed	5.5 m/s	6.8 m/s	8.0 m/s
Parameter A (c=2)	6.23	7.66	9.06
Average factor for the turbine power, k_t	0.15	0.25	0.35
k_{dCu}	0.07	0.14	0.24
k_{dHy}	0.50	0.61	0.69
k_{dFt}	0.35	0.47	0.57
$k_{d\mu}$	0.38	0.50	0.60

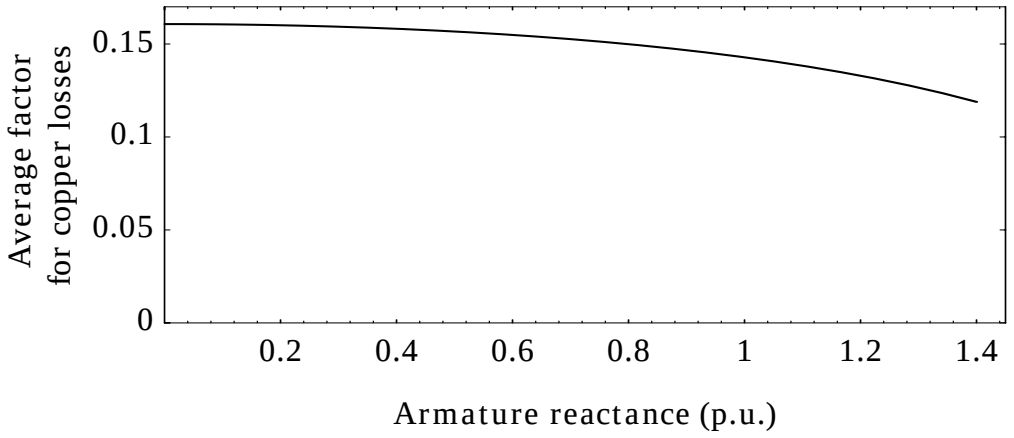

Figure 3.3 The value of the average factor for the copper losses k_{dCu} as a function of generator reactance at the medium wind speed site.

losses is shown as a function of armature reactance for the site with an average wind speed of 6.8 m/s. The average loss factor decreases with increasing reactance. For generators with high force density the reactance is usually between 0.7 and 1.2 p.u. Consequently, it is reasonable to use a reactance of value 1 p.u. when the average loss factor for the copper losses is calculated.

In electrically excited generators, the flux linkage can be reduced at low power to maximize the efficiency at each load, as described by Grauers (1994, p. 90-91). If this control strategy is used, the average loss factor for the copper losses will be higher than for this permanent-magnet generator. The average loss factor for the core losses will instead be lower.

4 Generator Types

In this chapter a generator type suitable for direct-driven wind turbine generators is chosen. First, some different generator types are discussed briefly, and then the choice of rectifier is discussed more in detail. Finally, the chosen generator type is presented.

It is very difficult to compare generator types completely; to find which is the best for a given application. The aim of this chapter is solely to find a generator type well suited to be a direct-driven wind turbine generator.

4.1 Electrical Excitation or Permanent Magnets

Synchronous generators can be either electrically excited or excited by permanent magnets. The question of which type of excitation is best is determined mainly by comparing the cost of the permanent magnets with the total cost of the rotor pole, the field winding and the field winding losses.

The cost and the losses of an electrically excited generator depend on the pole pitch. A simplified way of showing this is to look into the required field current at no-load. The mmf required of the field pole is determined by the required air gap flux density and the magnetic air gap. The mmf required for the iron has been neglected. In the electrically excited generator, the magnetic air gap is the distance between the pole shoe and the stator teeth. As the pole pitch is reduced, the no-load mmf required of each pole is constant. Consequently, the total field mmf has to be constant, although there is less room for the field winding as the pole pitch decreases. To allow constant no-load field mmf, the field pole will have to be higher as the pole pitch is decreased. In Figure 4.1, generator poles with electrical excitation are shown for three different pole pitches. The air gap flux density is 0.7 T and the air gap is 2 mm, which requires a no-load field mmf of 1100 ampere-turns. The the no-load field winding current density is assumed to be 2 A/mm^2 and the fill factor of the field winding is 0.5. In the figure it can be seen that it becomes difficult to decrease the pole pitch below 100 mm because there is not much room left for the field winding. Since the number of poles increases with decreasing pole pitch, the field winding losses will increase as the pole pitch decreases.

Permanent magnets are expensive but they eliminate the excitation losses and allow smaller pole pitches to be used than electrical excitation does. The pole pitch of a generator with permanent magnets can be very small. It is only limited by the leakage flux between the magnets. Just as for the electrically excited generator, the no-load mmf required of the magnet

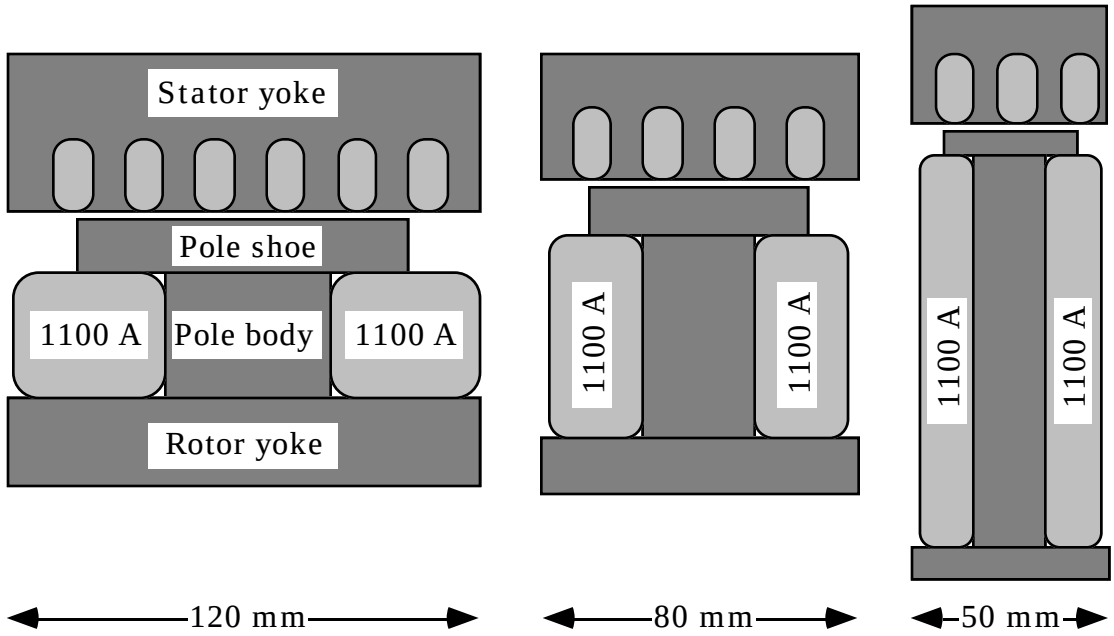

Figure 4.1 Electrical excitation for three pole pitches. No-load peak flux density in the air gap 0.7 T, air gap 2 mm.

does not depend on the pole pitch. The mmf produced by a magnet is the magnet height times the coercitivity of the permanent-magnet material. Therefore, the magnet height can be constant as the pole pitch decreases. In Figure 4.2 permanent magnet excitation is shown for three different pole pitches. In comparison with Figure 4.1 it is clear that permanent magnets are a better alternative than electrical excitation if the pole pitch has to be small.

This comparison is made in a simplified way, not including the armature reaction of stator currents. Still, it shows the main advantage of permanent magnets over electrical excitation when using a small pole pitch. For electrically excited generators the magnetic air gap is small

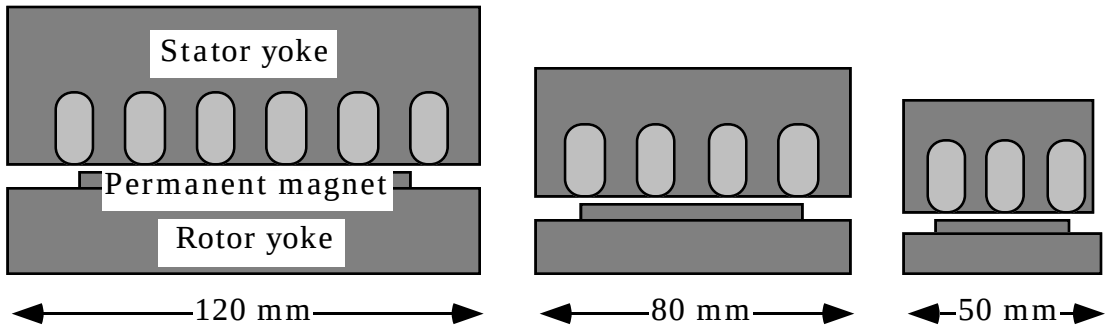

Figure 4.2 Permanent magnet excitation for three pole pitches, 120, 80 and 50 mm. No-load peak flux density in the air gap 0.7 T, air gap 2 mm.

and, as a consequence, the armature reaction will be important if the pole pitch is large. For rotors with surface-mounted permanent magnets, the magnetic air gap is much larger since the permeability of the permanent magnets is almost equal to that of air. Consequently, the armature reaction is much smaller in a permanent magnet generator with surface magnets than in electrically excited generators.

Even though the permanent magnets are very expensive, the losses of the field winding make permanent-magnet excitation better than electrical excitation for small pole pitches. Jöckel (1996) has shown that even expensive NdFeB magnets (≈150 ECU/kg) lead to a lower total cost than electrical magnetization does. Besides reducing losses, the permanent magnets lead to a lighter design.

Induction generators are electrically excited, but in contrast to the electrically excited synchronous generator the magnetizing current flows in the stator winding. Although the design differs from the design of electrically excited synchronous generators, induction generators also suffer from the same negative effects as the pole pitch is reduced. The magnetizing mmf is constant, but as the pole pitch is reduced a larger part of the stator current will be needed to magnetize the air gap. This effect causes the power factor to decrease as the pole pitch decreases. The practical limit for the minimum pole pitch of induction machines with an air gap of 2 mm is in the order of 100 mm. An other reason why induction generators cannot be made with a small pole pitch even if the air gap can be made small is that the stator winding should be made with at least two slots per pole and phase to keep the space harmonics of the air gap flux wave low. Two slots per pole and phase requires at least a 100 mm pole pitch in a three phase generator.

4.2 Direct Grid Connection or Frequency Converter

Grid connected generators are required to have a frequency of 50 or 60 Hz and to damp oscillations between the grid and the rotor. Direct-driven wind turbine generators can only generate 50 Hz with a very large number of poles, for example 188 poles for a 500 kW generator with a rated speed of 32 rpm.

With a required pole pitch of more than 100 mm, diameter for electrically excited generators will be very large, more than 6 m for the 500 kW generator. Therefore, electrically excited, direct-driven wind turbine generators should not be designed for a 50 Hz frequency and, consequently, should not be direct grid connected.

The pole pitch can be made 50 mm, or even less, by using permanent magnets. The generator can then provide a 50 Hz frequency with a reasonable diameter, 3 m for a 500 kW generator with a rated speed of

32 rpm. Nevertheless, damper windings cannot be made efficient with such a small pole pitch and, therefore, the permanent magnet generator cannot be direct grid connected. There is one solution to this problem; mechanical damping of a moving stator, discussed by Westlake et al. (1996). That solution requires a complicated mechanical structure and is not further analysed in this thesis.

It is clear from the discussion above that it would be very difficult to design a direct-driven wind turbine generator that is to be direct connected to the grid if the diameter must remain small. Connecting a frequency converter between the generator and the grid will solve these problems. To use a frequency converter is, however, not only a way to avoid problems: A frequency converter also improves the wind energy converter performance. It makes it possible to operate the wind turbine at variable speed, which increases the energy production and reduces the noise at low wind speeds. The frequency converter can also reduce mechanical loads and it allows the generator to be optimized with less restrictions.

4.3 Surface Magnets or Flux Concentration

In permanent magnet generators the magnetization can either be achieved by magnets directly on the rotor surface or by magnets inside the rotor. One rotor design with surface-mounted magnets and one rotor design with flux concentration are shown in Figure 4.3.

Magnets on the rotor surface have to have a remanent flux density higher than the required air gap flux density. Subsequently, it is necessary to use expensive magnets, like Samarium-Cobalt (SmCo) or Neodymium-Iron-Boron (NdFeB). SmCo has a remanent flux density of about 1 T and NdFeB about 1.2 T. The magnet material is utilized best when the flux density in the air gap is half the remanent flux density. If the air gap flux density has to be close to the remanent flux density, the amount of permanent

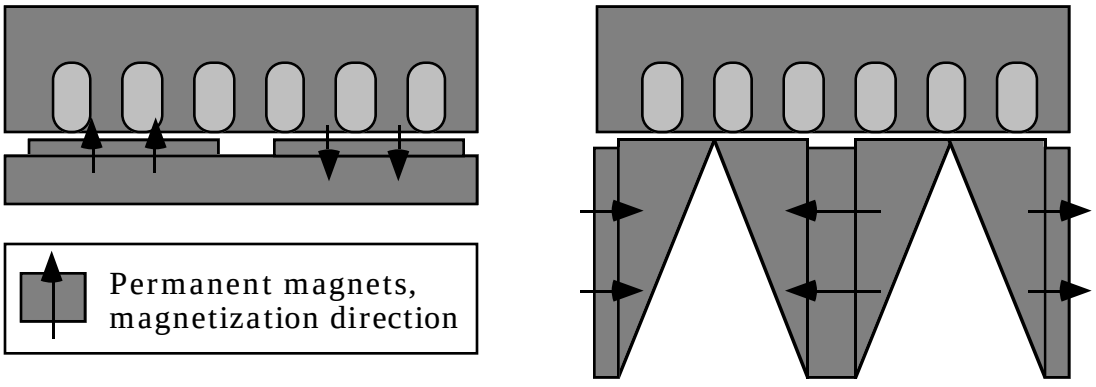

Figure 4.3 Surface mounted NdFeB magnets (left) and ferrite magnets with flux concentration (right).

magnets required will be large. Nevertheless, surface magnets lead to a very simple rotor design with a low weight.

Flux concentration can be used to utilize cheap low-energy magnets and still obtain a high air gap flux density. The magnets are then placed inside the rotor and the flux is guided in magnetic circuits which are narrower at the air gap than at the magnets. A common low-energy magnet material is ferrite which has a remanent flux density of about 0.4 T.

A more complicated rotor is required for flux concentration than for surface magnets and it would also normally be heavier, while the cost for magnets can be much lower than for surface magnets. Today, NdFeB magnets cost about 30 times more than ferrite magnets and their maximum magnetic energy product is about 10 times higher than it is for ferrite.

4.4 Slot Winding or Air Gap Winding

Normally, the armature windings in electrical machines are placed in slots in the iron core, but in certain machines air gap windings have been used. A conventional slot winding and an air gap winding are shown in Figure 4.4.

The air gap winding is interesting for several reasons: more copper can be placed in the space between the stator yoke and the rotor; cogging torque caused by the teeth is avoided; and the reactance of the stator winding is reduced. Nevertheless, the use of air gap windings also results in some disadvantages: the magnetic air gap is large, requiring a large field current or much permanent magnet material to be used; the forces act on the stator winding instead of on the stator iron; the cooling surface between the windings and the stator core is smaller if an air gap winding is used; and the conductors of the air gap winding will be penetrated by the air gap flux, which will cause eddy current losses in the windings. The last disadvantage is not important if the windings are made of thin

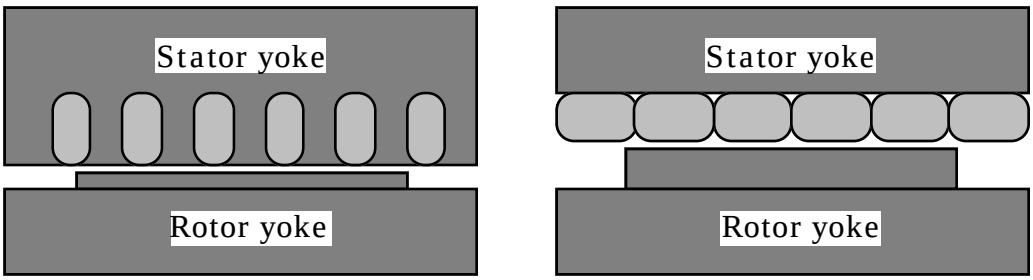

Figure 4.4 A conventional slot winding (left) and an air gap winding (right).

wire. In windings made of copper bars with a large cross section, the eddy current losses caused by the main flux may singnificantly increase the winding temperature.

Several authors propose air gap windings instead of conventional slot windings. Air gap windings have been proposed for large turbogenerators by Davies (1971), for several small machines and also for direct-driven, wind turbine generators by Honorati et al. (1991) and by Alatalo (1991). Except for turbogenerators, which have a very large pole pitch, air gap windings are used in combination with permanent magnet excitation.

Turbogenerators have a large air gap, in the order of 100 mm, even with a conventional slot winding. Consequently, the air gap winding does not necessarily increase the necessary magnetizing mmf. The windings are also usually directly water-cooled. Still, there can be problems with air gap windings in turbogenerators: The eddy current losses in the winding, for example, have not been discussed by Davies (1971); since turbogenerators generally have thick copper bars, these losses can be very high.

In small electrical machines, the air gap winding can be very useful because it simplifies the manufacturing of the machine. In these small machines the windings can be easily glued to the stator, since the forces are very small. The cooling of the winding is also effective because of thin windings and the windings are made of thin wire, leading to low eddy current losses.

In direct-driven wind-turbine generators, the air gap winding seems to have some disadvantages. The winding is normally indirectly cooled in generators of this size and, therefore, the decreased cooling surface between the air gap winding and the stator yoke is a disadvantage. The air gap is normally only a few millimetres in a slotted machine but in a machine with air gap windings, the air gap will become several times larger, leading to a large amount of permanent magnets. The eddy current losses in the winding can also be a problem, but one that can be avoided if the winding can be made of stranded wire.

4.5 Radial-, Axial- and Transversal-flux Machines

There are several generator types that are possible to use as direct-driven wind turbine generators. In this section, the radial-flux, axial-flux and transversal-flux generators are discussed. Since the radial-flux machine is the most conventional of the alternatives to be compared, it is used as a reference in the comparisons. The design of the different machine types can be seen in Figures 1.4–1.8 in Section 1.3.

Axial-flux machines can, in many respects, be designed in a way similar to radial-flux machines. One important restriction for axial-flux machines is that the amount of windings in the air gap is limited by the available space at the inner radius. The air gap at larger radius cannot be fully utilized because of this and the utilization of the iron core and magnets is slightly less efficient in axial-flux machines than in radial-flux machines. In radial-flux machines, the length of the stator and the air gap diameter can be chosen independently. If necessary, the radial-flux machine can be made with a small diameter by using a long stator. To reduce the diameter of the axial-flux machine, while keeping the rated torque constant, the difference between inner and outer radius has to be increased. The maximum torque of an axial-flux machine is, however, achieved when the inner radius is about 0.6 times the outer radius (di Napoli 1991). A smaller inner radius will only decrease the rated torque. Consequently, the diameter of the axial-flux machine cannot be reduced as much as that of the radial-flux machine. One way of avoiding a large diameter is to stack a number of axial-flux machines with a small diameter on the same shaft. Thus, the rated power can be increased without increasing the diameter. This will, however, lead to an expensive generator.

To allow a small air gap, the rotor and stator structures have to withstand the high magnetic force in the air gap. It is easier to make a rotor stiff in the radial direction than in the axial direction, especially in generators with a large diameter. Therefore, it is easier to make radial-flux generators with a small air gap. However, the thermal expansion of the rotor and stator will in a radial-flux generator influence the air gap, while in an axial-flux machine it does not affect the air gap. Axial-flux machines are also difficult to manufacture with a slotted stator, because the slot pitch varies on stator laminations for different radii.

The axial-flux machine can be made with a double-sided stator more easily than a radial-flux machine. A double-sided stator is shown in Figure 1.7. This stator eliminates the need for a rotor yoke as a return path for the flux. Subsequently, the active weight of the generator can be reduced. Nevertheless, it is only a rotor yoke made of cheap solid iron that is eliminated. A more complex non-magnetic rotor structure has to be used instead to hold the magnets. The double-sided stator also allows the winding to be divided into two, half as thick parts. In a radial-flux machine an equivalent electromagnetic design can be achieved by doubling the stator length instead of using two stator halves. Such a solution will lead to a lower amount of end windings than the double-sided stator. If the machine length is not restricted, the axial-flux machine with a double-sided stator will not be better than a radial-flux machine with a long stator, from an electromagnetic point of wiev.

A special type of axial-flux generator is the toroidal stator machine (Shown in Figure 1.6). Besides the above mentioned advantages and disadvantages of axial-flux machines, the toroidal stator winding leads to simple end windings, but it becomes more difficult to fix the stator to the generator structure. One further disadvantage is that the windings, which have high losses in direct-driven wind turbine generators, are in the middle part of the machine where they are difficult to cool without direct air- or water-cooling.

The transversal-flux machine is rather different from the other machine types, and it is difficult to make any simple comparisons between it and radial-flux machines. The major difference between radial- or axial-flux machines and the transversal-flux machine is that the transversal-flux concept allows an increase in the space for the windings without decreasing the available space for the main flux; this allows for very low copper losses. The transversal-flux machine can also be made with a very small pole pitch compared with the other types. These differences make the transversal-flux machine capable of producing a higher force density in the air gap than the other machine types. Unfortunately, the electromagnetic structure is more complicated than for conventional generator types, which may make it more expensive to manufacture. The transversal-flux generator is probably better than the radial-flux machines from an electromagnetic point of view, but a comparison of these generator types must include a detailed mechanical investigation and has, therefore, not been included in this thesis.

4.6 Forced-commutated Rectifier or Diode Rectifier

To make a direct-driven generator small, it is important that the force density in the air gap is high. A high force density requires a high current loading, which leads to a high armature reactance. Because of the reactance, the type of rectifier has a large influence on the phase angle of the armature current and on the achievable force density.

There are two major types of rectifiers that can be used for variable-speed generators: machine-commutated rectifiers and forced-commutated rectifiers. In this section, a machine-commutated diode rectifier is compared with a forced-commutated sine-wave rectifier. The diode rectifier is simpler, cheaper and more efficient than a forced-commutated rectifier. The diode rectifier, however, cannot control the current phase angle and, if the reactance of the generator is high, the generator will not be well utilized. The forced-commutated rectifier can supply the generator with reactive power and, therefore, the phase angle between the current and the internal emf can be kept small, allowing a high force density, even if the reactance is high.

A comparison of rectifiers will be made regarding the power at rated current and peak power. In some wind energy converters, the generator must be able to produce a peak power higher than the rated power, often about 150 % of the rated power. The peak power is only required for short times, in the order of some seconds. During that short time, the heating of the winding is not assumed to be a problem and, therefore, the current can be allowed to be much higher than the rated current.

4.6.1 Generator Model

The generator is assumed to be a three-phase permanent-magnet generator with sinusoidal no-load voltages. Its equivalent circuit is shown in Figure 4.5. In a permanent-magnet generator of the type discussed in Chapters 5–7, the synchronous-, transient- and sub-transient reactances are almost equal. In this thesis, the value of the synchronous reactance X_a is used in all calculations. The per unit base is the no-load emf of the generator and the rated current. The per unit resistance of the armature winding will be a few percent, and has not been included in this comparison of rectifiers.

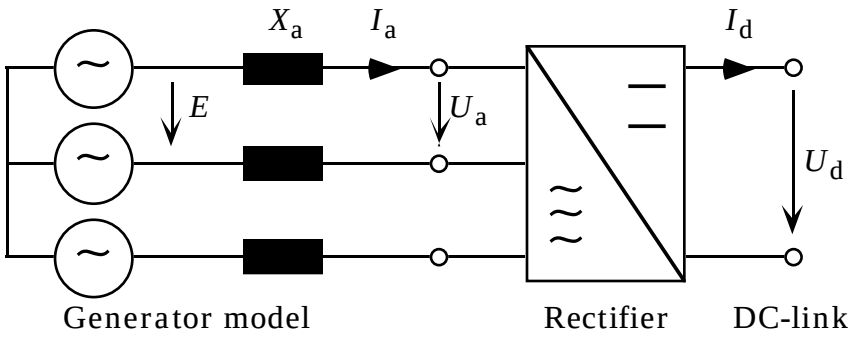

Figure 4.5 The equivalent circuit of the generator used for a comparison of rectifiers.

4.6.2 Diode Rectifier

The commutation voltage drop makes the output voltage U_d of a diode rectifier depend on the dc current I_d. The currents in two phases overlap during the time it takes to commutate the current from one phase to another. The overlap can be measured as an electrical angle and, when the overlap angle is less than 60 degrees, the voltage can be calculated as

$$U_d = \frac{3}{\pi}\sqrt{2}\,E - \frac{3}{\pi}\,X_a\,I_d \qquad (4.1)$$

where E is the internal line-to-line emf of the generator and X_a is the armature reactance (Thorborg 1988, p. 117). If the overlap angle exceeds 60 degrees, the diode bridge will be completely short-circuited during a

part of the period. The dc voltage starts to decrease more rapidly with increasing current and the dc voltage eventually becomes zero. The output power as a function of the current can be calculated from the output voltage. Since the voltage always decreases with increasing current, the output power will have a maximum value which cannot be exceeded, no matter how high the current is. The output dc voltage and the active power of a diode rectifier fed by a generator, with a reactance of 0.5 p.u. and zero resistance, are shown in Figure 4.6. The voltage and active power as functions of current will always have the same shape, regardless of the value of the armature reactance. It is only the scales of the current axis and the power axis which will change if the reactance is changed.

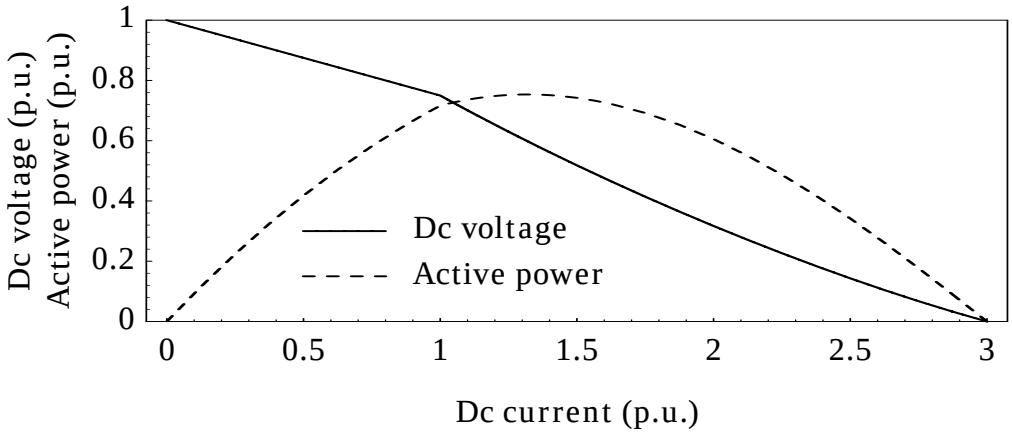

Figure 4.6 The dc voltage and active power of a diode rectifier fed by a generator with an internal emf of 1 p.u. and a reactance of 0.5 p.u.

4.6.3 Forced-commutated Rectifier

If a forced-commutated rectifier is used, the terminal voltage of the generator can be controlled by supplying the generator with reactive power. The rated armature current I_{aN} and rated phase voltage U_{apN} are usually the limit for the generator power, and depending on how the phase angle of the armature current is controlled, different values of the active power can be achieved at rated current. To maximize the active power at rated current, the product of the voltage, current and power factor has to be maximized.

Three different ways to control the generator terminal voltage, and the corresponding kVA ratings required of the generator armature and the rectifier, are shown in Figure 4.7. Maximizing the terminal power factor (control a) does not maximize the power, because the terminal voltage must be lower than the internal emf. Since the generator armature and

the rectifier both has to be rated for the no-load emf, which is higher than the terminal voltage at rated load, the required kVA ratings are high.

Instead, the terminal voltage can be kept at the same level as the no-load emf (control b), by supplying reactive power from the rectifier. This control method maximizes the active power from a generator and rectifier with equal kVA rating and will be used in the following discussion.

If the generator is designed with an emf lower than the rated voltage, the power can be increased by keeping the phase angle between the internal emf and the armature current zero (control c). The advantage of this generator design is that less permanent magnet material is used than if control b is used and core losses at no-load are lower. The stator flux is kept high only at high load by supplying reactive power to the armature winding. One drawback is that the rated active power of the generator is not maximized. The same generator would be capable of producing slightly higher power, if the internal emf were increased to the rated voltage and rectifier control b were used. Control b does not only allow a lower generator armature kVA rating than control c, it also requires a lower kVA rating of the frequency converter.

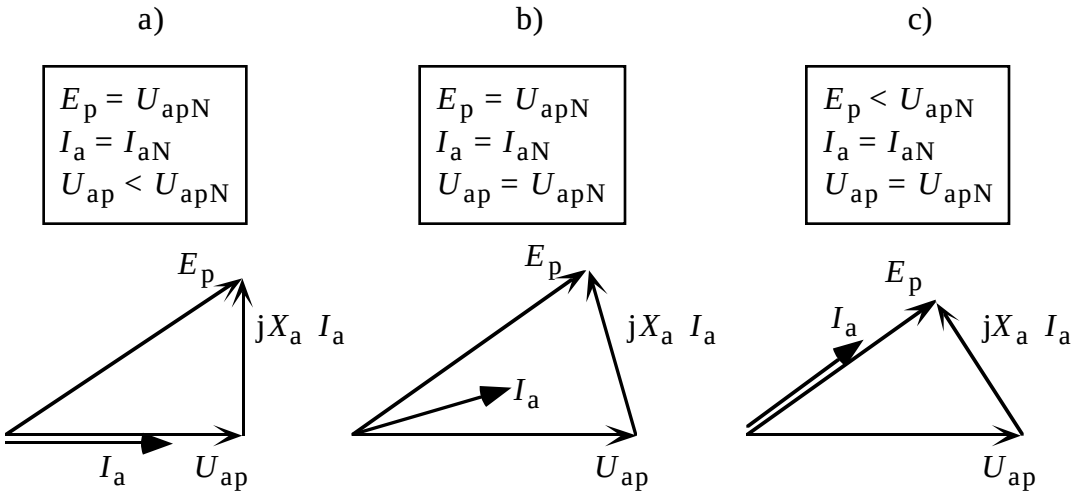

Rating (kVA) if x_a = 0.8 p.u.	a)	b)	c)
Frequency converter	1.28 P_N	1.09 P_N	1.28 P_N
Generator armature	1.28 P_N	1.09 P_N	1.28 P_N

Figure 4.7 Phasor diagrams of a generator loaded by a forced-commutated rectifier at rated current and the neccesary frequency converter and generator armature kVA ratings. E_p is the induced no-load phase voltage, U_{ap} the armature phase voltage and I_a the armature current.

a) cos(φ)=1 at the terminals and E_p equal to the rated voltage.
b) U_{ap} and E_p equal to the rated voltage.
c) U_{ap} equal to and E_p lower than the rated voltage.

The active power as a function of current, for a generator with a reactance of 0.5 p.u. connected to a forced-commutated rectifier using control b, is plotted in Figure 4.8. The output power increases linearly with increasing current as the current starts to increase from zero. The reason for this is that the forced-commutated rectifier can keep the terminal voltage constant and that the power factor is almost 1. As the current increases further, the power factor decreases because the rectifier has to supply reactive power. Therefore, the increase in active power is no longer linear. Eventually, the active power reaches a maximum value, at a generator load angle of 90 degrees. If the current increases further, it will only lead to a decrease in active power.

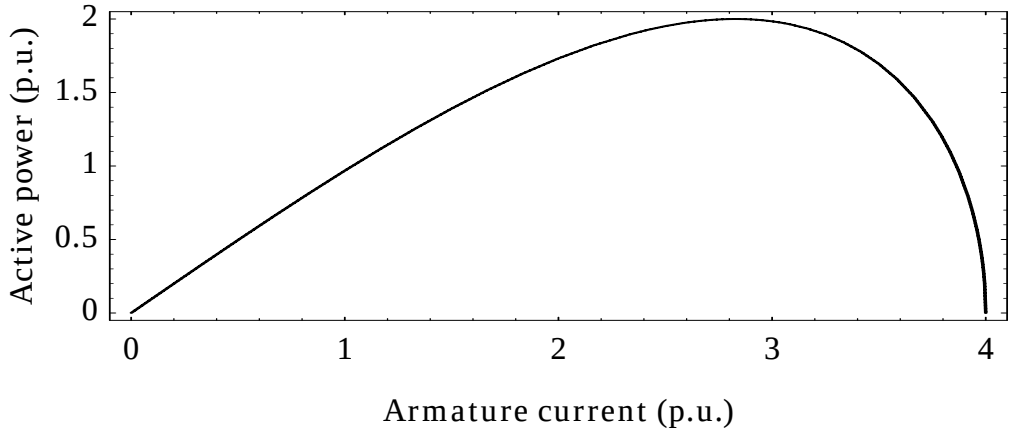

Figure 4.8 The active power of a generator with a reactance of 0.5 p.u. connected to a forced-commutated rectifier. The rectifier keeps the generator terminal voltage constant.

4.6.4 Rectifier Comparison

The diode rectifier and the forced-commutated sine-wave rectifier were compared regarding the output power at rated armature current. The active powers of a generator connected to the two types of rectifiers are shown in Figure 4.9, as functions of armature current. The value of the generator reactance does not change the shape of the curves, only the scaling of the current and power axes. As can be seen in the figure, the difference in rated power between a diode rectifier and a forced-commutated rectifier depends on how high the rated current of the generator is.

If the rated current is I_1, which corresponds to a reactance of 0.15 p.u., the rated power of the forced-commutated rectifier is 12 % higher than if a diode rectifier is used. A sub-transient reactance of 0.15 p.u. is usual for a conventional, four-pole, synchronous generator, but it is a low value for a direct-driven wind turbine generator.

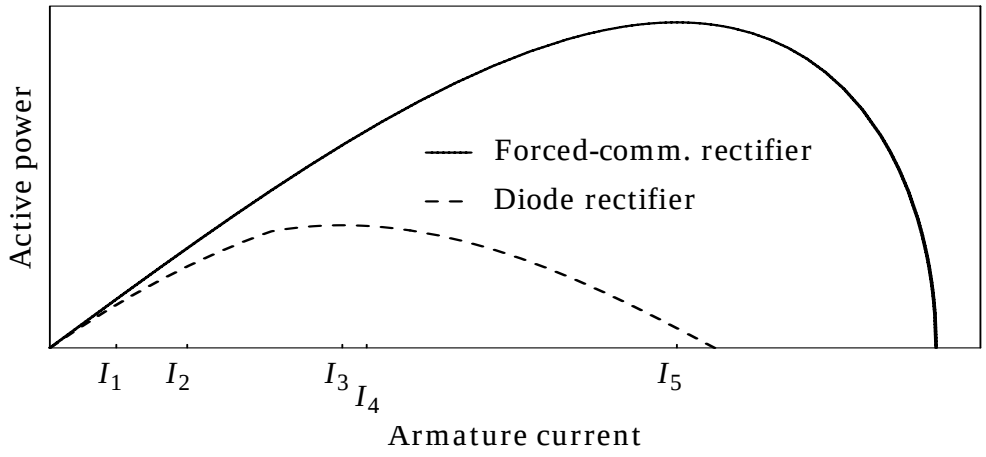

Figure 4.9 The active powers of a generator, connected to a diode rectifier or a forced-commutated rectifier, as functions of armature current.

In some wind energy converters, the generator has to be able to produce a peak power of 150 % of the rated power. In this case, the rated current cannot be higher than I_2 if a diode rectifier is used. The rated current I_2 corresponds to a reactance of 0.31 p.u. At the same rated current, the generator can produce 22 % higher power if it is instead connected to a forced-commutated rectifier. The copper losses are almost the same as if a diode rectifier is used and, therefore, the forced-commutated rectifier increases generator efficiency.

If the rated current is I_3, corresponding to a reactance of 0.66 p.u., the generator reaches its peak power if it is connected to a diode rectifier. If connected to a forced-commutated rectifier instead of the diode rectifier, the same generator can be capable of producing 65 % higher power with almost the same copper losses.

Connected to a forced-commutated rectifier, the generator can have a rated current of I_4 and still be capable of producing a peak power of 150 %. The rated current I_4 corresponds to a per unit reactance of 0.71 p.u. If a diode rectifer is used, the maximum reactance for a generator with 150 % peak power is only 0.31 p.u. Consequently, a forced-commutated rectifier allows more than twice as high reactance as a diode rectifier does for a generator system required to produce a peak power of 150 % of the rated power.

If cooling and efficiency considerations do not limit the current and the peak power is not required to be higher than the rated power, the generator is utilized best if the rated current is I_5 and a forced-commutated rectifier is used. In this case, the reactance is 1.41 p.u. and the generator can produce a power which is 165 % higher than

(2.65 times) its peak power connected to a diode rectifier. The copper losses of the generator, however, are 360 % higher (4.6 times) at the current I_5 than they are at the current I_3, which means much lower efficiency even though the rated power is 165 % higher. This power is the absolute peak power the generator can produce if the armature voltage is limited to the no-load voltage.

Peak power and power at rated current of the generator are presented as functions of the per unit reactance in Figure 4.10. It can be seen that the peak power of the generator connected to a forced-commutated rectifier is always 2.65 times the value obtained for a generator connected to a diode rectifier. The difference in power at rated current, if a forced-commutated rectifier is used instead of a diode rectifier, is less than 20 % for reactances below 0.3 p.u., but it increases quickly as the reactance increases. The diode rectifier should probably not be used for a generator with a reactance higher than 0.5 p.u., while generator reactance of up to 1.4 p.u. can be allowed if a forced-commutated rectifier is used.

The choice of rectifier depends on the total cost for the generator plus rectifier and the total average efficiency. The diode rectifier is cheap and very efficient, but it may require a much larger generator and it also decreases the efficiency of the generator. If it is important that the generator is small, a high reactance of the generator is difficult to avoid. Of the two compared rectifier types, the forced-commutated rectifier is probably the best for a direct-driven wind turbine generator.

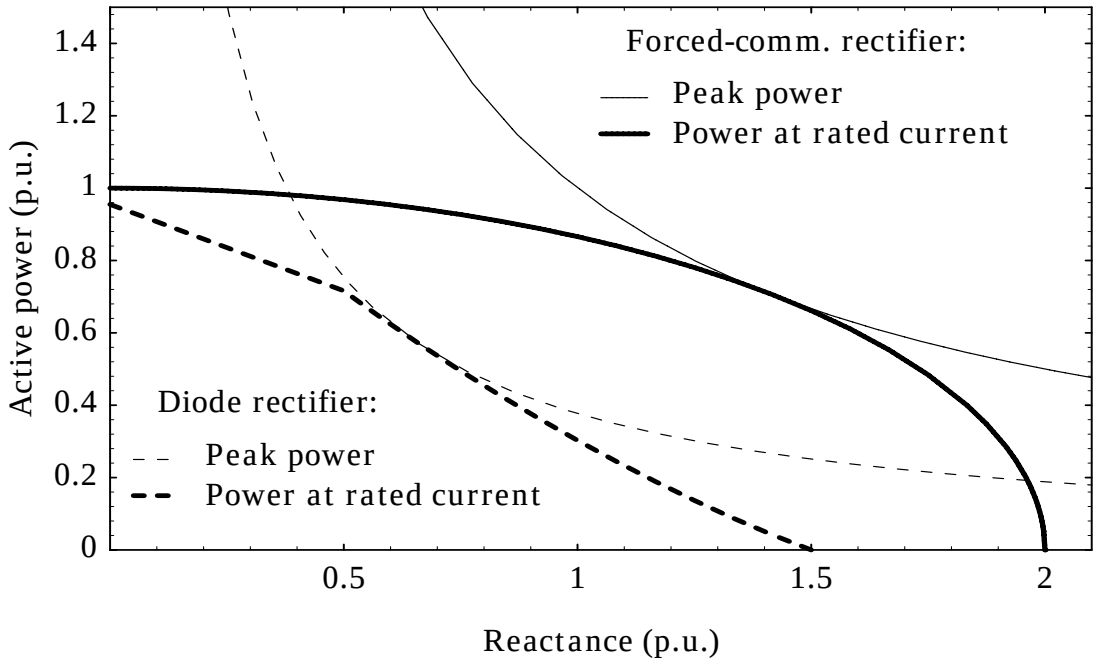

Figure 4.10 Peak power and power at rated current as a function of armature reactance of the generator.

4.7 Chosen Generator Type

In this section, the generator type chosen and the reason for using it are presented. The comparisons made earlier in this chapter indicate that the radial-flux permanent-magnet generator has several advantages and that it is well suited to be used as a direct-driven wind turbine generator.

4.7.1 Basic Generator Concept

Permanent-magnet excitation is chosen because it gives an efficient generator in which the pole pitch can be made small, leading to a light core and low end-winding losses. The magnets are of NdFeB material and are placed on the rotor surface. This placement gives a simple and light rotor design, however these magnets are more expensive to use than ferrite magnets.

Radial-flux design is used because it allows a simple generator structure, good utilization of the active materials and it can easily be made with a slotted stator. Radial-flux design also allows a small diameter since the stator can be long. The air gap can more easily be made small in a radial-flux machine than in an axial-flux machine, which leads to a low amount of permanent-magnet material.

A stator with a slot winding is used because the cost of the permanent magnets would otherwise be very high and a slot winding makes it easier to cool the winding indirectly, through the stator core.

A frequency converter is used since the generator diameter otherwise has to be very large and also because it allows variable turbine speed and lower grid interference. The rectifier is a forced-commutated sine-wave rectifier to allow for high inductance and a small generator.

4.7.2 Details of the Chosen Generator

The winding has three phases and only one slot per pole and phase to allow for a small pole pitch, without having slots which are very narrow. Narrow slots lead to a low copper fill factor. A two-layer winding is used to make the end windings simple, and since it is an integer slot winding, all slots will contain two coils belonging to the same phase. The slots are constructed semiclosed to limit losses in the rotor due to slot harmonics and to limit the cogging torque.

The windings and magnets must be cooled efficiently. Almost all losses are dissipated in the stator, since the only rotor losses are the losses in the magnets. The generator is to be totally enclosed (class IP54 described in IEC Publication 529). Ambient air is not allowed to enter the generator, in order to reduce the risk of water condensation on the windings and salt and dust in the generator.

Forced cooling directly on the outer surface of the stator core will be used. The stator yoke is fixed to a circular beam which guides the cooling air. Air is forced round the circumference of the stator by means of external fans. A principal drawing of the cooling system is shown in Figure 4.11. To achieve a low temperature rise between the stator yoke and the cooling air, the air velocity is 15 m/s and extra cooling fins are made at the outer surface of the stator core. The circular stator beam is divided into two or more separate cooling circuits, in order to make the cooling more efficient. Internally, the rotor and the end windings are cooled by the circulation of the inner air. The rotor is equipped with a radial fan which forces the air to pass the end windings and then out to be cooled at the end shields.

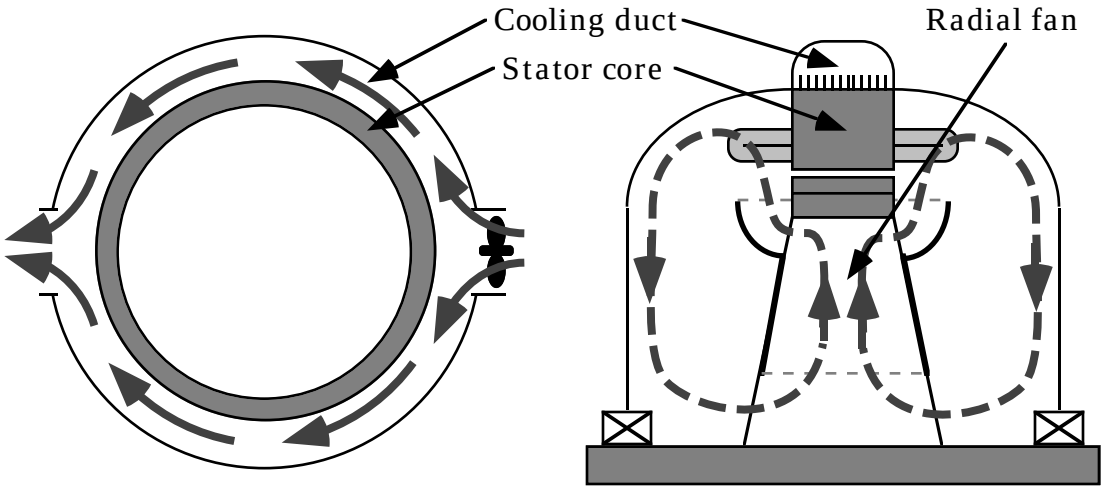

Figure 4.11 Left: Axial view of the cooling of the stator iron core. An external fan forces air through the cooling duct at the stator core back.

Right: Tangential view of the cooling of the rotor and end windings. The rotor is equipped with a radial fan circulating the internal air.

4.7.3 Materials

The winding is made of stranded wire that has a copper fill factor of 0.8, excluding the coil insulation. Each coil has an insulation that is 0.5 mm thick. The slot is made 1 mm wider than the insulated coil. That extra space is filled with resin during the impregnation, leading to a total insulation thickness of 1 mm. The value of the total fill factor of the slot, excluding the slot wedge, is 0.58 for a 40 mm high and 10 mm wide slot with a two-layer winding.

The magnet material is NdFeB with a remanent magnet flux density of 1.22 T at room temperature. The remanent flux density at operating temperature, i.e. below 120˚C, will be 1.1 T or higher. NdFeB is chosen instead of SmCo because of its lower price and higher remanent flux density.

The stator core is made of 0.5 mm thick, low-loss, electrical steel for large generators. The losses at 50 Hz and 1.0 T are 1.20 W/kg and the fill factor of the stator core is 0.97.

5 Design Method for a Permanent-magnet Generator

In this chapter, an analytical design method is derived for the proposed three-phase radial-flux generator with a forced-commutated rectifier. The design variables are discussed in Section 5.1 and the design equations and the thermal model in Section 5.2. In Section 5.3, the calculation method is described. Finally, the analytical design method is compared with finite element calculations and the sensitivity of the thermal model is discussed in Section 5.4.

Many of the calculations are based on simplified models. The models have been estimated to be sufficient for a preliminary generator design. If the design method should be used for other purposes, needing higher accuracy, the models can be changed to more detailed ones.

Some steps in the complete design of a generator have not been included. Parts which can be considered as final adjustments and checks, are left for the detailed design that has to be carried out before a generator is manufactured. The steps remaining for the final design are: adjusting the rated voltage to the desired level; rounding off the number of pole pairs to the nearest integer value; and checking that the permanent magnets do not risk irreversible demagnetization. The demagnetization calculations can be included in the design method, but it has been found during this investigation that the demagnetization is not a problem in this type of generator, as long as the pole pitch is kept small.

5.1 Design Variables

It is important that the variables chosen for the design calculations are independent. By starting with the geometrical variables and the current density in the windings as basic variables, it is easy to assure that they are independent. The proposed generator is described by 16 basic variables, the 15 in Figure 5.1 and the stator length. The generator is completely defined by these 16 basic variables and the material data. All the basic variables have to have values before the generator data can be calculated.

Nine of the basic variables are assumed to be constant or are defined as functions of other variables. The stator and rotor yoke heights are determined by the allowed flux densities in the yokes. The tooth tip height, the slot wedge height, the slot opening and the coil insulation thickness are constant. The air gap is kept at its minimum value, limited by mechanical considerations to 0.1 % of the air gap diameter. The slot pitch is determined by the required number of slots per pole and phase and the magnet width is kept as a constant fraction of the pole pitch.

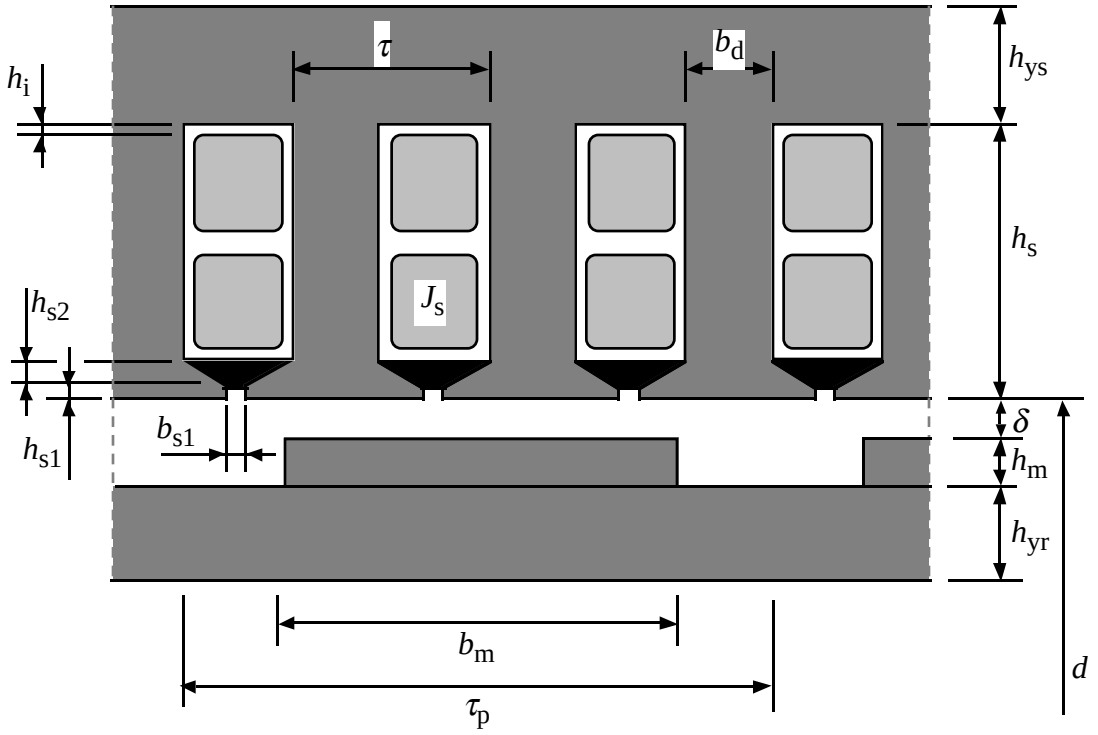

Figure 5.1 Basic variables of the proposed generator.

Five of the basic variables are used directly as design variables: the air gap diameter, the stator length, the slot height, the pole pitch and the current density. The two remaining variables, the magnet height and the tooth width, are defined as functions of the peak, no-load, air gap flux density and the peak, no-load, teeth flux density, respectively. The reason for using flux densities as design variables rather than geometrical variables is that the optimum flux densities can be assumed to vary rather little as the generator size changes.

The variables are summarized in Table 5.1. Seven variables are used as design variables. These variables can be used to calculate generator designs of different rated power and with different temperatures of the windings. If a generator with a specified rated power and specified winding temperature is designed, two of the design variables can no longer be chosen freely. The stator length is adjusted to get the right rated power of the generator and the current density is adjusted to get the right winding temperature. The other five design variables can still be varied freely.

The rated voltage and current are not included in the preliminary design. It is assumed that the top and bottom conductor in the slots are connected parallelly. Thus, the phase current is equal to the total current in a slot.

By adjusting the number of slots and the number of branches connected parallelly and in series, the voltage level can be adjusted.

The pole pitch is used as a variable instead of the number of pole pairs. Since there are no restrictions on the pole pitch, the number of pole pairs is usually not an integer in the design calculations. For a generator having a large number of pole pairs, this will simplify the numerical optimization of the generator without introducing any significant errors.

Table 5.1 The variables used in the design method.

Design variables		**Corresponding basic variables**	
d	Air gap diameter	d	Air gap diameter
l	Stator length	l	Stator length
h_s	Slot height	h_s	Slot height
τ_p	Pole pitch	τ_p	Pole pitch
J_s	Current density	J_s	Current density
$\hat{B}_{\delta 0}$	Peak air gap flux density	h_m	Magnet height
$\hat{B}_{d0}$	Peak teeth flux density	b_d	Tooth width

Constants and fixed relations		**Corresponding basic variables**	
$\hat{B}_{ys} = 1.2$ T	Peak stator yoke flux density	h_{ys}	Stator yoke height
$\hat{B}_{yr} = 1.2$ T	Peak rotor yoke flux density	h_{yr}	Rotor yoke height
$h_{s1} = 1$ mm	Tooth tip height	h_{s1}	Tooth tip height
$h_{s2} = 4$ mm	Slot wedge height	h_{s2}	Slot wedge height
$b_{s1} = 3$ mm	Slot opening	b_{s1}	Slot opening
$h_i = 1$ mm	Insulation thickness	h_i	Insulation thickness
$\delta = 0.001\, d$	Mechanical air gap	δ	Mechanical air gap
$q = 1$	No. of slots per pole & phase	τ	Slot pitch
$b_m = 0.7\, \tau_p$	Magnet width	b_m	Magnet width

5.2 Design Equations

5.2.1 General Definitions

The diameter and pole pitch determine the number of pole pairs

$$p = \frac{\pi\ d}{2\ \tau_p} \tag{5.1}$$

The number of slots per pole and phase q is set to one to allow for a small pole pitch without getting a low slot fill factor because of narrow slots. The number of phases m is three. The total number of slots of the stator is

$$Q = 2\,p\ \ m\ \ q \tag{5.2}$$

The slot pitch is

$$\tau = \frac{\tau_p}{m\ \ q} \tag{5.3}$$

The slot and the two-layer winding are shown in Figure 5.2. The slot is described by its depth h_s and its width b_s. The slot width can be calculated from the slot pitch and tooth width b_d as

$$b_s = \tau - b_d \tag{5.4}$$

The slot opening b_{s1} is assumed to be 3 mm, the tooth tip height h_{s1} 1 mm, and the slot wedge height h_{s2} 4 mm. The winding height is

$$h_{s3} = h_s - h_{s1} - h_{s2} \tag{5.5}$$

The conductor height h_{Cu} and width b_{Cu} are determined by the winding

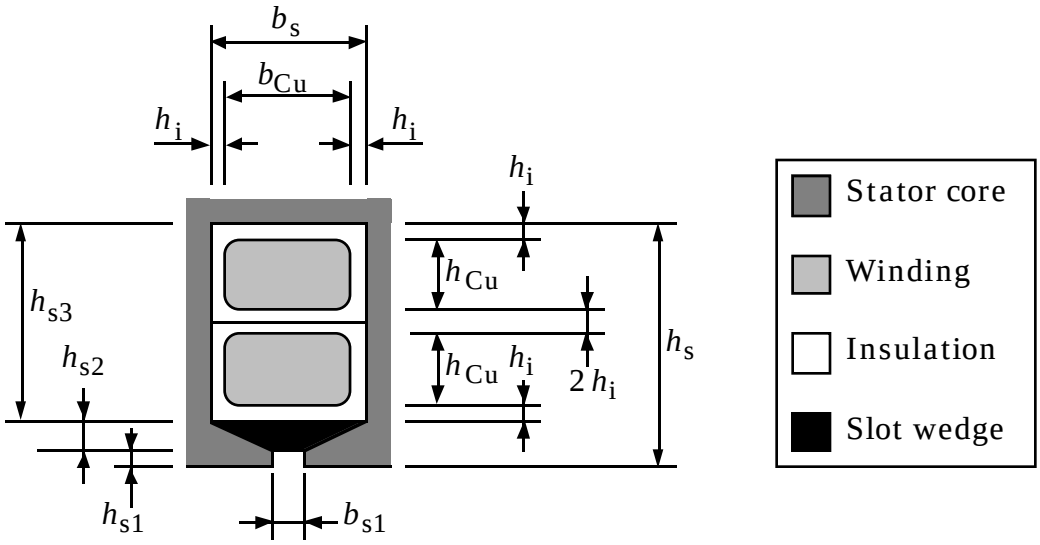

Figure 5.2 The slot and the two-layer winding.

height, slot width and the coil insulation thickness h_i, i.e.,

$$h_{Cu} = \frac{h_{s3} - 4\ h_i}{2} \tag{5.6}$$

$$b_{Cu} = b_s - 2\ h_i \tag{5.7}$$

respectively.

For a three-phase machine for which the magnet cost per torque should be kept low, the ratio of magnet width to pole pitch should be between 0.6 and 0.9 (Lampola et al. 1996a). In the proposed generator the magnet width is kept at 0.7 times the pole pitch, i.e.,

$$b_m = 0.7\ \tau_p \tag{5.8}$$

The winding is a full-pitch winding and, therefore, the winding pitch is

$$W = \tau_p \tag{5.9}$$

The end winding length is assumed to be

$$l_b = 2\ W \tag{5.10}$$

The equivalent core length is approximated by

$$l_e = l + 2\ \delta \tag{5.11}$$

The useful iron length is

$$l_u = k_{Fes}\ l \tag{5.12}$$

where k_{Fes} is the stator iron fill factor. The frequency at rated speed is

$$f = p\ n_N \tag{5.13}$$

where p is the number of pole pairs. The air gap should be small to minimize the amount of permanent magnets needed. The mechanical stiffness and the thermal expansion of the generator limits the minimum air gap which can be used. In this thesis the relation

$$\delta = 0.001\ d \tag{5.14}$$

is used. Because the slot opening is narrow compared with the air gap, the Carter factor will be 1. The outer diameter of the stator and the approximate total length of the stator, including the end windings, are

$$d_{se} = d + 2\ h_s + 2\ h_{ys} \tag{5.15}$$

$$l_{tot} = l + 3\ W \tag{5.16}$$

respectively. (Error found after the defence of the thesis: The total winding length is overestimated, in equation 5.16 the total length is more likely to be approx. $l_{tot} = l + 2\ W$. This error will lead to a small overestimation of the copper weight and copper losses)

5.2.2 Magnetic Circuit

The stator yoke thickness, the rotor yoke thickness, and the stator tooth width are

$$h_{ys} = \frac{\hat{B}_{\delta 0}\ b_m\ l_e}{2\ \hat{B}_{ys}\ l_u} \tag{5.17}$$

$$h_{yr} = \frac{\hat{B}_{\delta 0}\ b_m\ l_e}{2\ \hat{B}_{yr}\ l} \tag{5.18}$$

$$b_d = \frac{\hat{B}_{\delta 0}\ \tau\ l_e}{\hat{B}_{d0}\ l_u} \tag{5.19}$$

respectively, where $\hat{B}_{\delta 0}$ is the no-load peak air gap flux density and $\hat{B}_{d0}$ the no-load peak teeth flux density.

The mmf:s of the iron core can be calculated from the magnetization curves for the stator and rotor core materials, i.e., $H_s(B)$ and $H_r(B)$. In the stator yoke the mmf needed for the magnetic flux between two poles can be approximated as

$$\hat{v}_{ys} = c\ \left(\tau_p + \frac{\pi\ (h_s + 0.5\ h_{ys})}{p}\right)\ H_s(\hat{B}_{ys}) \tag{5.20}$$

where c takes into account the variation of the field strength in the yoke. For the stator, c is assumed to be 0.5.

The mmf needed for the teeth can be expressed approximately as

$$\hat{v}_d = H_s(\hat{B}_{d0})\ (h_{s3} + 0.5\ h_{s2}) + H_s(\hat{B}_{\delta})\ (0.5\ h_{s2} + h_{s1}) \tag{5.21}$$

The mmf of the rotor yoke is

$$\hat{v}_{yr} = c\ \left(\tau_p - \frac{\pi\ (\delta + h_m + 0.5\ h_{yr})}{p}\right)\ H_r(\hat{B}_{yr}) \tag{5.22}$$

where c is assumed to be 0.5 for the rotor. Because h_m is included in this expression, the required magnet height has to be calculated by iteration. The required magnet height can be calculated analytically by replacing h_m with $2\ \delta$ in equation (5.22). This causes an error in the order of 1 % in $\hat{v}_{yr}$.

The mmf drops of the magnet and the air gap are

$$\hat{v}_m = h_m\ \frac{\hat{B}_{\delta 0}}{\mu_m\ \mu_0} \tag{5.23}$$

$$\hat{v}_{\delta} = \delta_{ef}\ \frac{\hat{B}_{\delta 0}}{\mu_0} \tag{5.24}$$

respectively. μ_m is the relative permeability of the permanent magnet material.

The sum of the mmf:s around the magnetic circuit of two poles is zero

$$2 H_c h_m - \hat{V}_{ys} - \hat{V}_{yr} - 2 \hat{V}_d - 2 \hat{V}_\delta - 2 \hat{V}_m = 0 \tag{5.25}$$

where H_c is the coercitivity of the permanent-magnet material. The needed magnet height can now be calculated from Equations (5.23) and (5.25)

$$h_m = \frac{0.5 \hat{V}_{ys} + 0.5 \hat{V}_{yr} + \hat{V}_d + \hat{V}_\delta}{H_c - \frac{\hat{B}_{\delta 0}}{\mu_m \mu_0}} \tag{5.26}$$

The flux density wave of a permanent magnet generator with uniform air gap and surface magnets is ideally square-shaped. Due to fringing effects, the real shape is smoother. Since the winding is a full-pitch winding, the harmonics of the flux wave result in rather large voltage harmonics. The voltage harmonics can contribute to the active power produced by the generator if the armature current is non sinusoidal. Usually the contribution from the harmonics is very small, thus, only the fundamental components of the flux density wave and the voltage are considered in the following calculations.

The shape of the flux density wave in the air gap depends mainly on the magnet width, the pole pitch, the air gap and the magnet height. The shape of the flux wave with a smooth stator surface was calculated by the finite element method for several combinations of air gap, magnet height and pole pitch, including combinations more extreme than what will occur in the direct-driven generators in this thesis. In the calculations, the magnet width was kept at 0.7 times the pole pitch. The fundamental component was calculated from the air gap flux wave. The analysis showed that the approximate relation

$$B_{\delta(1)} = \hat{B}_{\delta 0} \left(0.81 - \frac{0.30 \ (h_m + \delta)}{\tau_p} \right) \tag{5.27}$$

for

$$\tau_p \geq 4 \ (h_m + \delta) \tag{5.28}$$

can model the RMS value of the fundamental flux density $B_{\delta(1)}$ within about 2 % of the values calculated with the finite element method.

5.2.3 Stator Inductance and Resistance

In order to calculate the output power of the generator, the inductance and resistance of the armature winding must be known. In the calculation of the tooth tip leakage inductance and magnetizing

inductance, the permanent magnets are assumed to have the same permeability as air.

The slot leakage inductance, tooth tip leakage inductance and end winding leakage inductance, for a winding without parallel branches, can be expressed as

$$L_{sl} = 2\ p\ q\ \mu_0\ l_e\ \lambda_{sl} \tag{5.29}$$

$$L_{tl} = 2\ p\ q\ \mu_0\ l_e\ \lambda_{tl} \tag{5.30}$$

$$L_b = 2\ p\ q\ \mu_0\ l_b\ \lambda_b \tag{5.31}$$

where λ_{sl}, λ_{tl} and λ_b are the specific permeance of the slot leakage, tooth-tip leakage and end winding leakage, respectively. For the proposed generator, with equal current in the upper and lower conductor in the slots, the average specific permeance of the slot leakage for the two coil sides in the slot can be expressed as (Richter 1951, p. 269-271)

$$\lambda_{sl} = \frac{2\ h_{Cu}}{3\ b_s} + \frac{3\ h_i}{2\ b_s} + \frac{h_{s1}}{b_{s1}} + \frac{h_{s2}}{b_s - b_{s1}}\ \ln\left(\frac{b_s}{b_{s1}}\right) \tag{5.32}$$

The specific permeance of the tooth tip leakage can be calculated by an approximate expression (Richter 1953, p. 90)

$$\lambda_{tl} = \frac{\delta + h_m}{b_{s1} + 0.8\ (\delta + h_m)} \tag{5.33}$$

The specific permeance of the end winding leakage has been determined experimentally for different winding types in (Richter 1953, p. 91–92). For this two-layer winding the specific permeance is approximately

$$\lambda_b = 0.25 \tag{5.34}$$

The magnetizing inductance is used to calculate the required reactive power. Therefore, the total inductance is important, including the flux harmonics caused by the stator winding. The single-phase magnetizing inductance, for the winding with one slot per pole and phase, can be expressed as

$$L_m = p\ \mu_0\ l_e\ \lambda_m \tag{5.35}$$

where the specific permeance of the single-phase magnetizing inductance is

$$\lambda_m = \frac{\tau_p}{2\ (\delta_{ef} + h_m)} \tag{5.36}$$

The expressions (5.35) and (5.36) for the single-phase magnetizing inductance are derived in Appendix A.

The magnetizing inductance used in an equivalent Y-phase circuit is not the single-phase inductance. Because of the mutual inductance between the three phase windings, the apparent inductance of the equivalent Y-phase is higher. The equivalent Y-phase magnetizing inductance is 4/3 times the value of equation (5.35). The factor 4/3 includes the total flux generated by the stator winding and it is derived in Appendix A. For sinusoidally distributed windings this factor is, instead, 3/2.

There is no mutual inductance between the slot leakage and tooth tip leakage inductances of the different phases, and the magnetic coupling between the end winding inductances is included in the empirical permeance coefficient λ_b. The equivalent Y-phase inductance of the armature, therefore, is

$$L_a = \frac{4}{3} L_m + L_{sl} + L_{tl} + L_b \tag{5.37}$$

and the total leakage inductance is

$$L_\sigma = L_{sl} + L_{tl} + L_b \tag{5.38}$$

Since the resistance is temperature-dependent, its value depends on the generator load and the ambient temperature. The skin effect can be neglected since the winding is made of stranded wire. A typical value of the stator per phase resistance at rated load and average ambient temperature is

$$R_a = \rho_{Cu}(\theta_{CuAv}) \frac{2\ p\ q\ (l + l_b)}{k_{Cu}\ 2\ h_{Cu}\ b_{Cu}} \tag{5.39}$$

where $\rho_{Cu}(\theta)$ is the resistivity of copper at the temperature θ and θ_{CuAv} is the winding temperature at rated load and average ambient temperature. The annual average temperature in the southern part of Sweden is about 8˚C. Since the maximum ambient temperature is 40˚C and the maximum winding temperature according to the specification 130˚C, the temperature of the winding at rated load and average ambient temperature is

$$\theta_{CuAv} = 98^\circ C \tag{5.40}$$

5.2.4 Material Volume and Weight

In this section the material consumption for the active parts of the generator is calculated. The symbol ρ here is the density of the materials, not the resistivity.

The volumes of the different materials are calculated and multiplied by the specific weight of the material to find the material weight for the

windings m_{Cu}, stator yoke m_{Feys}, stator teeth m_{Fed}, rotor yoke m_{Feyr} and magnets m_m:

$$V_{Cu} = 2\,(l + l_b)\,Q\;\; h_{Cu}\;\; b_{Cu}\;\; k_{Cu} \tag{5.41}$$

$$m_{Cu} = \rho_{Cu}\; V_{Cu} \tag{5.42}$$

$$V_{Feys} = l_u\;\pi\;(d + 2\,h_s + h_{ys})\;h_{ys} \tag{5.43}$$

$$m_{Feys} = \rho_{Fe}\;\; V_{Feys} \tag{5.44}$$

$$V_{Fed} = l_u\;\; Q\;\left(b_d\,h_{s3} + \frac{(\tau - b_{s1}) + b_d}{2}\;\; h_{s2} + (\tau - b_{s1})\,h_{s1}\right) \tag{5.45}$$

$$m_{Fed} = \rho_{Fe}\;\; V_{Fed} \tag{5.46}$$

$$V_{Feyr} = l\;\;\pi\;\;(d\; -\; 2\,\delta\; -\; 2\,h_m\; - h_{yr})\,h_{yr} \tag{5.47}$$

$$m_{Feyr} = \rho_{Fe}\;\; V_{Feyr} \tag{5.48}$$

$$V_m = 2\;\; p\;\; l\;\; b_m\;\; h_m \tag{5.49}$$

$$m_m = \rho_m\;\; V_m \tag{5.50}$$

where ρ_{Cu}, ρ_{Fe} and ρ_m are the density of copper, iron and permanent-magnets, respectively. The total weight of the active parts of the generator is

$$m_{tot} = m_{Cu} + m_{Feys} + m_{Fed} + m_{Feyr} + m_m \tag{5.51}$$

5.2.5 Losses

The copper losses at a winding temperature of θ_{Cu} can be calculated from the resistivity of the copper $\rho_{Cu}(\theta_{Cu})$, the rms current density J_s and the copper volume V_{Cu}:

$$P_{Cu}(\theta_{Cu}) = \rho_{Cu}(\theta_{Cu})\;\; J_s^{\,2}\;\; V_{Cu} \tag{5.52}$$

The copper losses will be higher if the ambient temperature is high and lower if it is low. The thermal design of the generator must be carried out at the maximum ambient temperature with the maximum value of the copper losses, while the losses for the average efficiency should instead be the typical values of the copper losses. Consequently, two values of the copper losses are calculated: the maximum copper losses P_{CuMax} at an ambient temperature of 40˚C; and the typical copper losses P_{CuAv} at an ambient temperature of 8˚C,

$$P_{CuMax} = P_{Cu}(\theta_{CuN}) \tag{5.53}$$

$$P_{CuAv} = P_{Cu}(\theta_{CuAv}) \tag{5.54}$$

The core losses have to be calculated for each part of the iron core. They are divided into hysteresis losses and eddy current losses. The core losses can be calculated from the iron manufacturers loss data only if the losses are multiplied by empirical loss factors for the hysteresis and eddy current losses, k_{Hy} and k_{Ft} (>1). These empirical factors depend on the difference between the test conditions and the conditions in a real machine and they have different values for the yoke and the teeth. The iron used for the stator yoke, 0.5 mm thick *Surahammar CK-30*, has the approximate specific hysteresis and eddy current losses

$$p_{\mathrm{Hy}} = 2.04 \text{ W/kg} \tag{5.55}$$

$$p_{\mathrm{Ft}} = 0.76 \text{ W/kg} \tag{5.56}$$

respectively, at 50 Hz and 1.5 T. The core losses in the stator yoke are

$$P_{\mathrm{Hyys}} = k_{\mathrm{Hyys}} \; m_{\mathrm{Feys}} \; p_{\mathrm{Hy}} \left(\frac{f}{50 \text{ Hz}}\right) \left(\frac{\hat{B}_{\mathrm{ys}}}{1.5 \text{ T}}\right)^2 \tag{5.57}$$

$$P_{\mathrm{Ftys}} = k_{\mathrm{Ftys}} \; m_{\mathrm{Feys}} \; p_{\mathrm{Ft}} \left(\frac{f}{50 \text{ Hz}}\right)^2 \left(\frac{\hat{B}_{\mathrm{ys}}}{1.5 \text{ T}}\right)^2 \tag{5.58}$$

The empirical loss factors are approximately

$$k_{\mathrm{Hyys}} = 2 \qquad k_{\mathrm{Ftys}} = 1.8 \tag{5.59}$$

for the yoke (Richter 1951, p. 213). The teeth losses are

$$P_{\mathrm{Hyd}} = k_{\mathrm{Hyd}} \; m_{\mathrm{Fed}} \; p_{\mathrm{Hy}} \left(\frac{f}{50 \text{ Hz}}\right) \left(\frac{\hat{B}_{\mathrm{d0}}}{1.5 \text{ T}}\right)^2 \tag{5.60}$$

$$P_{\mathrm{Ftd}} = k_{\mathrm{Ftd}} \; m_{\mathrm{Fed}} \; p_{\mathrm{Ft}} \left(\frac{f}{50 \text{ Hz}}\right)^2 \left(\frac{\hat{B}_{\mathrm{d0}}}{1.5 \text{ T}}\right)^2 \tag{5.61}$$

The empirical loss factor for the hysteresis losses in the teeth is approximately (Richter 1951, p. 213)

$$k_{\mathrm{Hyd}} = 1.2 \tag{5.62}$$

Because the flux wave is square-shaped, the eddy current losses in the teeth are higher than for sinusoidal flux waves. Therefore, the eddy current loss factor of 1.5, given by Richter (1951, p. 213), is increased to

$$k_{\mathrm{Ftd}} = 2.5 \tag{5.63}$$

It is assumed that the flux density in the iron, and, thereby, the core losses, at rated load are the same as at no-load. For a direct-driven wind turbine generator, connected to a forced-commutated rectifier that keeps the armature voltage constant, the core losses were found to be rather independent of load by Lampola et al. (1996b).

The core losses in the rotor yoke are small because the main flux is constant in the rotor. The major rotor losses are the eddy current losses in the magnets due to flux harmonics. The flux harmonics originate both from the no-load flux harmonics caused by the stator slots and the flux harmonics caused by the armature currents. The magnet losses are reduced by using small magnets to build a complete magnet pole. The magnet losses can be estimated by time stepping FEM calculations and the losses are assumed to have a constant loss density at the magnet surface. The magnet losses, therefore, can be expressed as

$$P_{\mathrm{Ftm}} = p_{\mathrm{Ftm}}\ 2\ p\ b_{\mathrm{m}}\ l \tag{5.64}$$

This estimation of the magnet losses is very rough. However, since the magnet losses are important mainly for the magnet temperature, the error will not be very important. In Section 5.4.2, it is shown that the magnet temperature is only to a minor extent determined by the magnet losses. In a paper by Lampola et al. (1996b) the specific rotor losses of the generator are about 100 W/m^2 at rated load. For the proposed generator, which is similar to the one investigated by Lampola et al. (1996b), the specific losses are assumed to be

$$p_{\mathrm{Ftm}} = 300\ \mathrm{W/m^2} \tag{5.65}$$

because of higher current loading.

Additional losses (stray load losses) in synchronous generators consist, according to Chalmers (1965), of losses due to slot leakage flux, losses due to end leakage flux, short-circuit iron losses due to the armature mmf and rotor pole face losses. In the proposed generator the winding is made of stranded wire, which eliminates eddy current losses due to slot leakage. The rotor surface losses P_{Ftm} are dealt with separately and, thus, are not included in the additional losses in these calculations. The rest of the additional losses are mainly core losses. They are at rated load assumed to be about 20 % of the core losses at no load, i.e.,

$$P_{\mathrm{ad}} = 0.2\ (P_{\mathrm{Hyys}} + P_{\mathrm{Ftys}} + P_{\mathrm{Hyd}} + P_{\mathrm{Ftd}}) \tag{5.66}$$

The additional losses are assumed to be proportional to the square of the armature current. In the thermal calculations, the additional losses are assumed to be located in the stator tooth tips.

Friction and windage losses are caused by the losses in the generator bearings, the windage losses of the rotor and the radial fan on the rotor used to circulate the internal air. The bearing braking torque is not determined so much by the generator design as by the loading from the turbine. It is assumed to be 0.5 % of the rated torque and to be independent of the speed. The losses of the radial fans can be calculated approximately and they are found to be very small, less than 100 W for a 500 kW

generator. Because of the low air gap speed, the windage losses are neglected. The total friction and windage losses at rated speed are assumed to be

$$P_{\mu} = 0.005\, P_{N} \tag{5.67}$$

The power of the external cooling fans, blowing air through the cooling ducts at the outer surface of the stator yoke, are not included in this calculation. The total losses at rated load can now be calculated as

$$P_{lossMax} = P_{CuMax} + P_{Ftys} + P_{Hyys} + P_{Ftd} + P_{Hyd} + P_{Ftm} + P_{ad} + P_{\mu} \tag{5.68}$$

The average losses can be calculated by using the average loss factors derived in Chapter 3:

$$P_{lossAv} = k_{dCu}\,(P_{CuAv} + P_{ad}) + k_{dFt}\,(P_{Ftys} + P_{Ftd} + P_{Ftm}) + \\ + k_{dHy}\,(P_{Hyys} + P_{Hyd}) + k_{d\mu}\,P_{\mu} \tag{5.69}$$

5.2.6 Voltage, Power and Efficiency

The induced fundamental no-load armature phase voltage is

$$E_{p} = 2\,p\;q\;k_{w(1)}\;B_{\delta(1)}\;l_{e}\;v_{\delta} \tag{5.70}$$

where v_{δ} is the velocity of the flux wave in the air gap, given by

$$v_{\delta} = \pi\;d\;n_{N} \tag{5.71}$$

and $k_{w(1)}$ is the winding factor for the fundamental flux density wave. Because the winding is a full-pitch winding, the winding factor $k_{w(1)}$ is 1. The generator phase voltage is at rated speed controlled by the forced-commutated rectifier to be equal to the no-load phase emf

$$U_{apN} = E_{p} \tag{5.72}$$

The rated rms phase current is

$$I_{aN} = J_{s}\;2\,h_{Cu}\;b_{Cu}\;k_{Cu} \tag{5.73}$$

where k_{Cu} is the fill factor of copper inside the stranded coils, excluding the coil insulation, equal to 0.8. The phase current from the rectifier will include harmonics and, therefore, the fundamental component is lower than the total rms current. The rms value of the fundamental component is assumed to be 98 % of the total rms value of the armature current, i.e.,

$$I_{(1)} = 0.98\, I_{aN} \tag{5.74}$$

From the rated voltage, rated current and the current phase angle, the rated electrical output power can be calculated as

$$P_{aN} = 3\ U_{apN}\ I_{(1)}\ \cos(\varphi_N) \tag{5.75}$$

where, according to (3.25)

$$\cos(\varphi_N) = \sqrt{1 - \left(\frac{I_{(1)}\ 2\ \pi\ f_N\ L_a}{2\ U_{apN}}\right)^2} \tag{5.76}$$

The rated mechanical shaft power can now be calculated from the electrical output power and the losses, i.e.,

$$P_N = P_{aN} + P_{lossMax} \tag{5.77}$$

The efficiency at rated load is

$$\eta_N = \frac{P_{aN}}{P_N} \tag{5.78}$$

By using the average factor for the turbine power, derived in Chapter 3, the average input power can be calculated as

$$P_{Av} = P_N\ k_t \tag{5.79}$$

The average efficiency is

$$\eta_{Av} = 1 - \frac{P_{lossAv}}{P_{Av}} \tag{5.80}$$

The armature reactance is in this thesis expressed in per unit. The per unit base values used are

$$U_{base} = U_{apN} \tag{5.81}$$

$$I_{base} = I_{aN} \tag{5.82}$$

5.2.7 Thermal Model and Temperature Rise

The aim of the thermal calculations is to find the maximum temperature of the stator winding and the magnets. The generator is represented by a lumped-parameter thermal network model.

The thermal model represents the generator by the circuit shown in Figure 5.3. The temperature differences in the circumferential direction of the generator are neglected. The generator cooling is symmetrical in the axial direction and, therefore, the two end windings of a coil are modelled as one. The thermal network model is derived in Appendix B.

The losses in the thermal model are copper losses in the stator winding, core losses in the stator teeth and yoke, eddy current losses in the magnets and additional losses. Friction and windage losses are assumed not to increase the temperature rise of the winding and magnets. Thus, they are neglected in this thermal model. The copper losses are divided into losses in the end windings, losses in the bottom-layer coil sides in the slots, and

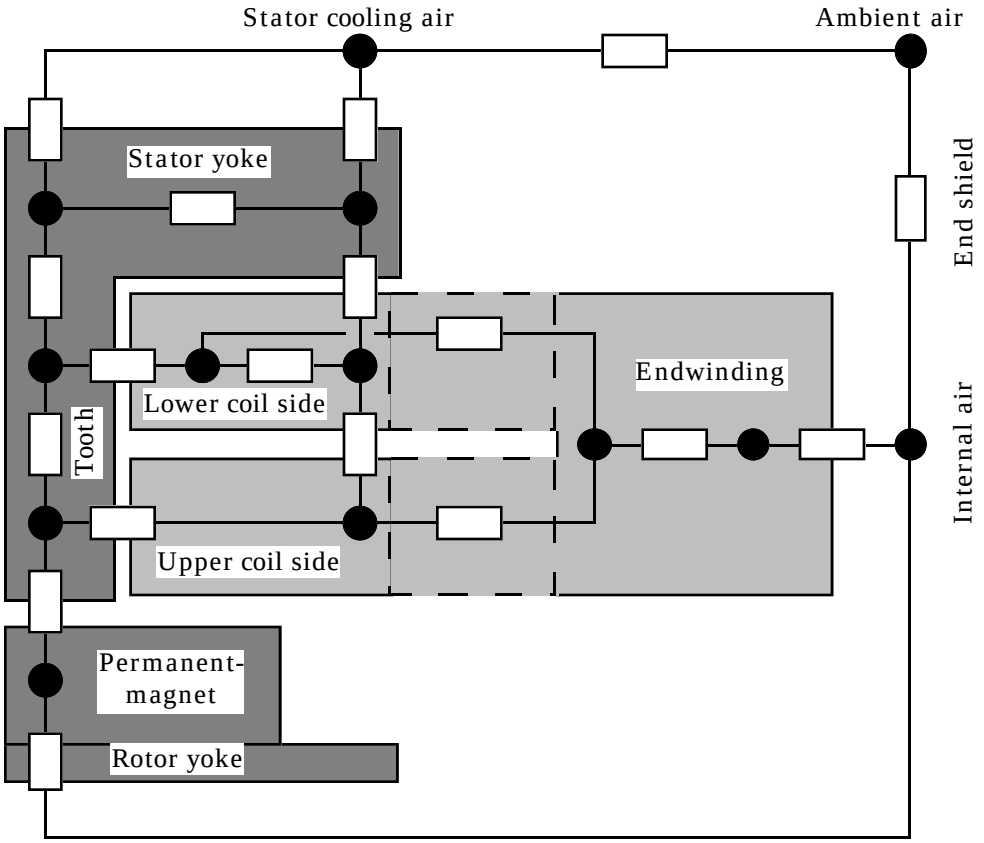

Figure 5.3 The thermal model based on one slot pitch, one rotor pole, one coil, internal air and end shield.

losses in the top-layer coil sides. The magnet losses are assumed to be distributed homogenously in the magnets, while additional losses are assumed to be located in the tooth tip. The temperature rise of the cooling air along the cooling ducts at the outer surface of the stator yoke is included in the thermal model as an equivalent thermal resistance.

Because the major part of the losses is cooled at the outer surface of the stator yoke, the maximum winding temperature is the end winding temperature.

5.2.8 Irreversible Demagnetization

Irreversible demagnetization can be a problem in permanent-magnet generators. The magnets will be demagnetized if the flux density in them is lower than a minimum flux density of $B_{\min}$. The high-temperature NdFeB material used in these calculations can withstand at least 0 T at the assumed maximum operating temperature of 120˚C. The minimum flux density may in many cases also be a negative value, usually at low temperatures.

Of course, the magnets must not be demagnetized by the rated current and it is also important that they can withstand the most probable faults, for instance, short circuits. During normal operation the armature winding generates a peak flux density in the air gap and magnet that depends on the peak value of the stator mmf $\hat{\hat{v}}_s$ and the magnetic air gap. It is given by

$$\hat{\hat{B}}_s = \mu_0 \frac{\hat{\hat{v}}_s}{\delta + h_m/\mu_m} \tag{5.83}$$

For the proposed generator type with three phases and one slot per pole and phase, the peak mmf generated by the armature is the peak value of the current in one slot

$$\hat{\hat{v}}_s = \hat{I}_{aN} \tag{5.84}$$

To avoid demagnetization of the magnets, the stator must not generate a higher peak flux density $\hat{\hat{B}}_s$ than

$$\hat{\hat{B}}_s < \hat{\hat{B}}_{\delta 0} - B_{min} \tag{5.85}$$

Equation (5.85), however, does not take the risk of local demagnetization into account. The flux density may locally be lower than B_{min} because of, for instance, flux leakage at the magnet ends. The minimum flux density should be checked in the final design by a finite element calculation.

The risk of demagnetization at a short circuit at the generator terminals is discussed by Slemon (1992). For a generator with sinusoidally distributed windings there is no risk of demagnetization if the ratio between leakage inductance and magnetizing inductance is

$$\frac{L_\sigma}{L_m} > \frac{8 \sin(0.5\,\alpha_M)}{\pi\left(1 - \dfrac{B_{min}\,(\delta + h_m/\mu_m)}{B_r\ h_m/\mu_m}\right)} - 1 \tag{5.86}$$

where α_M is the magnet angle. For a generator with large resistance, the factor 8 can be changed to 4. The proposed type of generator does not have a sinusoidally distributed winding. Equation (5.86) is still used as an indication of the risk of demagnetization during short circuit. Since the minimum flux density here is zero and the magnet angle is 126˚, the expression becomes

$$\frac{L_\sigma}{L_m} > 1.27 \tag{5.87}$$

Because of the small pole pitch and the large air gap, demagnetization is generally not a problem in the proposed type of generator. This was verified by checking that the peak flux density generated by the stator winding is below the value in Equation (5.85) and that the leakage

inductance to magnetizing inductance ratio is larger than described by Equation (5.87).

If there is a risk of irreversible demagnetization, the risk can be eliminated by increasing the air gap and at the same time increasing the magnet height in such a way that the air gap flux density is unchanged. Then, the stator will generate lower flux density at rated current and the magnetizing inductance will be reduced. The reduced magnetizing inductance will also increase the possible peak power. Of course, the price for this change is increased cost for the magnets.

5.3 Calculation Procedure

The design method is implemented in the computer program Matematica (Version 2.1 for Machintosh), which facilitates easy use of symbolic mathematics. The generator design starts by executing all the definitions in Section 5.2 and Appendix B. Once that is done, the program can calculate any of the defined quantities if only the design variables are given values. In this thesis seven variables are used. If, for example, the average efficiency of a generator is to be calculated, the seven design variables are given their values and the definition for the average efficiency is executed giving the value of the average efficiency of that particular generator. The active weight of the same generator can now be calculated simply by executing that definition, without changing the variable values. A new generator can be calculated by changing one or more of the variables and executing the definitions again.

The rated power and winding temperature of a generator does not automatically fulfil the specification, with arbitrary values of the seven design variables. The proper winding temperature and rated power is achieved by adjusting two variables iteratively. In this thesis, the stator length and winding current density are used to reach a feasible generator design. Before the iteration, these variables have to have starting values. The variables are adjusted until the error of the winding temperature is smaller than 0.1 K and the error of the rated power is smaller than 0.1 W. During the optimization of the generator, the starting values for the length and current density are the final values of the generator designed in the previous step in the optimization.

In the way that the design calculations are carried out, only the definitions of the quantities which are sought are executed. There is no program which has to be run through completely for each new generator. During the optimization procedure only the cost function is executed. The other definitions will only be used once the performance and data of the optimized generator are calculated.

Generator optimization is made using a numerical Matematica function which finds a minimum of a multi-variable function. The generator is optimized regarding air gap diameter, pole pitch, air gap flux density, teeth flux density, slot height, and the temperature of the windings. The search is unconstrained and if any optimum variables are outside the allowed limits, the optimization is repeated with a fixed value of that variable. In practice, it is only the winding temperature that sometimes has an optimum value not allowed by the specification.

5.4 Test of the Design Method

5.4.1 Comparison with Finite Element Calculations

To verify and test the design method, a generator with an air gap diameter of 2.5 m, a stator length of 0.5 m and a rated speed of 30 rpm was designed. The generator is a rather typical 550 kW generator, but it was not optimized. The variables used in the calculations are shown in Table 5.2.

To verify some of the analytical calculation methods, the performance of the test generator was also calculated by the finite element method. The finite element calculations were both steady state calculations and time-stepping calculations with a rotation of the rotor. A program called "FCSMEKB" which has originally been developed at Helsinki University of Technology was used. The program has been modified for permanent magnet machines by Antero Arkkio and Jorma Luomi at Chalmers University of Technology. A comparison of the analytical design method and the finite element calculations is shown in Table 5.3.

The voltage and the rated torque calculated with the analytical model correspond well to the results of the finite element calculations. The

Table 5.2 The variable values of the test generator

Variable		Value
Air gap diameter	d	2.5 m
Stator length	l	0.5 m
Pole pitch	τ_p	60.4 mm
Slot height	h_s	55 mm
Current density	J_s	4.27 A/mm^2
Peak air gap flux density	$\hat{B}_{\delta 0}$	0.72 T
Peak tooth flux density	$\hat{B}_{d0}$	1.63 T

Table 5.3 Comparison of the analytical design calculations and FEM calculations for the test generator.

	Analytical method	FEM
Open circuit fundamental voltage	246 V	240 V
Torque at rated current	175 kNm	177 kNm
Reactances (in d- and q-axis)	x_a = 0.97 p.u. ($x_q = x_d = x_a$ assumed)	x_d = 0.88 p.u. x_q = 0.82 p.u.
Stator core losses	2982 W	2314 W
Magnet losses	824 W	311 W
Rotor yoke losses	included in magnet losses	93 W
No-load torque ripple	not calculated	± 0.8 kNm

analytically calculated inductance is 10% higher than predicted by the finite element calculations, but the results cannot be expected to be much better since there are simplifications in the inductance calculation methods. The analytical method is expected to overestimate the inductance since the mmf of the stator core was not included in the inductance calculations. The core losses are lower for the finite element calculations than for the analytical method. However, the analytical model includes empirical corrections for non-ideal manufacturing which the finite element calculations do not. The magnet losses of the analytical model are based on a rough estimation, and the finite element calculation shows that they are at least not underestimated for this generator. Torque ripple has not been included in the design calculations because the semi-closed slots will keep the torque ripple low. The finite element calculations verify this assumption.

5.4.2 Test of Thermal Model

Since the generator has not been built yet, the thermal model cannot be verified by measurements. One way of showing how the errors of the model can influence the design of the generator is to vary the uncertain parameters of the thermal model to see what effect they have on the winding temperature and magnet temperature. First the temperatures of the test generator were calculated using the normal values of the parameters in the thermal model. The calculations were made for the test generator described in Section 5.4.1. and the results are shown in Table 5.4.

The influence of the uncertain thermal parameters on the overall generator design was tested by changing the parameter values to twice and to half the nominal values. For each new parameter value, the temperature of the windings and the magnets were calculated. The calculations with a parameter value causing a temperature increase were selected (either twice or half of the nominal parameter value). The resulting temperature increases in the windings and the magnets can be found in Figure 5.4. The parameters that were changed are: heat transfer coefficients at the outer surface of the stator yoke, in the air gap, at the end shields, at the end windings and at the inner surface of the rotor yoke; the thermal conductivity of the slot insulation; and the losses in the magnets. It is not the thermal conductivity of the slot insulation that is the uncertain parameter, but rather the thickness of the insulation. However, the thickness cannot be changed in the calculations because that will increase the conductor cross-section and, therefore, increase the rated power and the copper losses of the generator. Changing the thermal conductivity instead will have the same effect on the heat transfer as changing the insulation thickness, although the generator performance will not be changed.

Figure 5.4 shows that the winding temperature is very sensitive to the heat transfer coefficient at the outer surface of the stator yoke. The only other parameter with an important influence on the winding temperature is the thermal conductivity of the slot insulation. The reason for this is that almost all the losses in the windings are cooled through the slot insulation and the stator yoke.

The magnet temperature is also very sensitive to the thermal resistance between the stator yoke and the cooling air. The reason is that good thermal contact between the stator and the rotor makes the magnet

Table 5.4 The calculated temperatures at rated load in the test generator.

Ambient temperature	40 ˚C
Stator cooling air	50 ˚C
Stator yoke	98.6˚C and 99.3 ˚C
Lower teeth	107 ˚C
Upper teeth	113 ˚C
Lower coil side	115 ˚C
Upper coil side	121 ˚C
End winding	122 ˚C
Magnets	96 ˚C
Internal air	77 ˚C

temperature almost as high as the stator teeth temperature. An increase in stator teeth temperature will cause an almost as large increase in magnet temperature. Also the thermal resistance at the end shields and the inner surface of the rotor yoke, as well as the losses in the magnets, influence the magnet temperature. It is important to note that the magnet losses do not influence the magnet temperature very much. The temperature of the magnets will be a little lower than the temperature of the stator teeth even if the magnet losses differ greatly from what has been estimated. Since the winding is not allowed to be warmer than 130˚C and the teeth are about 10 ˚C colder, it must always be possible to keep the magnet temperature below 120 ˚C, which is the limit in the specification.

The winding and magnet temperatures can become very high if the stator cooling is not as efficient as assumed. However, the assumed heat transfer coefficient at the outer surface of the stator yoke is not higher than what is achieved in a normal induction machine (Kylander 1993, p. 66).

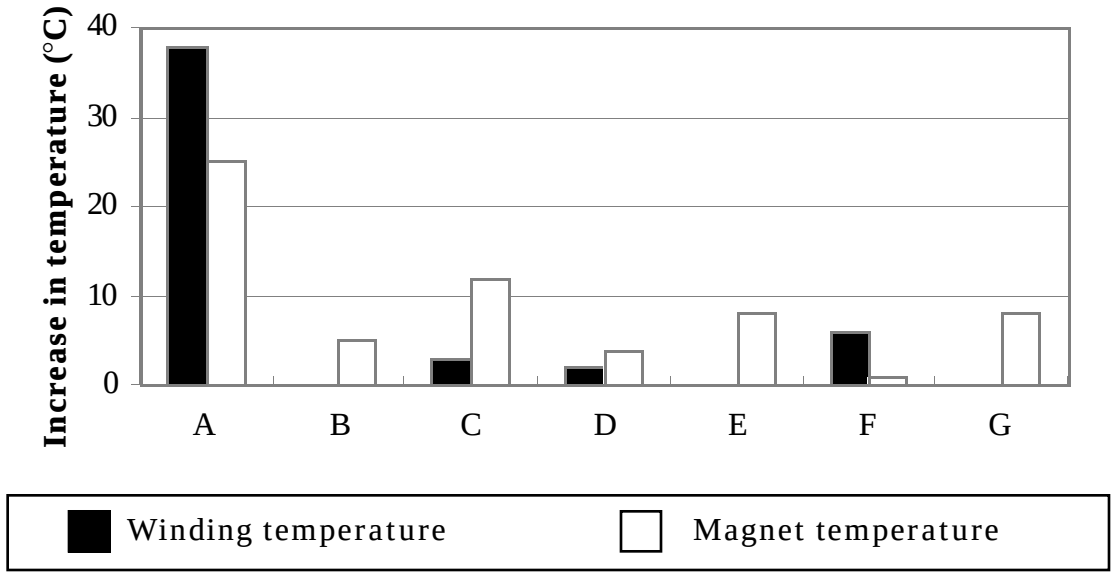

Figure 5.4 The increase in the temperatures of the windings and magnets as different thermal parameters are doubled and halved. The changed parameters are:
A) Heat transfer coefficient at the stator yoke;
B) Heat transfer coefficient in the air gap;
C) Heat transfer coefficient at the end shields;
D) Heat transfer coefficient at the end windings;
E) Heat transfer coefficient at the rotor yoke;
F) Thermal conductivity of the slot insulation and ;
G) Losses in the magnets.

6 Generator Optimization

In this chapter, the generator design method is used together with a numerical optimization method to investigate the optimization of a generator of the proposed type. A 500 kW generator has been choosen since that is a normal size for today's commercial wind energy converters.

In Section 6.1, five 500 kW generators are optimized. The first generator is optimized using the nominal cost function, and that generator will be used as a reference design throughout this chapter. Three other generators are also optimized with the nominal cost function, but they were required to produce either 50 Hz or 200 % peak power, or both 50 Hz and 200 % peak power. The fifth generator is optimized using a cost function with the losses at rated load instead of average losses.

The influence of different variables on the generator design is investigated in Section 6.2 and the influence of the cost function in Section 6.3. The optimum diameter of the generator is especially interesting since the problems of manufacturing and transportation can be expected to depend on the generator diameter to a great extent. In Section 6.4, the optimum diameter is discussed in detail. In Section 6.5 the typical size, average efficiency and active weight of a 500 kW generator of the proposed type are summarized.

6.1 Optimum 500 kW Generators

6.1.1 Optimized Reference Generator

In this section, a 500 kW generator is optimized using the nominal values of the cost function parameters. The cost of the average losses is 6000 ECU/kW and the cost of iron, copper and permanent magnets are 4, 6 and 100 ECU/kg, respectively. The reference diameter of the structure is 2 m, the reference length 1 m, the cost of the reference structure is 20 000 ECU and the exponent for the structure cost is 3. A medium wind speed site is assumed, i.e., the average loss factors for a site with an average wind speed of 6.8 m/s are used. The rated speed of the 500 kW generator is 32 rpm and the rated torque is 148 kNm. Data for the optimized reference generator are presented in Table 6.1.

The optimum diameter of the generator is 2.15 m and the stator length is 0.55 m. Both the flux density in the air gap and the teeth have normal optimum values and the optimum winding temperature is lower than what is allowed in the specification. A higher winding temperature would lead to an uneconomically low efficiency. The frequency of the optimized

Table 6.1 Data of the optimized 500 kW reference generator.

Ratings:

Rated torque	T_N	148 kNm
Rated speed	n_N	32 rpm

Optimized variables:

Air gap diameter	d	2.15 m
Slot height	h_s	64.0 mm
Pole pitch	τ_p	68.3 mm
Air gap flux den.	$\hat{B}_{\delta 0}$	0.77 T
Teeth flux dens.	$\hat{B}_{d0}$	1.64 T
Winding temp.	Θ_{CuN}	107 ˚C

Electrical data:

Frequency	f	26.5 Hz
Reactance	x_a	0.95 p.u.
Current density	J_s	3.60 A/mm^2
Current in a slot	I_{aN}	1540 A

Losses, efficiency:

Copper losses	P_{CuN}	22700 W
Stator yoke losses	P_{Feys}	760 W
Stator teeth losses	P_{Fed}	1950 W
Magnet losses	P_{Ftm}	780 W
Additional losses	P_{ad}	540 W
Frict. & windage	P_{μ}	2500 W
Average losses	P_{dAv}	6430 W
Average eff.	η_{Av}	94.9 %
Full-load eff.	η_N	94.2 %

Geometry:

Stator length	l	0.55 m
Tooth width	b_d	11.1 mm
Slot width	b_s	11.7 mm
Air gap	δ	2.15 mm
Magnet height	h_m	6.3 mm
Stator yoke height	h_{ys}	15.9 mm
Rotor yoke height	h_{yr}	15.4 mm
End wind. length	l_b	137 mm
Conductor width	b_{Cu}	9.7 mm
Conductor height	h_{Cu}	27.5 mm

Weights:

Magnet weight	m_M	124 kg
Copper weight	m_{Cu}	779 kg
Stator yoke w.	m_{Fes}	467 kg
Teeth weight	m_{Fed}	888 kg
Rotor yoke weight	m_{Fer}	431 kg
Total active w.	m_{tot}	2690 kg

Miscellaneous:

Magnet temp.	Θ_m	90 ˚C
Induct. ratio [1)]	–	1.7
Stator flux dens.	$\hat{B}_s$	0.33 T
Cost of losses	C_d	38500 ECU
Cost of active part	C_{act}	24200 ECU
Cost of structure	C_{str}	16000 ECU

1) Leakage inductance divided by magnetizing inductance.

generator is only 26.5 Hz and the reactance is 0.95 p.u., which is a high reactance value compared with grid-connected generators. Such a high reactance is possible only because the generator is not required to produce a high peak torque.

The weights of the stator and rotor yokes are low. From a mechanical point of view, the stator yoke may have to be made thicker than 16 mm to be stiff enough. The magnet weight is 124 kg, which means that the magnets will cost about 12 400 ECU. This cost is about the same as the cost for 2 kW of average losses.

The magnet temperature and the risk of demagnetization have not been included in the optimization and, thus, have to be checked. As predicted, the magnet temperature is lower than the limit, and the peak flux density $\hat{B}_s$ in the air gap caused by the stator winding at rated current is only 0.4 times the flux density generated by the permanent magnets. Therefore, the magnets will not be demagnetized during normal operation. The ratio of the leakage inductance to the magnetizing inductance is 1.7, which is enough to avoid demagnetization during a sudden short circuit according to equation (5.87).

Both the losses at rated load and the average losses of the generator are illustrated in Figure 6.1. The copper losses totally dominate at rated load, but since the average copper losses for the chosen wind energy converter site are only 14 % of the ones at rated load, the copper losses are still only half of the average losses. The other loss components are, on the average, approximately half of their rated load values. Since the total average losses are 22 % of the total losses at rated load and the average power produced by the turbine is 25 % of the rated power, the average efficiency is higher than the efficiency at rated load. The average efficiency is 94.9 %, while the efficiency at rated load is 94.2 %. For conventional, grid-connected, four- or six-pole wind energy converter generators, the average efficiency is lower than the efficiency at rated load.

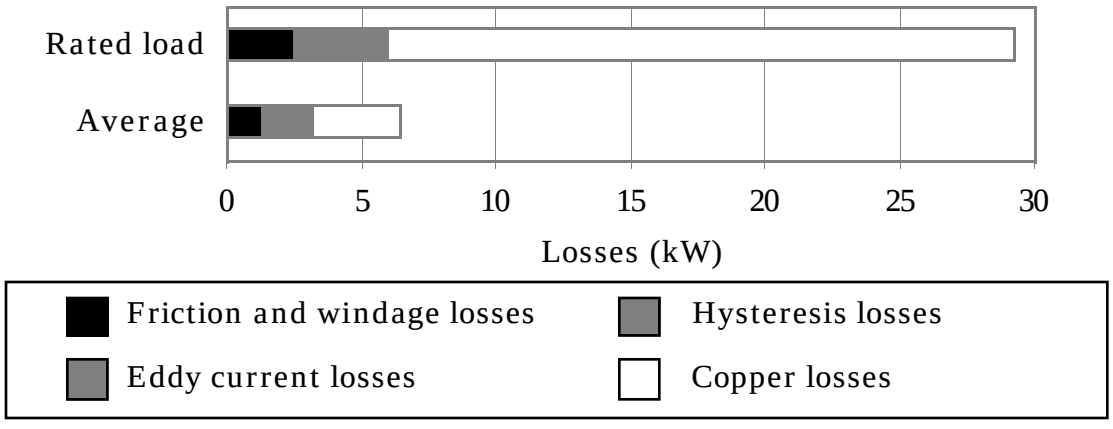

Figure 6.1 The losses of the optimized 500 kW generator at rated load and average losses.

6.1.2 Optimized Generators for 50 Hz and 200 % Peak Power

The reference generator is designed for a variable-speed, pitch-controlled wind turbine and requires neither any specified frequency, nor a peak power higher than the rated power. In this section, a generator for direct grid-connection is designed (for a pitch- or stall-controlled wind turbine), as well as a generator for stall-controlled, variable-speed wind turbines. A generator which is direct connected to the grid has to produce a frequency of 50 Hz and, for stability reasons, it must have a peak power of about 200 % of the rated power. A stall-controlled wind energy converter with variable speed also requires about 200 % peak power, to control the turbine speed, but does not require a frequency of 50 Hz.

A generator design with a frequency of 50 Hz is achieved by keeping the number of pole pairs constant, which means that the pole pitch is no longer a free variable. A peak power of 200 % is assured by limiting the allowed armature reactance to be no more than 0.52 p.u. This maximum value of the armature reactance acts as a second limit for the current density, beside the maximum winding temperature.

In Table 6.2, the different generator designs are compared with the reference generator. To make the comparison more complete, a 50 Hz generator without any required peak power is also included in the comparison. The generators are compared regarding average efficiency, active weight and size. The generator size is, here, expressed as the volume of the rotor.

The comparison shows that a demand for 200 % peak power leads to about a 25 % larger rotor volume than for the reference generator, while the

Table 6.2 Generators designed with or without requirement of 200 % of the rated power and requirement of 50 Hz.

Frequency (Hz)	Peak power to rated power (%)	Air gap diameter (m)	Stator length (m)	Average efficiency (%)	Active weight (kg)	Rotor volume (m^3)
26.5	120	2.15	0.55	94.9	2690	2.00
29.7	**200**	2.33	0.60	94.5	2401	2.56
50	124	2.39	0.56	93.6(1	1928	2.51
50	**200**	2.51	0.60	93.4(1	1795	2.97

(1 The average efficiency is calculated for variable speed operation. At constant speed the average efficiency will be lower.

average efficiency is 0.4 % lower and the active weight 10 % lower. The lower active weight depends mainly on the increased air gap diameter. Requiring 50 Hz frequency of a generator also leads to about a 25 % larger rotor volume than of the reference generator. To keep the diameter low, the pole pitch has become only approximately 40 mm and, therefore, the slots are narrow. Narrow slots lead to a low copper fill factor and higher resistance. As a consequence, the average efficiency is 1.3 percent-units lower for the 50 Hz generator than for the reference generator. The active weight is almost 30 % lower than for the reference generator. About two thirds of the weight reduction is because of the reduced pole pitch, the other third because of increased air gap diameter.

A generator for direct grid-connection, both 50 Hz and 200 % peak power, will have about 50 % larger rotor volume than the reference generator. The active weight is about 30 % lower than for the reference generator partly because of the increased air gap diameter, partly because of reduced yoke thickness owing to a smaller pole pitch. The average efficiency is 1.5 percent-units lower than for the reference generator. More data of the direct grid-connected generator is presented in Table 6.3. No damper windings were included in this design, so the direct grid-connected generator has to be provided with mechanical damping of the type presented by Westlake et al. (1996). Damping by means of damper windings is possible only with a much larger generator diameter.

Table 6.3 Data of an optimized 500 kW generator for direct grid-connection. The frequency is 50 Hz and the peak power 200 % of the rated power.

Optimized variables:

Air gap diameter	d	2.51 m
Slot height	h_s	34.0 mm
Pole pitch	τ_p	42.2 mm
Air gap flux den.	$\hat{B}_{\delta 0}$	0.74 T
Teeth flux dens.	$\hat{B}_{d0}$	1.68 T
Winding temp.	Θ_{CuN}	108 ˚C

Efficiency:

Average eff.(1	η_{Av}	93.4 %
Full-load eff.	η_N	92.6 %

Electrical data:

Reactance	x_a	0.52 p.u.

Geometry:

Stator length	l	0.60 m
Tooth width	b_d	6.5 mm
Slot width	b_s	7.6 mm

Miscellaneous:

Cost of losses	C_d	49300 ECU
Cost of active part	C_{act}	22700 ECU
Cost of structure	C_{str}	25700 ECU

(1 The average efficiency is calculated for variable speed operation. At constant speed the average efficiency will be lower.

6.1.3 Optimization Using the Losses at Rated Load

Because the average factor for the copper losses is only 0.14 while the average factors for the core losses are about 0.50–0.60, a generator optimized with the average losses in the cost function can be expected to have high copper losses at rated load compared with the core losses. If the losses at rated load are used in the cost function, instead of the average losses, the optimum generator will have lower copper losses and higher core losses. The effect of using average losses in the cost function, instead of the losses at rated load, was tested by changing the cost function for the optimization. To make sure that the generator is comparable with the reference generator, the diameter was fixed at 2.15 m and the cost of the losses at rated load was adjusted until the average efficiency was 94.9 %, as it is for the reference generator. Data of a 500 kW generator, optimized using the losses at rated load in the cost function, are shown in Table 6.4.

The differences between this generator and the reference generator are rather small. The current density is 12 % lower, the slot 7 % higher and the stator 11 % longer than for the reference generator. The efficiency at rated load is 0.5 percent units higher. The cost of the active parts of the generator has increased slightly along with the cost of the structure.

Table 6.4 Data of a 500 kW generator optimized with the losses at rated load in the cost function.

Optimized variables:

Slot height	h_s	68.4 mm
Pole pitch	τ_p	57.9 mm
Air gap flux den.	$\hat{B}_\delta$	0.75 T
Teeth flux dens.	$\hat{B}_d$	1.64 T
Winding temp.	Θ_{CuN}	92 °C

Electrical data:

Reactance	x_a	0.94 p.u.
Current density	J_s	3.17 A/mm^2

Miscellaneous:

Cost of av. losses	C_d	38500 ECU
Cost of active part	C_{act}	25300 ECU
Cost of structure	C_{str}	20200 ECU

Geometry:

Air gap diameter	d	2.15 m
Stator length	l	0.61 m
Tooth width	b_d	9.2 mm
Slot width	b_s	10.1 mm

Losses, efficiency:

Copper losses	P_{CuN}	18700 W
Stator yoke losses	P_{Fevs}	842 W
Stator teeth losses	P_{Fed}	2760 W
Magnet losses	P_{Ftm}	861 W
Additional losses	P_{ad}	720 W
Frict. & windage	P_μ	2500 W
Average eff.	η_{Av}	94.9 %
Full-load eff.	η_N	94.7 %

The losses at rated load and the average losses for this generator and the reference generator are illustrated in Figure 6.2. The difference between the generator loss distributions is not very large. This low difference indicates that the very high copper losses of the reference generator are not only a consequence of the cost function, but also a natural loss distribution in this type of low-speed generator. Moreover, the efficiency curves for the two generators were calculated, using the *g*-functions from Chapter 3. The efficiency curves, plotted in Figure 6.3, are found to be rather similar, but with the peak efficiency at different powers.

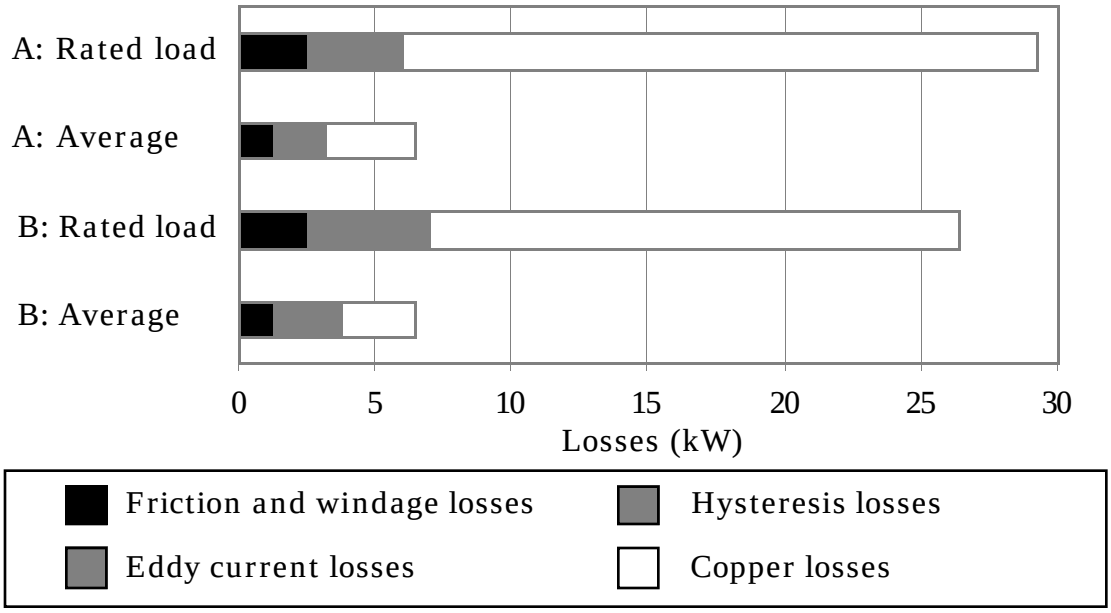

Figure 6.2 The losses of two generators with equal average efficiency: Generator A: Reference generator; Generator B: Optimized using the cost of the losses at rated load.

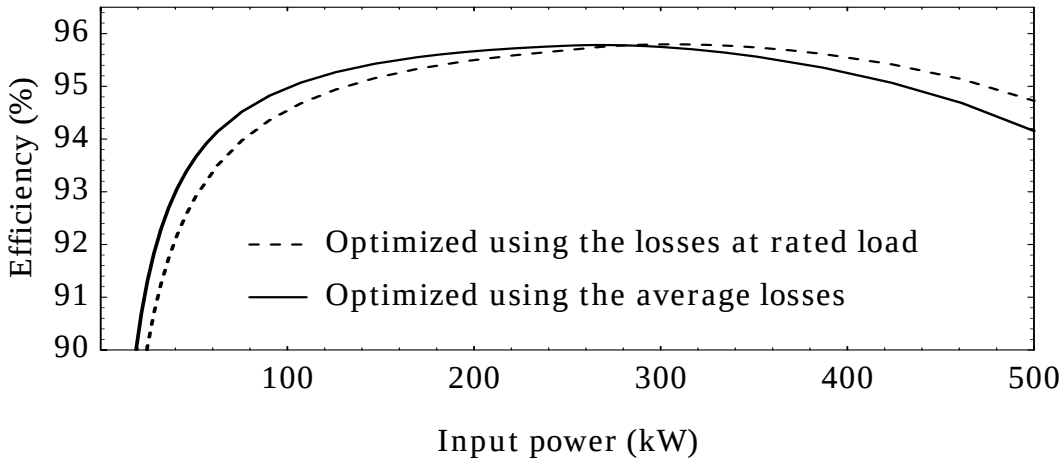

Figure 6.3 Efficiency curves of two generators. One is optimized with the losses at rated load in the cost function and one with the average losses. Both generators have equal average efficiency.

The generator optimized regarding average losses will be smaller and have a slightly lower total cost than if the losses at rated load are used. However, one reason to design a generator with high efficiency at rated load, even if the average efficiency is not improved, would be because the cooling system might be made simpler and cheaper.

6.2 Sensitivity to Variable Changes

In this section, the influence of six design variables on the stator length, the active weight, the losses and the cost function is investigated. The influence of a variable is tested by changing its value to 0.9 or 1.1 times the optimum value, while the rest of the variables are kept at their optimum values. A new generator is calculated for each variable that is changed. The generator is not optimized; only the stator length and current density are adjusted to get the right rated power and right winding temperature. The results are presented in Table 6.5.

The main result from this investigation is that the total cost of the generator is rather insensitive to changes in any of the design variables. This insensitivity indicates a flat minimum in the cost function. The flux densities in the air gap and the teeth have the highest influence on the total cost, but the total cost increases only by approximately 3 % as the flux densities are changed 10 %.

The pole pitch has almost no influence on the total cost of the generator. The active weight and the cost of the active parts increase as the pole pitch increases. However, the core losses decrease at the same time.

A 10 % change in the air gap diameter increases the total cost of the generator by approximately 1.5 %. As the diameter decreases, the stator length along with the cost of the active part increase. The copper losses increase with decreasing diameter while the core losses remain almost constant.

The slot height has very little effect on the total cost of the generator. A decrease in the slot height requires an increase in stator length because the current in a slot has to be decreased in order to maintain the original winding temperature. The copper losses increase as the slot height decreases. At the same time, however, the core losses decrease since the major part of the core losses are losses in the teeth. The total influence on the average losses is minor.

The air gap flux density has the largest influence on the total cost of the generator. If the flux density is reduced, the stator length has to be increased and both copper and core losses increase. The amount of permanent magnets is decreased as the flux density is decreased, leading to a lower cost for the active part of the generator. The influence of the

teeth flux density on the generator is similar to the influence of the air gap flux density, although the total cost is changed slightly less.

The winding temperature has a very low influence on the total cost. The influence on the copper losses is large, but while the copper losses increase much with increasing winding temperature the core losses decrease much, reducing the influence on the average losses. Decreased winding temperature requires a longer stator and, therefore, the cost of the active part of the generator increases.

Table 6.5 The influence of the design variables on the generator. The design variables are changed one by one while the rest have their optimum values. The changes are expressed in percent.

Changed variables	Stator length	Active weight	Copper losses	Core losses	Average losses	Cost of active part	Total cost
$\tau_p = 0.9\ \tau_{pOpt}$	+0	−5	+1	+9	+3	−2	+0
$\tau_p = 1.1\ \tau_{pOpt}$	+0	+5	−1	−6	−2	+3	+0
$d = 0.9\ d_{Opt}$	+23	+9	+8	+0	+4	+5	+2
$d = 1.1\ d_{Opt}$	−17	−7	−6	+0	−3	−4	+1
$h_s = 0.9\ h_{sOpt}$	+4	−3	+3	−2	+1	−1	+0
$h_s = 1.1\ h_{sOpt}$	−3	+4	−2	+2	−0	+2	+0
$\hat{B}_\delta = 0.9\ \hat{B}_{\delta Opt}$	+12	+6	+11	+4	+6	−4	+3
$\hat{B}_\delta = 1.1\ \hat{B}_{\delta Opt}$	−5	−0	−6	+2	−2	+15	+3
$\hat{B}_d = 0.9\ \hat{B}_{dOpt}$	+6	+5	+6	−1	+3	−1	+2
$\hat{B}_d = 1.1\ \hat{B}_{dOpt}$	−4	−2	−5	+2	−2	+14	+3
$\Theta_{CuN} = 0.9\ \Theta_{CuNOpt}$	+7	+6	−14	+7	−5	+7	+1
$\Theta_{CuN} = 1.1\ \Theta_{CuNOpt}$	−5	−5	+13	−5	+5	−5	+0
Reference generator	0.55 m	2690 kg	22700 W	3490 W	6420 W	24200 ECU	78700 ECU

6.3 Sensitivity to Cost Function Changes

The cost function used in this thesis is only a rough estimate of the real costs. Therefore, it is important to investigate how the cost function influences the generator design. In this section, the cost of losses, cost of iron and copper, cost of permanent magnets and the cost of the structure are changed to see how they influence the optimum generator.

6.3.1 Cost of Losses

The effect that the specific cost of losses has on the optimized 500 kW generator is investigated by changing the cost of average losses between 0, 10, 50, 100, 200 and 1000 % of the nominal value. The extreme values 0, 10 and 1000 % are, of course, not realistic. Nevertheless, they have been used to show more clearly which parameters are important for the average efficiency. Data of the generator optimized with different specific cost of losses are shown in Table 6.6. With increasing specific cost of losses the diameter increases slightly, the active weight increases considerably and, of course, the average efficiency increases. The average losses with no cost of the losses are 8 percent-units and 3.5 percent-units at the highest cost of the losses. The increased efficiency is mainly reached by increasing the slot height and decreasing the current density. Thus, a higher efficiency causes a higher active weight. The efficiency increase is, to some extent, also reached by increasing the diameter. The air gap flux density, however, is not increased as the cost of losses is increased.

The average losses of three of the optimized generators are shown in Figure 6.4. It can be seen that the decrease in average losses is mainly caused by a decrease in copper losses. The eddy current losses are

Table 6.6 Generators optimized using different loss costs.

Cost of losses	Average efficiency (%)	Air gap diameter (m)	Active weight (kg)	Slot height (mm)	Current density (A/mm^2)	Air gap flux density (T)	Winding temperature (°C)
0 %	92.0	2.05	1814	46	5.6	0.67	130
10 %	92.6	2.04	1907	48	5.3	0.70	130
50 %	93.7	2.07	2187	55	4.7	0.75	130
100 %	94.9	2.15	2689	64	3.6	0.77	107
200 %	95.6	2.32	3274	71	2.7	0.76	89
1000 %	96.5	2.73	5369	93	1.5	0.75	71

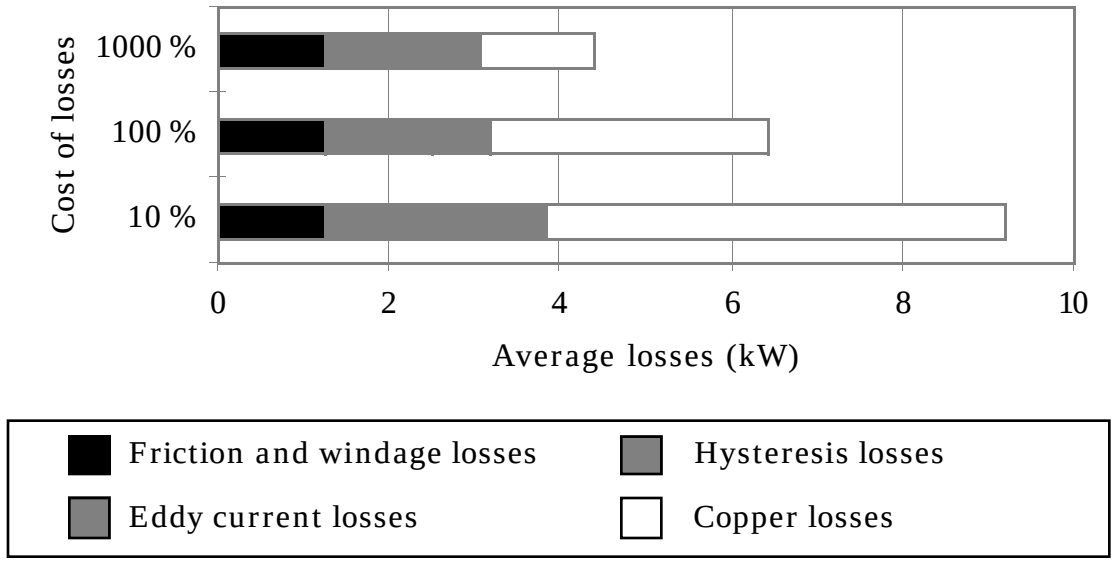

Figure 6.4 The average losses of three generators optimized using different specific costs of the losses (10, 100 and 1000 % of the nominal cost of the average losses).

approximately halved but the hysteresis losses remain almost constant. The windage and friction losses are assumed constant and cannot be changed by optimization.

One way of decreasing the core losses, which is not included in the optimization in this thesis, is to use iron with lower losses and perhaps also thinner laminations.

6.3.2 Cost of Iron and Copper

The influence of the cost of the active iron and copper on the optimum generator is tested by changing the cost of these two materials to 0 %, 10 %, 50 %, 200 % and 1000 % of their nominal costs. The results are shown in Table 6.7.

Decreased specific cost of iron and copper leads to a more efficient generator with a smaller diameter but a higher active weight. The average losses change between 4.5 and 7.0 percent-units, the diameter changes from 2.07 to 2.59 m and the weight from 3887 to 1443 kg as the costs of iron and copper change from 0 to 1000 % of their nominal values.

The costs of iron and copper mainly influence the active weight. The weight increases as copper and iron costs decrease because of the higher slots and also because of a slightly increased pole pitch. The pole pitch increases because the slot width increases. The copper losses are reduced as the costs of iron and copper decrease since the slots are made higher and the current density decreases.

Table 6.7 Generators optimized with different specific copper and iron costs.

Cost of iron and copper	Average efficiency (%)	Air gap diameter (m)	Active weight (kg)	Magnet weight (kg)	Slot height (mm)	Stator length (m)	Winding temperature (˚C)
0 %	95.5	2.07	3887	134	88	0.60	90
10 %	95.4	2.08	3677	132	84	0.59	92
50 %	95.1	2.11	3106	127	72	0.57	100
100 %	94.9	2.15	2689	124	64	0.55	107
200 %	94.4	2.21	2223	120	55	0.52	118
1000 %	93.0	2.59	1443	118	36	0.47	130

6.3.3 Cost of Permanent Magnets

The specific cost of the permanent magnets is a rather uncertain parameter. The permanent magnets are expensive, but the price has been falling for a number of years. It is, therefore, interesting to see what effect magnet price has on the optimum generator. The specific cost of the magnets has been changed from 0 to 1000 % of the nominal value, 100 ECU/kg. Some data of the different optimized generators are shown in Table 6.8.

It can be seen that the amount of magnets increases considerably as the specific cost of the magnets is reduced. The differences in the air gap and

Table 6.8 Generators optimized with different specific magnet costs.

Cost of magnets	Average efficiency (%)	Air gap diameter (m)	Active weight (kg)	Air gap flux density (T)	Magnet height (mm)	Teeth flux density (T)	Magnet weight (kg)
0 %	95.3	2.00	3142	0.89	16.2	1.83	285
10 %	95.2	2.03	2988	0.87	12.3	1.78	219
50 %	95.0	2.10	2802	0.81	7.9	1.70	148
100 %	94.9	2.15	2689	0.77	6.3	1.64	124
200 %	94.6	2.23	2549	0.72	5.1	1.59	104
1000 %	93.1	2.49	1977	0.60	3.3	1.49	76

teeth flux densities are, however, not very large. Even with a very low specific cost of the magnets, the optimum air gap flux density is only about 0.1 T higher than for the generator optimized with the nominal value of the specific cost of the magnets. The diameter decreases with decreasing magnet cost and the active weight increases, but the average efficiency changes only slightly. The conclusion of these results is that the average efficiency, the diameter and the active weight are not very dependent on the specific cost of the magnets. The specific cost of the magnets will mainly influence the material cost of the generator.

Since the generator is only slightly improved by increasing flux density, flux concentration will not lead to any significantly different generator performance than surface magnets do. Ferrite magnets and flux concentration, however, may lead to a cheaper generator.

6.3.4 Cost of the Structure

The approximate cost of the structure has several parameters. In this section, the reference structure cost c_{str}, the structure exponent a and the reference length l_{ref} are changed in order to see which effect they have on the optimum generator. The results of the changed cost of the structure are presented in Table 6.9. The parameters have been changed one at a time, while the other two have their nominal values. The nominal values of the parameters are c_{str} = 20 kECU, a = 3 and l_{ref} = 1 m.

Even major changes in the cost of the structure have little influence on the generator efficiency and active weight. The size of the generator is not changed drastically, unless c_{str} is reduced to 0 or 2 kECU or a is decreased to 1. For all other tested values of the cost function parameters, the diameter varies between 1.97 to 2.50 m and the average efficiency between 94.4 and 95.2 %. The weight of the active parts varies between 2048 and 3129 kg.

If the structure is not included (c_{str}=0), the optimization is only carried out for the electromagnetic part of the generator. The optimum diameter then becomes much larger than if the cost of the structure is included. Note, however, that the average efficiency of the very large generator is not much different from that of the reference generator. The cost of the active part does not decrease much compared with the reference generator. A large diameter, therefore, is not motivated.

The conclusion from this investigation is that the cost of the structure must be included in the optimization, because it is the main limiting factor for the diameter. Exactly how the cost of the structure varies with diameter does not have to be known in order to find an approximate optimum diameter.

Table 6.9 Generators optimized with different structure costs.

Changed cost parameter	Average efficiency (%)	Air gap diameter (m)	Active weight (kg)	Stator length (m)	Current density (A/mm^2)	Reac-tance (p.u.)	Winding temp. (°C)
c_{str}=0 kECU	95.7	6.33	1902	0.12	2.8	0.80	87
c_{str}=2 kECU	95.6	3.26	2366	0.32	3.1	0.89	93
c_{str}=10 kECU	95.2	2.39	2664	0.50	3.4	0.93	99
c_{str}=20 kECU	94.9	2.15	2689	0.55	3.6	0.95	107
c_{str}=40 kECU	94.4	1.97	2611	0.58	4.0	0.98	121
c_{str}=200 kECU	93.9	1.78	2690	0.62	4.1	1.00	130
a=1	95.5	3.39	2181	0.28	3.2	0.90	97
a=2	95.1	2.46	2534	0.45	3.4	0.94	102
a=3	94.9	2.15	2689	0.55	3.6	0.95	107
a=4	94.7	2.01	2749	0.60	3.7	0.96	111
l_{ref} = 0.5 m	94.4	2.50	2048	0.36	4.1	1.00	130
l_{ref} = 1 m	94.9	2.15	2689	0.55	3.6	0.95	107
l_{ref} = 2 m	94.9	1.98	3129	0.73	3.4	0.92	96

6.4 Optimum Generator Diameter

The diameter of a direct-driven generator is of great importance to a wind energy converter manufacturer. The optimum diameter is a compromize between the electromagnetic part and the structure of the generator. Since the cost of the structure is highly uncertain, it is interesting to investigate the influence of the diameter on the optimization.

The main variables that link the optimization of the electromagnetic part to the structure are the diameter and the length. In Figure 6.5 the length of the stator is plotted as a function of air gap diameter for optimized generators. Because the cost of the structure increases both with increasing length and with increasing diameter, the cost of the structure will have a minimum value. Both large and small diameters will lead to a high structure cost.

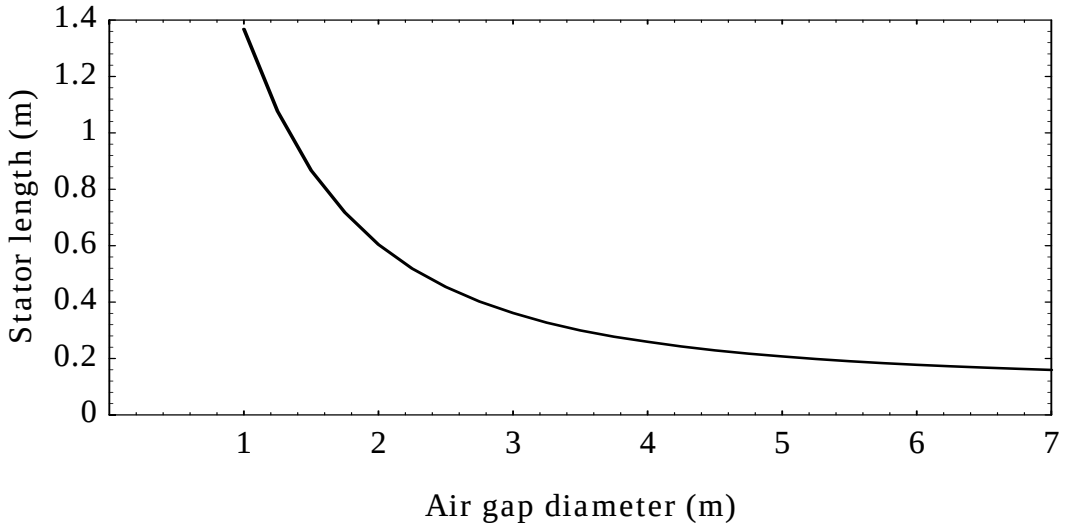

Figure 6.5 The optimum stator length as a function of diameter.

The cost of the active part, the cost of the losses and the cost of the structure were calculated as functions of air gap diameter. The generator was optimized for each fixed value of the diameter. The results are shown in Figure 6.6.

The losses, and consequently the cost of the losses, decreases rapidly as the diameter increases from 1 to 2 m. As was shown in Section 6.2, the core losses are rather diameter-independent. The reason the losses decrease with increasing air gap diameter is that the active parts of the windings are reduced. At small diameters, when the stator is rather

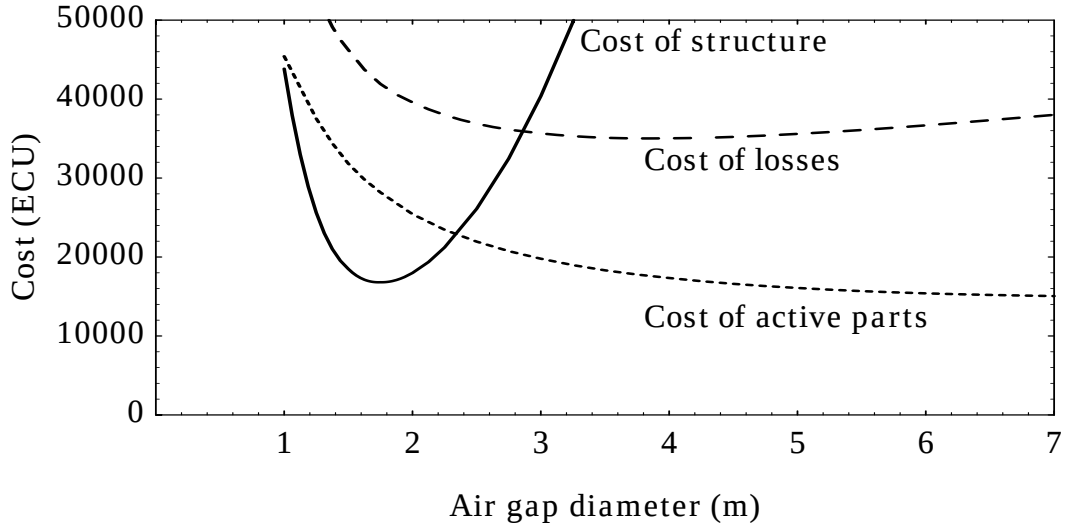

Figure 6.6 The three parts of the cost function as functions of air gap diameter. The generator is optimized for each value of the air gap diameter.

long, this phenomenon reduces the losses as the diameter increases. At large diameters, the stator is short and the end windings become more important. While the active part of the winding decrease with increasing diameter the amount of end windings increases. If the air gap diameter is between 3 and 5 m, the total losses are almost independent of the diameter. For diameters larger than 5 m the losses increase slightly with increasing diameter.

The cost of the active part of the generator is more diameter-dependent than the cost of the losses. If the generator diameter is decreased, the amount of active material is increased. Since the generator cost function will keep the optimum stator short, the increased cost depends mostly on increasing slot height and increasing flux density. Increasing flux density leads to high magnet weight. Under a diameter of 2 m, the cost of the active material increases rapidly and, therefore, the diameter cannot be much less than 1.5 m for this 500 kW generator.

At large diameters, over 2 m, the stator is short and the cost of the structure is determined mainly by the diameter. Consequently, the cost of the structure increase along with the diameter. For small diameters, under 1.5 m, the stator is long and, thus, the cost of the structure is determined mainly by the stator length. Therefore, the cost of the structure increase as the diameter is decreased below 1.5 m. A large diameter has to be avoided because of transportation and manufacturing problems and a small diameter has to be avoided because a long generator structure is difficult to manufacture.

If only the cost of the active parts and the cost of the losses are considered, the optimum diameter would be more than 6 m. If the cost of the structure is included in the optimization, the optimum diameter is decreased drastically, to about 2 m. The reason is easily seen in Figure 6.6; the cost of the losses and the cost of active materials are rather diameter-independent for diameters above 2.5 m.

The optimum generator diameter is not very sensitive to changes in the shape of the cost function for the structure. The reason is a significant increase in the cost of the active material and the cost of the losses as the diameter decreases below 1.75 m, in combination with a very slow decrease in those costs as the diameter increases beyond 2.5 m. As a consequence, the optimum diameter is likely to be within 1.75–2.5 m.

6.5 Typical 500 kW Permanent-magnet Generator

Ranges for the efficiency, active weight and air gap diameter can be found from the data in Section 6.3. The maximum and minimum values of the average efficiency, active weight and air gap diameter are presented in Table 6.10. Only the values for generators optimized with specific costs c_d,

c_{Fe}, c_{Cu}, l_{ref}, c_{str} equal to 50 or 200 % of the nominal cost and a equal to 2 and 3 were used. The generators optimized with more extreme values of the cost function parameters were excluded.

The 500 kW permanent-magnet generator will have an average efficiency of about 94.6 %, an active weight of about 2600 kg and a diameter of about 2.2 m. The efficiency can increase slightly if the specific cost of the losses is high or if the specific costs of the iron and copper are low. The increased efficiency will lead to an increase of the active weight. An increase in the diameter only leads to a small increase in the efficiency and a small decrease in the active weight; a decrease in the diameter will increase the active weight and decrease the efficiency.

Table 6.10 Data of a typical 500 kW direct-driven, permanent-magnet generator of the proposed type.

Average efficiency	Active weight	Air gap diameter
94.6 ± 1 %	2600 ± 700 kg	2.2 ± 0.3 m

7 Design and Comparison

In this chapter the performance and data of the proposed generator type is presented and discussed. Direct-driven generators are designed and optimized for rated powers from 30 kW to 3 MW. A comparison is made of the average efficiency and the size of direct-driven generators of the proposed type and conventional drive trains, consisting of a gear and a grid-connected induction generator. Some other direct-driven generators are also compared with the proposed generator type.

7.1 Generators from 30 kW to 3 MW

Direct-driven generators are interesting for all sizes of wind energy converters. Wind energy converters from about 30 kW and up to 3 MW are of the same basic design and can be assumed to follow Equations (2.1) and (2.2) as pertains to rated speed and rated torque as functions of rated power. Therefore, generators within that power range were investigated. The calculated generator sizes are 30, 50, 100, 170, 300, 500, 1000, 1700 and 3000 kW. All the generators were optimized using the nominal values of the cost function parameters presented in Table 2.3. The efficiency, size and active weight of the direct-driven generators are presented in Section 7.1.1. Optimum values of the design variables and other results from the electromagnetic design are discussed in Section 7.1.2. In Section 7.1.3 the differences between generators of different rated power are discussed.

7.1.1 Generator Data

Both the average efficiency and the efficiency at rated load of the optimized generators are shown in Figure 7.1. The efficiency of the direct-driven generators increases with the rated power, as it also does for conventional generators. An important reason for the increase in efficiency is that the rotor surface velocity increases; a higher rotor surface velocity means that a higher active power can be produced per square meter of air gap surface, with a given force density. The average efficiency increases from 92.5 % for a 30 kW generator to 95.8 % for a 3 MW generator, and the rotor surface velocity increases from 2.58 to 4.56 m/s. The efficiency at rated load is about 1 percent-unit lower than the average efficiency.

The size of the direct-driven generator is important. Generators will be more difficult to manufacture the larger they are, but an even more important problem might be the transportation to the site. The optimum air gap diameter and stator length of the generator are shown in Figure 7.2. An optimized 30 kW generator has an air gap diameter of 0.8 m and a 3 MW generator 4.1 m. The corresponding stator lengths are

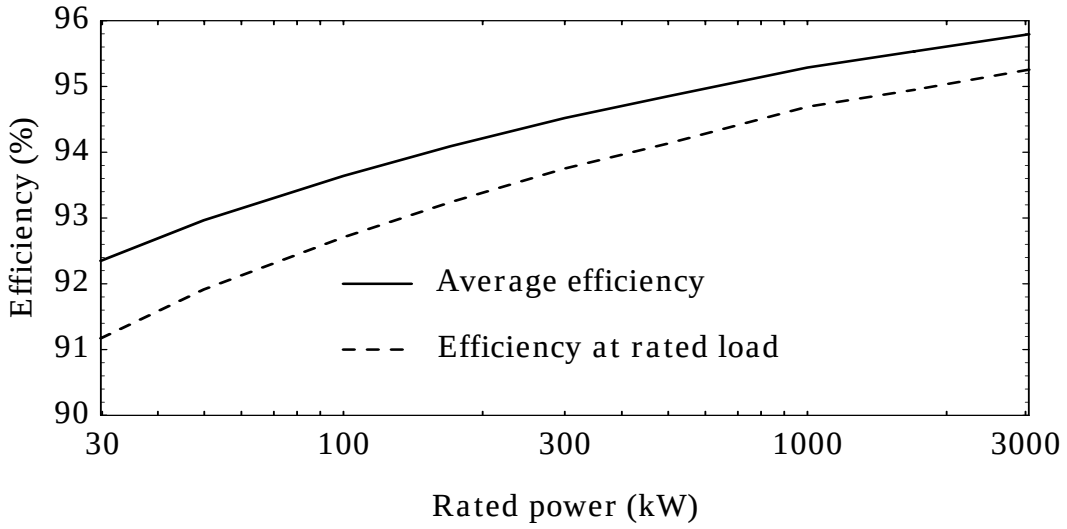

Figure 7.1 The efficiencies of the direct-driven generators

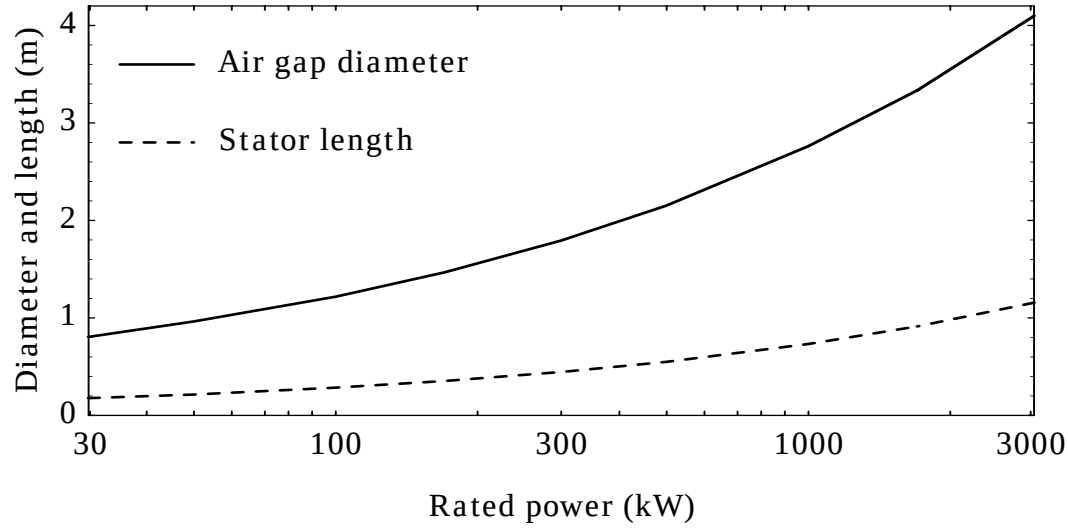

Figure 7.2 The air gap diameter and stator length of the direct-driven generators.

0.2 m for the 30 kW generator and 1.1 m for the 3 MW generator. The length-to-diameter ratio increases as the rated power increases, but even the 3 MW generator has a length-to-diameter ratio of less than one third.

The weight of the generator is usually not a problem for the wind energy converter during operation. Forces on the wind energy converter tower, for instance, are determined almost exclusively by the forces from the turbine, not by the generator weight. Nevertheless, the weight can be important for the erection of the wind energy converter. A heavy generator demands a larger crane or that the machinery be lifted in several parts.

Since the mechanical part of the generator has not been designed, only the active weight is calculated. The weight of the generator structure is expected to be much higher than the active weight. The active weight increases slightly less than linearly with the rated power, see Figure 7.3. The figures are 210 kg for a 30 kW generator, 1700 kg for a 300 kW generator and 14000 kg for a 3 MW generator.

Since it was not included in the design method, the risk of demagnetization of the magnets was also checked. The larger generators have a lower minimum flux density in the magnets than the smaller ones, but none of the generators risks irreversible demagnetization of the permanent magnets.

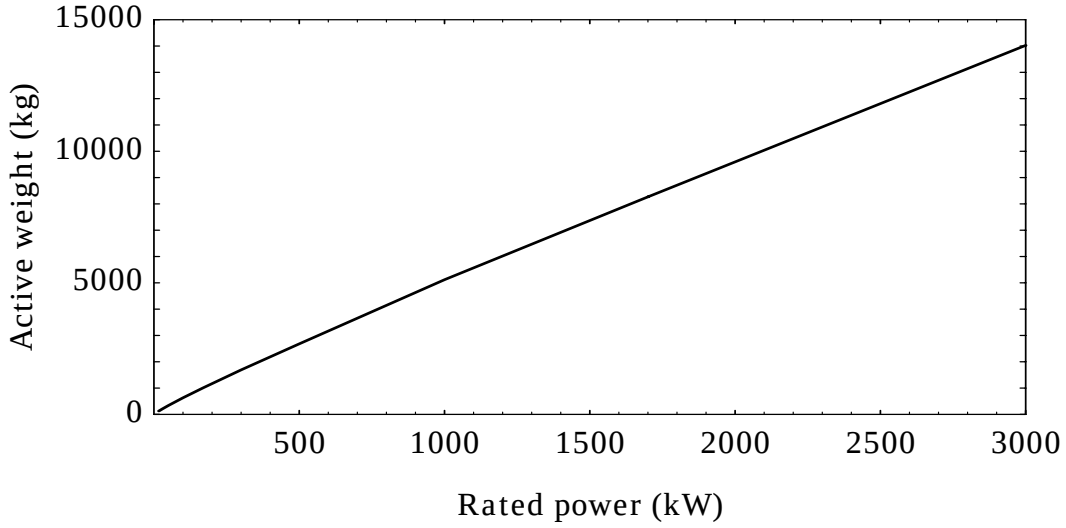

Figure 7.3 The active weight of the generator as a function of rated power.

7.1.2 Optimum Variables and Parameter Values

All the generators, from 30 kW to 3 MW, are of the same type and optimized with the same cost function. It is interesting, therefore, to see in what respect the generators of different rated powers are similar and in what respect they are different.

The optimum air gap flux density is about 0.76 T and the optimum teeth flux density about 1.65 T for all generator sizes. The variations are only about ±1 %.

The force density in the air gap of the generators is presented in Figure 7.4. The larger generators have a higher force density than the smaller ones. Since the flux density is constant, the higher force density is achieved by a higher current loading.

The optimum winding temperature also increases as the rated power of the generator increases. In Figure 7.5, the diagram shows that the temperature limit is reached as the rated power is 3 MW or larger. This means that the smaller machines can be made with simpler cooling systems than the larger ones. The magnet temperature is also plotted in the diagram. The magnet temperature is well below 120˚C for all of the generators.

The per-unit reactance of the optimized generators increases with increasing rated power. Figure 7.6 shows that the value of the reactance increases from approximately 0.75 p.u. for a 30 kW generator to 1.05 p.u. for a 3 MW generator.

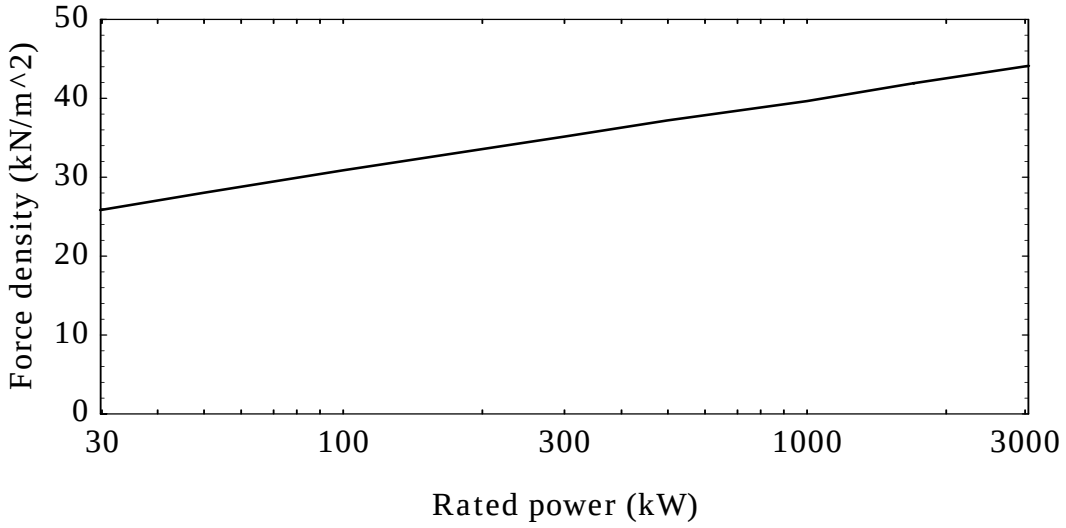

Figure 7.4 The force density in the air gap of the optimized generators

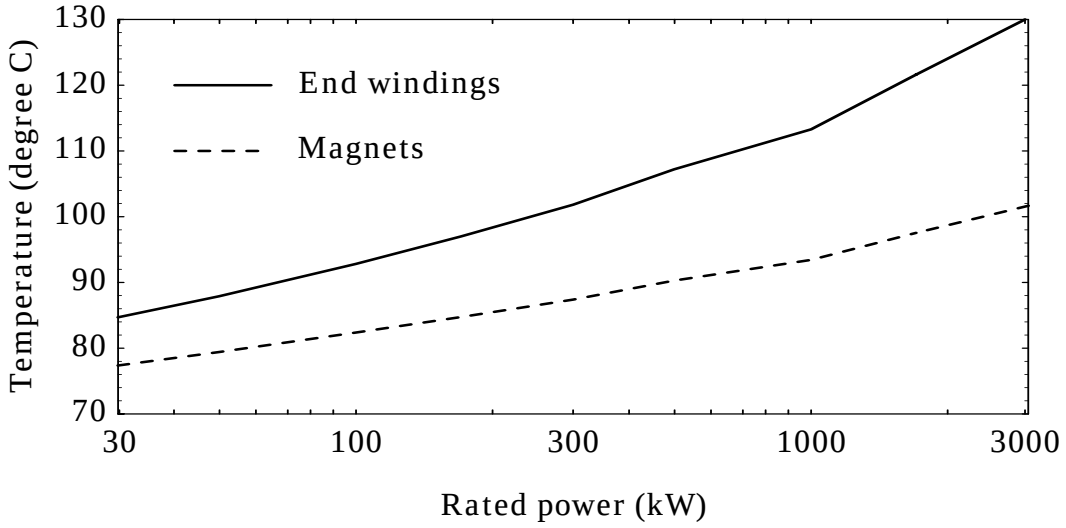

Figure 7.5 The maximum winding temperature and magnet temperature of the optimized generators.

The slot height and pole pitch of the optimized generators both increase with increasing rated power, as is shown Figure 7.7. It is the increasing current loading which causes the slot height to increase. The slot pitch and pole pitch are not optimized independently. Because the number of slots per pole is constant, the slot pitch is proportional to the pole pitch. Therefore, the optimum pole pitch and the slot pitch could have other values if they were optimized separately.

The results presented in this section are rather typical of the design of electrical machines in general. It is a well known phenomenon that larger generators have a higher force density than smaller ones. The higher force density is the reason for the increase in slot height, current

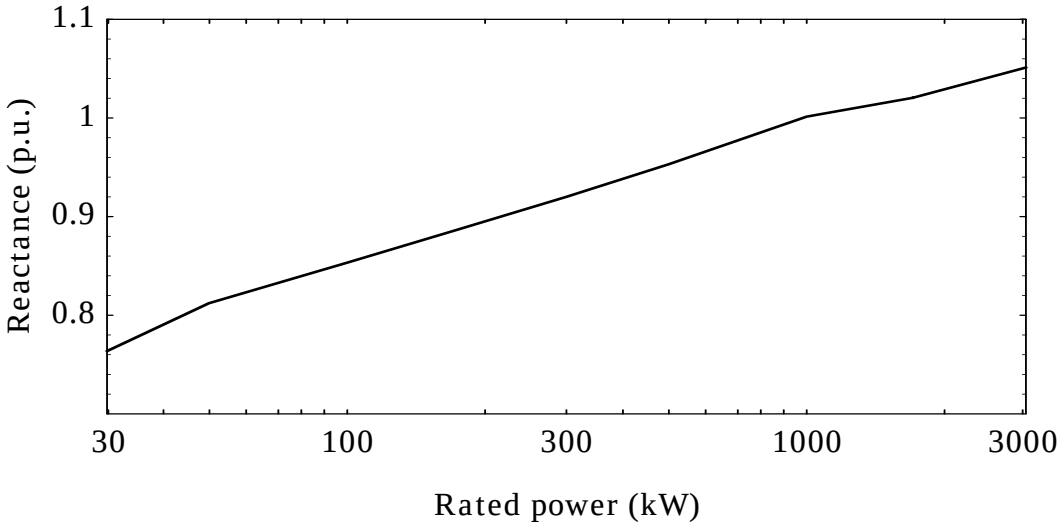

Figure 7.6 The reactance of the optimized generators.

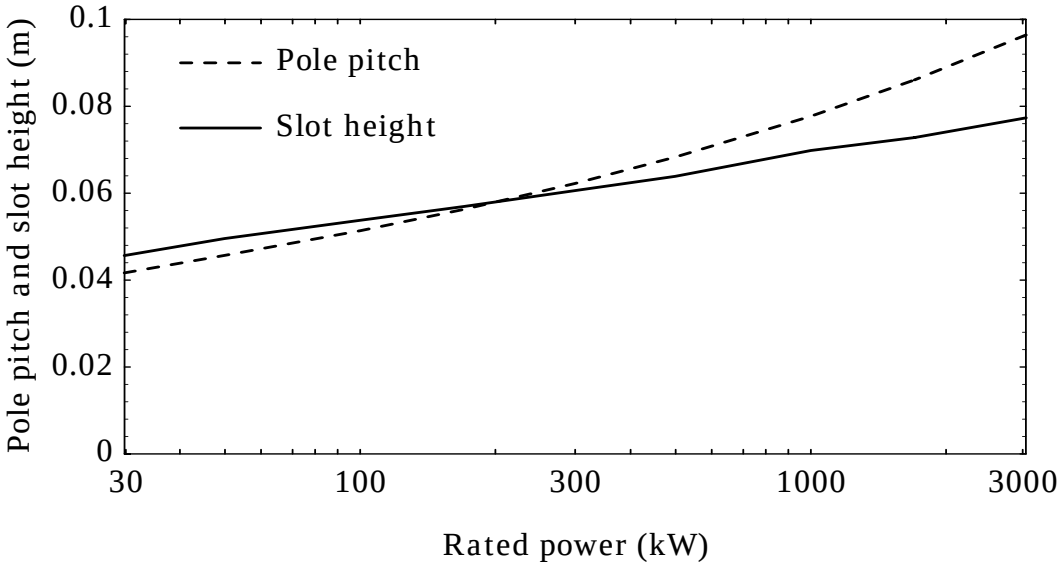

Figure 7.7 The slot height and pole pitch of the optimized generators.

loading, reactance and winding temperature as the rated power increases. The increased force density, however, is not a necessary consequence of increased generator size; it is caused by the optimization.

7.1.3 Power Limits For the Direct-driven Generators

This section examines whether or not there exists a practical upper or lower limit for the rated power of direct-driven generators. The reasons for such a limit may be the total cost, the weight or the size of the generator.

The three parts of the cost function only give a rough estimate of the cost of the generator. In Figure 7.8, the three parts of the cost function are shown to illustrate how the cost changes with rated power. All three parts of the cost function increase almost linearly with the rated power. This indicates that the specific cost, ECU per kW, of a direct-driven generator is about the same for all generator sizes.

The weights of the active materials are plotted as functions of the rated power in Figures 7.9 and 7.10. The iron weight and the copper weight increase slightly less than linearly and the magnet weight increases slightly more than linearly. Since the magnets are only a small part of the active weight, the total active weight still increases less than linearly with increasing rated power. Thus the specific active weight, kg per kW, will be slightly lower for a large generator than for a small one.

The estimated outer diameter of the generators is plotted as a function of the rated power in Figure 7.11. The diameter increases with increasing power, but the increase is rather small, because of the increase in force

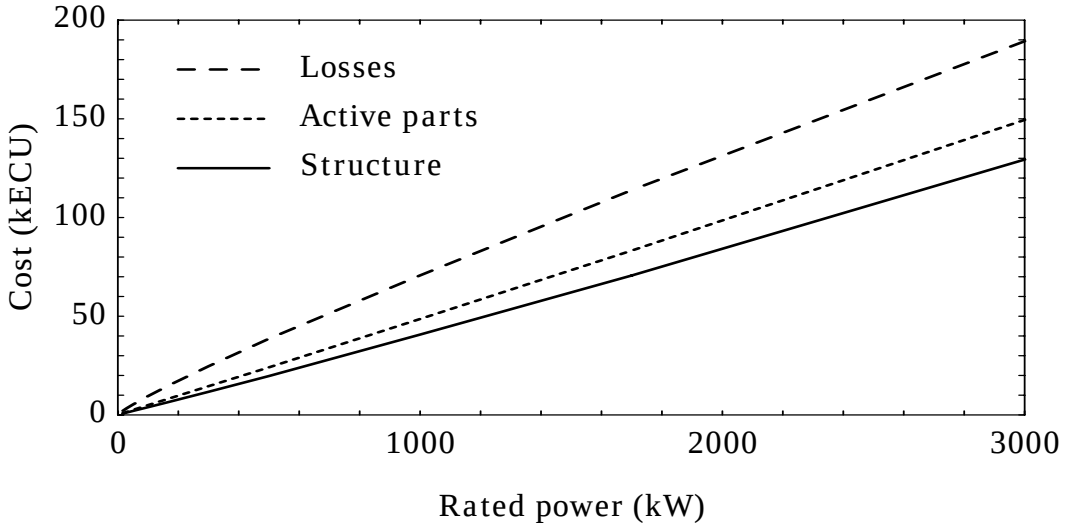

Figure 7.8 The cost of active parts, cost of losses and cost of structure for the generators as a function of rated power.

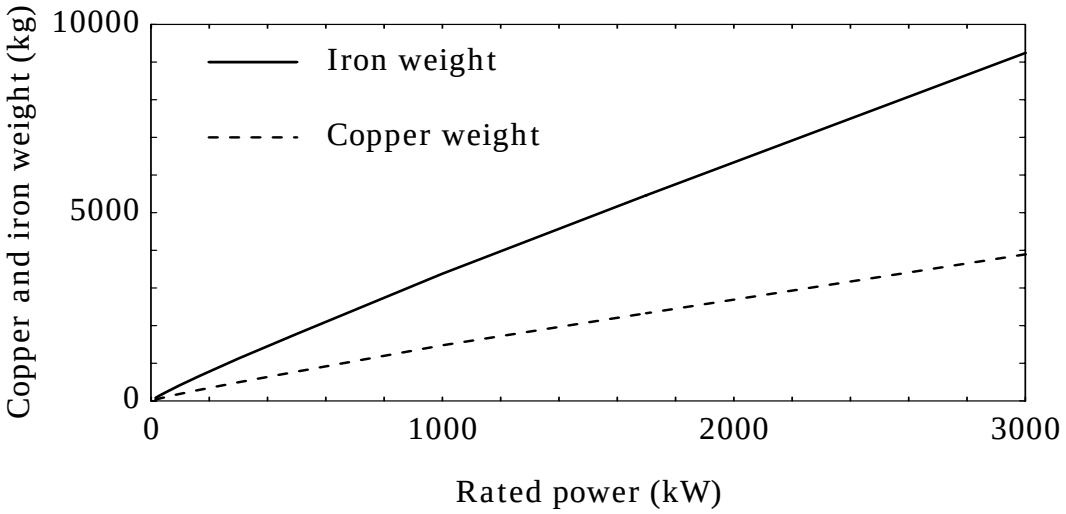

Figure 7.9 The weight of the iron core and winding as a function of rated power.

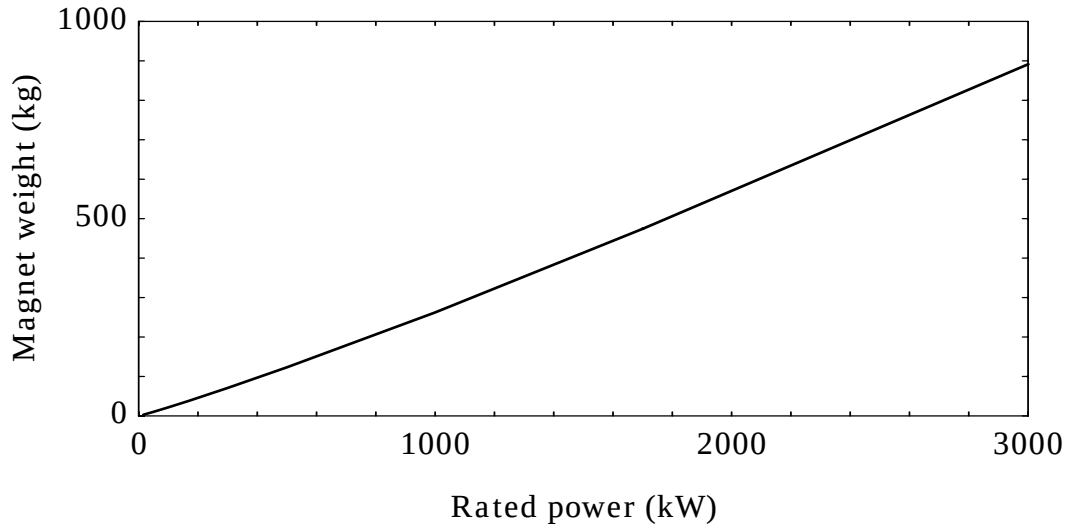

Figure 7.10 The weight of the permanent-magnets as a function of rated power.

density and length-to-diameter ratio with increasing rated power. If there is a definite maximum diameter, then this type of generator can be made with a smaller outer diameter than what is shown here. However, in that case the active weight will increase, the average efficiency decrease slightly and the length will increase.

The specific cost and specific active weight will not increase as the rated power increases. From these two aspects the upper power limit for direct-driven generators for wind energy converters seems to be more than 3 MW. Consequently, it is mainly the size of the generator that can act as a

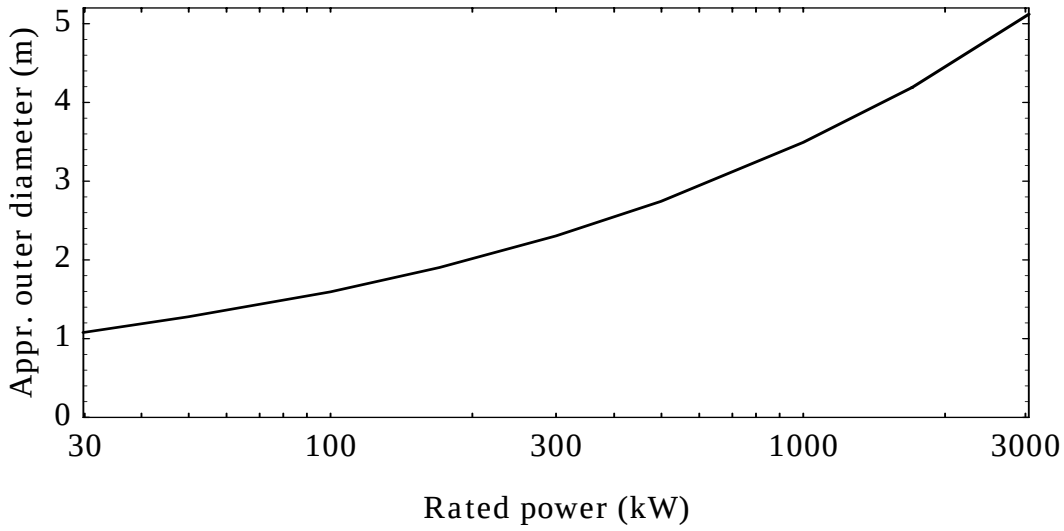

Figure 7.11 The approximate outer diameter of the direct-driven generators.

practical limit for large direct-driven generators. Compared with other parts of the wind energy converter, however, like the tower, the nacelle and the turbine blades, the diameter of the proposed generator type does not necessarily have to be a large problem.

7.2 Comparisons

Direct-driven generators have to be more cost effective than conventional systems with a gear and a four- or six-pole generator in order to be interesting. The main question is whether or not a direct-driven generator can bring down the cost of the produced energy. This comparison is not made regarding the total cost, however, since the cost function is too approximate for that purpose. Instead, the generator systems are compared regarding weight, efficiency and size.

7.2.1 Comparison with Conventional Generators and Gears

The proposed direct-driven generator type was compared with drive trains in conventional wind energy converters of three different rated powers. Four-pole generators were assumed rather than six-pole, since four-pole generators are smaller, have lower weight and higher efficiency. The comparison of the generator systems is shown in Table 7.1.

The weights of the gears and induction generators are based on data for commercial gears and standard generators. For the direct-driven generators the weights are only the active weight. The total weight of the gears and induction generators are 2.1 to 3.8 times the active weight of the

Table 7.1 A comparison of the proposed direct-driven generator type with conventional drive trains. Efficiency values refer to the efficiency from the turbine shaft to the grid.

Rated power	30 kW	500 kW	3000 kW
Weight of induction generator and gear	440 kg	7700 kg	53000 kg
Active weight of direct-driven generator	210 kg	2700 kg	14000 kg
Full-load efficiency of induction generator and gear	89.7 %	93.7 %	94.3 %
Full-load efficiency of direct-driven generator and frequency converter	87.4 %	90.3 %	91.4 %
Average efficiency of induction generator and gear	81.7 %	88.4 %	90.0 %
Average efficiency of direct-driven generator and frequency converter	88.3 %	90.7 %	91.6 %
Diameter and length of generator and gear combination	0.6 m 1.3 m	1.5 m 3 m	2.5 m 6 m
Outer diameter and length of the direct-driven generator	1.2 m 0.5 m	2.7 m 1.2 m	5 m 2 m

direct-driven generators. It seems realistic to expect that the total weight of the two alternative systems will be of the same order.

Both the efficiency at rated load and the average efficiency were compared. The efficiency of the direct-driven generators includes the frequency converter, which was assumed to be constructed with insulated-gate bipolar transistors. Its efficiency at rated load is assumed to be 95.9 % and the average efficiency is 95.6 %. (The average efficiency of the conventional systems and the frequency converter for the direct-driven generators are calculated in Appendix C).

At rated load the conventional systems are more efficient than the direct-driven generators, but they are less efficient on the average. The difference in average efficiency is 1.6 and 2.3 percent-units for the 3 MW and 500 kW systems, respectively. For the 30 kW system the difference is larger, 6.6 percent-units.

The size of the gear and generator is defined by their maximum diameter, at the gear box, and the total length, including a coupling on the high-speed shaft. The outer dimensions of the direct-driven generators are estimated; they will of course depend on how the structure is constructed.

Note that the compared systems are not completely equal. The conventional drive trains have a fixed turbine speed, while the direct-driven generator with a frequency converter allows variable turbine speed. Variable-speed turbines can produce about 5 to 10 % more energy, which will make the variable-speed, direct-driven generator more worthwhile than the grid-connected induction generator. The increased energy production by means of the variable turbine speed is not included in the efficiency comparison above. The efficiency discussed is only the efficiency from the turbine shaft to the grid.

High-slip generators have more recently often been used in large wind energy converters, in order to limit turbine power peaks and damp power oscillations. The rotor copper losses of the high-slip generators are 1–2 % higher at rated load than for the standard induction generators in Table 7.1. If two-speed generators are used the efficiencies of the induction generators will also be lower than what is shown here, about 0.5–1 percent-unit lower at rated load. In comparison with these types of generators, the use of direct-driven generators will lead to an even larger increase in average efficiency.

7.2.2 Comparison with Other Direct-driven Generators

In the previous section the proposed direct-driven generator type was compared with conventional drive trains; in this section it is compared with other direct-driven generators. The comparison is made with three theoretical design studies and one commercial generator. Unfortunately, the weight and efficiency of the commercial generator is not available. The values of the diameter, length, efficiency and active weight of the generators are shown in Table 7.2. The generators of the proposed type have all been optimized with the nominal cost function defined in Chapter 2.

Often, only electromagnetic losses are included in the theoretically calculated efficiency of generators, because the friction losses are difficult to determine without knowlegde of the mechanical design. In the efficiency of the proposed generator 0.5 % friction losses are included. As pertains to the other direct-driven generators it is not known which losses are or are not included in the efficiency figures.

The proposed generator is of about the same size and slightly less efficient at rated load when compared with a transversal-flux generator by Weh et al. (1988). The transversal-flux generator has a lower active weight but

it needs more permanent magnets than the proposed generator does. However, the presented transversal-flux generator is designed for diode rectifier connection which reduces its rated power. If the transversal-flux generator is designed for a forced-commutated rectifier, it will be smaller than the proposed generator.

The air gap diameter of the proposed generator is 8 % smaller and the stator is 38 % shorter than those of the similar generator, with surface

Table 7.2 Comparison of the proposed direct-driven generator with other direct-driven generators.

Generator, rated shaft power	Air gap diameter (Outer diameter)	Stator length (Outer length)	Efficiency at rated load (Average efficiency)	Active weight (Magnet weight)
Transversal-flux generator 60 kW at 78rpm	1.00 m (1.2 m)	– (0.35 m)	94 % –	176 kg (14 kg)
Proposed generator 60 kW at 78 rpm	0.91 m (1.15 m)[1)]	0.20 m (0.40 m)[1)]	93.4 % (93.9 %)	318 kg (9.4 kg)
Direct grid-connected Radial-flux generator 532 kW at 28.3 rpm	2.4 m –	0.91 m –	94.2 % –	4100 kg –
Proposed generator 532 kW at 28.3 rpm	2.28 m –	0.58 m –	94.0 % (94.8 %)	3088 kg (145 kg)
Axial-flux generator 1040 kW at 100 rpm	3.46 m [2)] 2.94 m [2)]	0.17 m [3)] 0.52 m [4)]	97 % –	3000 kg (>>100 kg)[1)]
Proposed generator 1040 kW at 100 rpm	1.90 m –	0.46 m –	96.9 % (95.6 %)	2456 kg (103 kg)
Electrically excited Radial-flux generator ≈540 kW[1)] at 40 rpm	4 m [1)] –	0.2 m [1)] –	– –	– (0 kg)
Proposed generator 540 kW at 40 rpm	2.06 m –	0.52 m –	94.8 % (95.3 %)	2487 kg (111 kg)

1) Values estimated by the author
2) Outer and inner diameter of the stator
3) Axial length of the active part of the generator.
4) Active stator length = two times the difference between inner and outer stator radii.

mounted NdFeB magnets, designed for 50 Hz direct grid-connection (Spooner and Williamson, 1992c). The efficiency at rated load is almost equal, and the proposed generator has 31 % lower active weight than the direct grid-connected generator. One important reason for this large difference in generator size is that the proposed generator has a reactance of 0.96 p.u. while the direct grid-connected generator has a reactance of only 0.31 p.u. The low reactance of the direct grid-connected generator is necessary to produce a high peak power.

Honorati et al. (1991) presents a 1 MW axial-flux generator designed for wind energy converters. The outer stator diameter of the axial flux generator is 82 % larger than the air gap diameter of the proposed generator, and the active stator length (two times the outer minus inner stator radius) is 13 % longer than the stator of the proposed generator. Since the stator is oriented in the radial direction in the axial-flux generator, however, the axial length of the active generator part is 63 % shorter than the stator length of the proposed generator. Both the axial-flux generator and the proposed generator have high efficiency. Such high efficiency is not realistic for a normal wind energy converter generator; the high efficiency depends on the very high rated speed of the generators. The active weight of the axial-flux generator is 22 % higher than that of the proposed generator. Since the axial-flux generator has an air gap winding, the amount of permanent magnets needed can be expected to be very high in comparison with the 103 kg needed for the proposed generator type.

A commercially used electrically excited generator was included in the comparison, even if the data of that generator are only approximate. The generator is used in the Enercon E-40 wind energy converter (Anon., 1994a). The comparison shows that the electrically excited generator has a 94 % larger diameter and a 62 % shorter stator than the proposed generator. The rotor volume of the electrically excited generator is about 50 % larger than that of the proposed generator type.

The comparisons in this section show that the proposed radial-flux permanent-magnet generator with a forced-commutated rectifier can have a small size compared with the other direct-driven wind turbine generators. It is much smaller than the electrically excited generator, the axial-flux generator and the direct grid-connected radial flux generator. It is of about the same size as the transversal flux generator with a diode rectifier. The reason for the small size of the proposed generator is mainly that a high peak power is not required. The efficiency at rated load is similar for the proposed generator type and the alternatives, but the average efficiency cannot be compared since it has not been given for the other generators.

8 Conclusions

A radial-flux permanent-magnet generator is a good option for direct-driven wind turbine generators. Connected to the grid via a frequency converter, it can be made small and efficient. The generator type can be used in wind energy converters, from at least 30 kW up to 3 MW, and it is more efficient than conventional four-pole induction generators with gears. By allowing the rated torque to be close to the pull-out torque, the proposed generator type can be made smaller than many other direct-driven generators in the literature.

8.1 Different Generator Types

Several generator topologies can be used for direct-driven wind turbine generators, for instance, radial-flux, axial-flux and transversal-flux topologies. Radial-flux generators are slightly more efficient and need slightly less active material than axial-flux generators do. Moreover, radial-flux topology allows a smaller outer diameter than axial-flux topology does. The transversal-flux generator is very small, efficient and light. There is one drawback, however; its structure is more complicated than the structure of a radial-flux generator. The final choice of the generator type cannot be made based exclusively on the analysis of the active part of the generators. The choice depends, to a large extent, on manufacturing aspects.

Electrically excited generators are difficult to use as direct-driven wind turbine generators, because a large air gap is required and that leads to large losses due to the magnetizing current. By making the pole pitch large the losses due to the magnetizing current can be reduced, but that results in a very heavy generator. Permanent-magnet generators are more efficient than electrically excited generators and, if the pole pitch is made small, they are also lighter.

Generators with low-energy magnets and flux-concentration or high-energy magnets mounted on the rotor surface will have similar efficiency and size. Low-energy magnets for flux-concentration are cheaper than surface-mounted, high-energy magnets, but a rotor for flux-concentration is more complicated and heavier.

Direct grid-connected generators are more difficult to design than generators connected to the grid via a frequency converter. A direct grid-connected 500 kW generator, of the proposed type, is about 50 % larger and 1.5 % less efficient than what a generator connected to a frequency converter can be. A 500 kW variable-speed generator required to produce a peak power of 200 % of the rated power will be about 25 % larger and 0.4 % less efficient than if no peak power capacity is required.

8.2 Generator Design and Optimization

A direct-driven radial-flux permanent-magnet generator with magnets mounted on the rotor surface was chosen for a theoretical investigation. This generator type has several favourable properties when compared with other types. The generator is connected to a forced-commutated rectifier in order to allow for a small diameter. An analytical design method was developed for this generator type. The cost function used for the generator optimization includes the cost of the active part of the generator, the cost of the average losses and the cost of the generator structure. A method to calculate the average losses of a wind turbine generator was also developed. The average losses were calculated by multiplying the losses at rated load with average loss factors for the different types of losses. This way of calculating the average losses is very easy to use in the optimization of a generator.

The cost function used for the optimization is approximate, but it is shown that the efficiency, active weight and size of an optimized generator do not change much even if the cost function is changed a great deal. If the efficiency is increased, the active weight of the generator increases. The diameter of the generator has a practical lower limit because the stator length, the losses and the active weight increase rapidly as the diameter is decreased below a certain diameter. An increase in diameter, above the practical lower limit, increases the efficiency and reduces the active weight only slightly. Therefore, the optimum diameter can be expected to be close to the practical lower limit.

8.3 Designed Generators and Comparison with Other Generators

Generators from 30 kW to 3 MW were designed. They are all feasible as wind turbine generators. The active weight per kW and total cost per kW are about the same for all the generator sizes. The maximum power of direct-driven generators may be limited by the diameter. The outer diameter of the proposed generator type, however, is not much larger than the width of the nacelle in a conventional wind energy converter.

The average efficiency of the proposed direct-driven generator, including the frequency converter losses, is higher than that of a gear and a direct grid-connected induction generator. Furthermore, the frequency converter allows variable turbine speed. The variable speed will increase energy production in comparison with the direct grid-connected generator system. Compared with some other direct-driven generators, the proposed generator type is small.

8.4 Further Work

The generator type proposed in this thesis is promising for use in future wind energy converters. There are aspects that should be investigated further, however. The mechanical structure should be investigated in detail, both for a final optimization of the generator and in order to determine the generator price. A prototype should be built to demonstrate that a generator with a high inductance can produce a high force density in the air gap when connected to a forced-commutated rectifier. Some parts of the design method can also be improved to increase accuracy. Inductance calculations can be improved by including the saturation, and the loss model can be improved. In addition, the optimum slot pitch and pole pitch should be investigated. In this thesis the number of slots per pole and phase was constant.

References

Adkins B, Harley R.G. 1975. *The general theory of alternating current machines*, London, Great Britain: Chapman and Hall, 279 p.

Alatalo M, 1991. "Konstruktionsstudie av en permanentmagnetiserad axialflödesmaskin." Göteborg, Sweden: Chalmers University of Technology, Department of Electrical Machines and Power Electronics, Technical Report No. 108L. 107 p.

Alatalo M, Svensson T, 1993. "Variable speed direct-driven PM-generator with a PWM controlled current source inverter." *European Community Wind Energy Conference (ECWEC'93)*, Lübeck-Travemünde, Germany, 8–12 March 1993, Proceedings, p. 639–642.

Anon., 1992, *Guidelines for Certification of Wind Turbine Power Plants*. Norway: Det Norske Veritas.

Anon., 1994a, Product description leaflet from the Enercon company, Germany, 4 p.

Anon., 1994b, *European Wind Turbine Catalogue*. Copenhagen, Denmark: Energy Centre Denmark, 63 p.

Bindner H, Søndergaard L, Damgaard E. 1995. "Undersøgelse af generatorkoncepter til vindmøller - opsummeringsrapport" (in Danish). Roskilde, Denmark: Forskningscenter Risø, Risø-R-857(DA), October 1995, 15 p.

Carrichi F, Crescimbini F, Honorati O, Santini E. 1992. "Performance evaluation of an axial-flux PM generator". *International Conference on Electrical Machines (ICEM'92)*, Manchester, U.K., 15-17 September 1992, Proceedings, vol. 2, p. 761-765.

Chalmers B.J. 1965. *Electromagnetic problems of A.C. machines*. London, Great Britain: Chapman and Hall Ltd, 102 p.

Davies E.J. 1971. "Airgap windings for large turbogenerators", *Proceedings IEE*, vol. 118, No 3/4 1971, p. 529-535.

de Haan S, van Engelen T, Frumau C, Veltman A, Wildenbeest E, Childs S, Torrey D. 1994. "Development of a gearless drive with variable reluctance generator for variable speed wind turbines". *European Wind Energy Conference (EWEC'94)*, Thessaloniki, Greece, 10–14 October 1994, Proceedings vol. III, p. 130–133.

Deleroi W. 1992. "Linear induction motor in generator use for windmills". *Symposium on Power electronics Electrical drives Advanced electrical motors (SPEEDAM)*, Positano, Italy, 19-21 May 1992, Proceedings, p. 71–76.

Di Napoli A, Carrichi F, Crescimbini F, Noia G. 1991. "Design criteria of a low-speed axial-flux PM synchronous machine". *International Conference on the evolution and modern aspects of synchronous machines (SM 100)*, Zurich, Switzerland, 27-29 August 1991, Proceedings part 3, p. 1119-1123a.

Grauers A. 1994. "Synchronous generator and frequency converter in wind turbine applications: system design and efficiency", Göteborg, Sweden: Chalmers University of Technology, Department of Electrical Power Engineering, Technical report No. 175 L, 125 p.

Gribnau W.H.J.K., Kursten J.P.J. 1991. "Electrical flexibillity versus mechanical complexity through direct conversion." *European Wind Energy Conference (EWEC'91)*, Amsterdam, The Netherlands, 14–18 October 1991, Proceedings Part I, p. 809-813.

Honorati O, Caricchi F, Crescimbini F, Noia G. 1991. "Gear-less wind energy conversion system using an axial-flux PM synchronous machine". *European Wind Energy Conference (EWEC'91)*, Amsterdam, The Netherlands, 14-18 October 1991, Proceedings Part I, p. 814-818.

Jöckel S, 1996, "Gearless Wind Energy Converters with Permanent Magnet Generators–An Option for the Future?". *European Union Wind Energy Conference (EUWEC'96)*, Göteborg, Sweden, 20–24 May 1996, Proceedings, (in press).

Kylander G. 1993. "Modellering och mätning av temperatur och förluster i mindre asynkronmaskiner" (In Swedish). Göteborg, Sweden: Chalmers University of Technology, Department of Electrical Machines and Power Electronics, Technical Report No. 147L, 107 p.

Lampola P, Perho J, Saari J. 1995a. "Electromagnetic and thermal design of a low-speed permanent magnet wind generator". *Stockholm Power Tech Conference*, Stockholm, Sweden, 18-22 June 1995, Proceedings vol. "Electrical machines and drives", p. 211-216.

Lampola P. 1995b. "Dirtectly driven generators for wind power applications". *EWEA special topic conference: The economics of wind energy*, Finland, 5-7 September 1995, Proceedings p. E4-1 to E4-6.

Lampola P, Perho J, Väänänen J. 1996a. "Analysis of a low-speed permanent-magnet wind generator". *European Union Wind Energy Conference (EUWEC'96)*, Göteborg, Sweden, 20–24 May 1996, Proceedings, (in press).

Lampola P, Perho J, Väänänen J. 1996b. "Analysis of a low-speed permanent-magnet wind generator connected to a frequency converter". *International Conference on Electrical Machines (ICEM'96)*, Vigo, Spain, 10-12 September 1996, Proceedings, vol II, p. 393-398.

Richter R, 1951. *Elektrische Machinen I*. 2nd ed. Basel, Germany: Verlag Birkhäuser. 630 p.

Richter R. 1953. *Elektrische Machinen II*. 2nd ed. Basel, Germany: Verlag Birkhäuser. 707 p.

Slemon G.R, Xian L. 1992. "Modeling and design optimization of permanent magnet motors" *Electric Machines and Power Systems*, vol. 20, 1992, p. 71-92.

Spooner E. 1992a "Direct-coupled, direct-connected, permanent-magnet generators". *Wind energy conversion 1992*, Nottingham, U.K., 25-27 March 1992, Proceedings, p. 149-154.

Spooner E, Williamson A.C. 1992b. "The feasiabillity of direct-coupled permanent-magnet generators for wind power applications". *Symposium on Power electronics Electrical drives Advanced electrical motors (SPEEDAM)*, Positano, Italy, 19-21 May 1992, Proceedings, p. 105-112.

Spooner E, Williamson A.C. 1992c. "Permanent-magnet generators for wind power applications". *International Conference on Electrical Machines (ICEM'92)*, Manchester, U.K., 15-17 September 1992, Proceedings, p. 1048–1052.

Spooner E, Williamson A.C, Thompson L. 1994. "Direct-drive, grid-connected, modular permanent-magnet generators". *Wind Energy Conversion 1994 (BWEA'94)*, Sterling, U.K., 15–17 June 1994, Proceedings, p. 339–343.

Søndergaard L, Bindner H, 1995, "Undersøgelse af generatorkoncepter til vindmøller - Direkt drevet generator til gearløs vindmølle" (in Danish). Roskilde, Denmark: Forskningscenter Risø, Risø-R-801(DA), 52 p.

Thorborg K. 1988. *Power Electronics*. United Kingdom: Prentice Hall, 504 p.

Veltman A, Thijssen G, de Haan S. 1994. "Direct drive generators for wind turbines". *European Wind Energy Conference (EWEC'94)* Thessaloniki, Greece, 10-14 October 1994, Proceedings vol. I, p. 541-546.

Weh H, Hoffman H, Landrath J,Mosebach H, Poschadel J. 1988. "Directly-driven permanent-magnet excited synchronous generator for variable speed operation". *European Wind Energy Conference (EWEC'88)*, Herning, Denmark, 6-10 June 1988, Proceedings p. 566-572.

Westlake A.J.G, Bumby J.R, Spooner E, 1996. "Damping the power-angle oscillations of a permanent-magnet synchronous generator with particular reference to wind turbine applications". *IEE Proc.-Electrical Power Applications* , Vol. 143, No. 3, p. 269-280.

Appendix A Magnetizing Inductance

In this appendix the magnetizing inductance of the armature winding is derived. The total air gap flux generated by the armature currents is included in the inductance calculations, while only the fundamental flux density wave from the magnets is included in the torque calculations. The reason is that no torque can be produced by flux-density harmonics since the armature currents are assumed to be sinusoidal, but the flux-density harmonics do increase the required reactive power consumed by the generator.

The assumptions for the inductance calculations are that:

- the number of slots per pole and phase is one;
- each slot contains two conductors which are parallel connected (Consequently, the total current in one slot is equal to the phase current);
- the winding pitch is equal to the pole pitch;
- the flux in the air gap is assumed to cross the air gap perpendicular to the rotor and stator surfaces;
- the permeabilities of the stator and rotor iron are assumed to be infinite and the relative permeability of the magnets is assumed to be 1.

In Figure A.1 the flux caused by a current in the R-phase is illustrated, the two other phase currents are assumed to be zero. The self-inductance of phase R can be expressed as

$$L_{RR} = \frac{\Psi_{RR}}{I_R} \tag{A.1}$$

where Ψ_{RR} is the total flux linkage of phase R caused by the current I_R. The total flux linkage is the pole flux Φ_{RR} times the number of pole pairs, i.e.,

$$\Psi_{RR} = p \ \Phi_{RR} \tag{A.2}$$

The air gap reluctance of a pole pitch is

$$\Re = \frac{\delta_{ef} + h_m}{\mu_0 \ l_e \ \tau_p} \tag{A.3}$$

and since the magnetizing mmf of one pole is I_R and the flux passes the air gap twice, the pole flux (excluding the leakage flux) becomes

$$\Phi_{RR} = \frac{I_R \ \mu_0 \ l_e \ \tau_p}{2 \ (\delta_{ef} + h_m)} \tag{A.4}$$

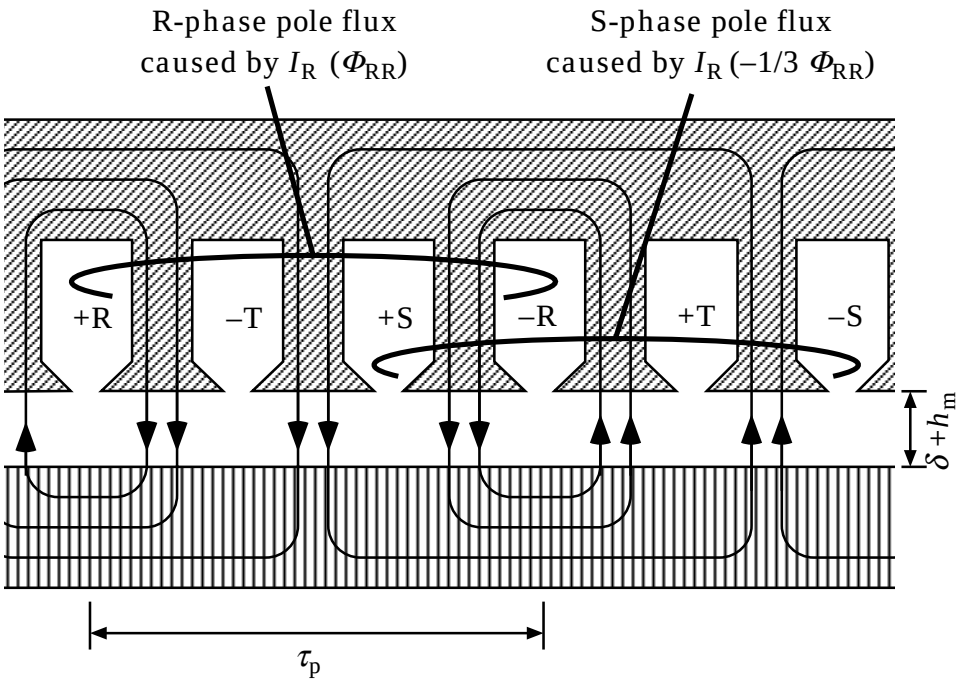

Figure A.1 The flux of the different phases caused by a current in the R-phase.

Now the self-inductance, for p pole pairs, can be expressed as

$$L_{RR} = p\ \mu_0\ l_e\ \frac{\tau_p}{2\,(\delta_{ef} + h_m)} \tag{A.5}$$

which makes it possible to identify the permeance coefficient λ_m of Equation (5.35). The mutual inductances between the phases will all be equal, and can be calculated in a way similar to the self-inductance, i.e.,

$$M = \frac{\Psi_{SR}}{I_R} \tag{A.6}$$

where Ψ_{SR} is the flux linkage of the S-phase caused by the current in the R-phase. Figure A.1 shows the pole flux linking to phase S to be minus one third of the pole flux linking to phase R. Consequently, the mutual inductance of the phases will be

$$M = -1/3\ L_{RR} \tag{A.7}$$

The equivalent Y-phase inductance must include both the self-inductance of one phase and the mutual inductance to the two other phases. The total flux linkage in phase R caused by all the windings is

$$\Psi_R = L_{RR}\ I_R + M\ \ I_S + M\ \ I_T \tag{A.8}$$

Since the neutral point of the Y-connected windings is not connected, the sum of the three phase currents is always zero. Therefore,

$$I_S + I_T = -I_R \tag{A.9}$$

The flux linkage of phase R can with Equations (A.8) and (A.9) be written

$$\Psi_R = (L_{RR} - M)\, I_R \tag{A.10}$$

Using Equation (A.7), the equivalent Y-phase inductance can be expressed as

$$L_{eq} = 4/3\, L_{RR} \tag{A.11}$$

Appendix B Thermal Model of the Generator

A thermal model of the generator is used to calculate the temperature of the hottest part of the stator winding, which is the end windings, and the magnet temperature. Only steady-state temperatures are calculated.

To make it easy to calculate the values of the thermal resistances in the complete model, the thermal resistances are first derived for thermal models of one slot pitch of the stator, one coil, one pole pitch of the rotor and the end shields. The values of these thermal resistances can be calculated by using definitions for one-, two- or three-dimensional heat flow in rectangular elements. The thermal model of the generator is derived by combining the detailed models for Q slots, Q coils, 2 p rotor poles, and two end shields. Finally, the complete thermal model of the generator is slightly simplified. All nodes which are not needed for the calculation of the winding and magnet temperatures are eliminated and series and parallel connected thermal resistances are replaced with the total thermal resistance. The result is a thermal network model with twelve nodes and eighteen thermal resistances.

Basic Theory

Three-dimensional heat flow can be approximately modelled by a lumped-parameter thermal circuit (Perez and Kassakian, 1979). The generator is divided into rectangular elements, like the one in Figure B.1, and they are represented by the simplified network models in Figure B.2. The total thermal resistances through the body in the x, y and z-directions are

$$R_x = \frac{l_x}{l_y \; l_z \; \lambda} \qquad R_y = \frac{l_y}{l_x \; l_z \; \lambda} \qquad R_z = \frac{l_z}{l_x \; l_y \; \lambda} \tag{B.1}$$

where l_x, l_y and l_z are the lengths of the body in x, y and z directions and λ

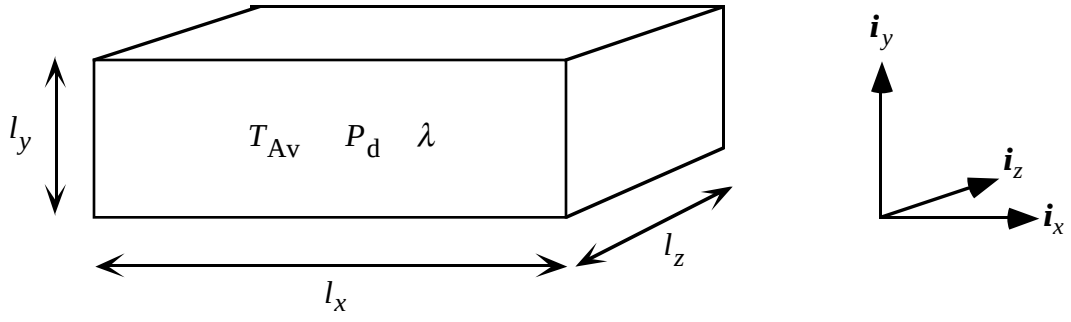

Figure B.1 A rectangular body with homogeneously distributed internal losses P_d, the heat conductivity λ and the average temperature T_{Av}.

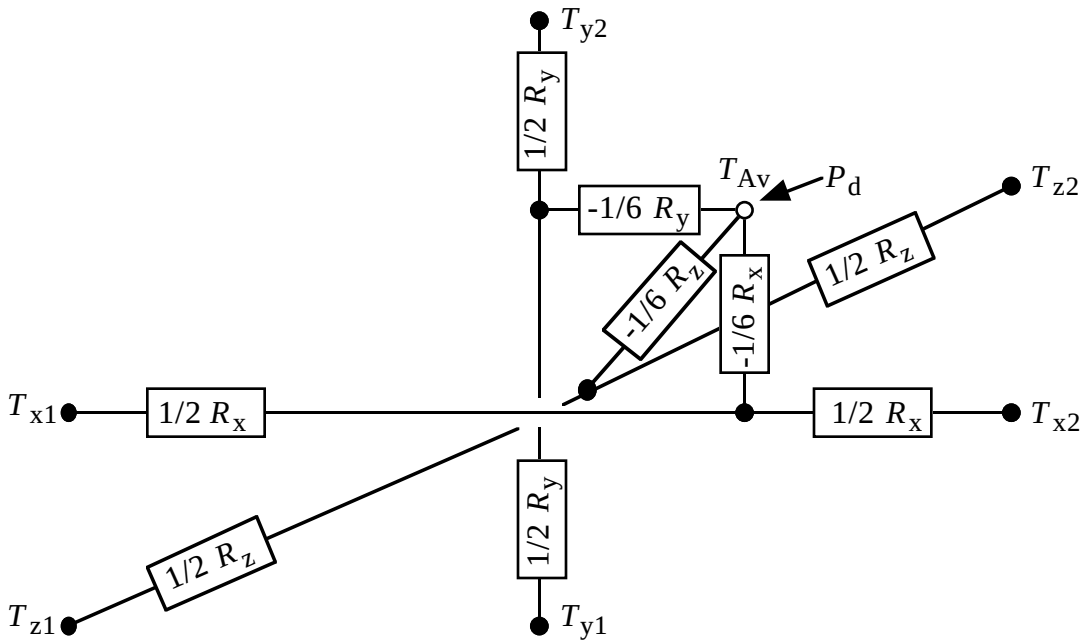

Figure B.2 Lumped-parameter thermal models for three-dimensional heat flow through the rectangular body.

is the thermal conductivity of the material. The average temperature of the body is T_{Av} and the power losses P_d are assumed to be homogeneously distributed within the body. If there is no heat flow in one direction, the corresponding thermal resistances are excluded (i.e., infinite thermal resistance).

The generator outer surface of the stator core is cooled by air forced through circumferential cooling channels. The temperature increase of the cooling air is included in the model, as an equivalent thermal resistance. The temperature increase of the cooling air depends on the heat flow P_c, the volumetric flow q_{vc}, the density ρ_c and the specific heat capacitivity k_{thc} of the cooling air. The temperature rise of the cooling air is

$$\Delta\theta_c = \frac{P_c}{q_{vc}\ \rho_c\ k_{thc}} \qquad \text{(B.2)}$$

This extra temperature rise will occur in the parts of the stator close to an outlet of the stator cooling channels. In the model, the cooling air at the stator yoke is assumed to have this temperature rise. The model then represents the warmest part of the stator. The magnet temperature is, therefore, overestimated by about 0.5 $\Delta\theta_c$. The error of the magnet temperature is in the order of 5˚C.

The temperature rise of the cooling air is included in the thermal model by introducing the equivalent thermal resistance of the cooling duct

$$R_{eq} = \frac{1}{q_{vc}\ \rho_c\ k_{thc}} \tag{B.3}$$

which represents the heating of the cooling air. The total volumetric cooling air flow depends on the number of cooling circuits and the flow in each circuit. It is assumed that the cooling channel length τ_{Air} should be 2 m. The number of cooling circuits has not been restricted to an integer number. Instead, it is defined as

$$N_{Air} = \frac{\pi\ d_{se}}{\tau_{Air}} \tag{B.4}$$

The volumetric flow in each cooling channel is determined by the stator length l, the height of the cooling channel h_{Air} and the cooling air velocity v_{Air} as

$$q_{vAir} = v_{Air}\ l\ h_{Air} \tag{B.5}$$

The total volumetric cooling air flow is

$$q_{vc} = N_{Air}\ q_{vAir} \tag{B.6}$$

The parameters for the stator cooling have the following values

ρ_c = 1.1 kg/m^3	(constant)
k_{thc} = 1010 J/(kg K)	(constant)
h_{Air} = 100 mm	(design variable)
v_{Air} = 15 m/s	(design variable)
τ_{Air} = 2 m	(design variable)

The Detailed Model

The detailed models of a slot pitch, a rotor pole, a coil and the two end shields are presented in Figures B.3 and B.4. Note that the thermal models of the two figures are connected. All parts of the generator are modelled by a one-, two- or three-dimensional version of the thermal model in Figure B.2. The definitions of the thermal resistances in these figures are found in Table B.1 and the values of the thermal constants used are found in Table B.2. Some clarifications of the model and the thermal resistances follow below.

The unconnected thermal conductors marked with I up to VII are connected to the other unconnected thermal conductor with the same number. P_a to P_f are losses in different parts of the generator.

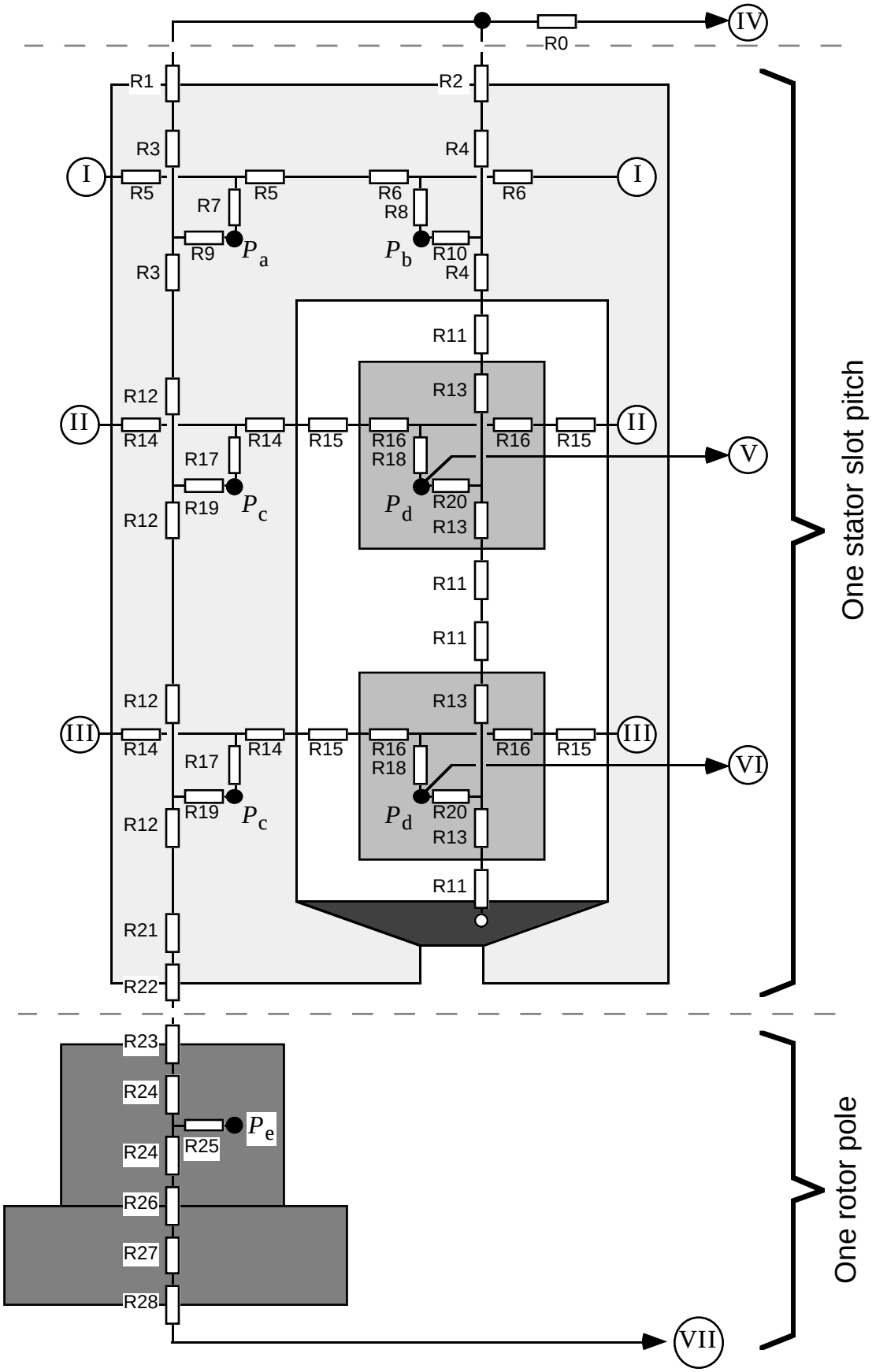

Figure B.3 The detailed model of the rotor and stator and the model of the radial and circumferential heat flow in the coil in the slots

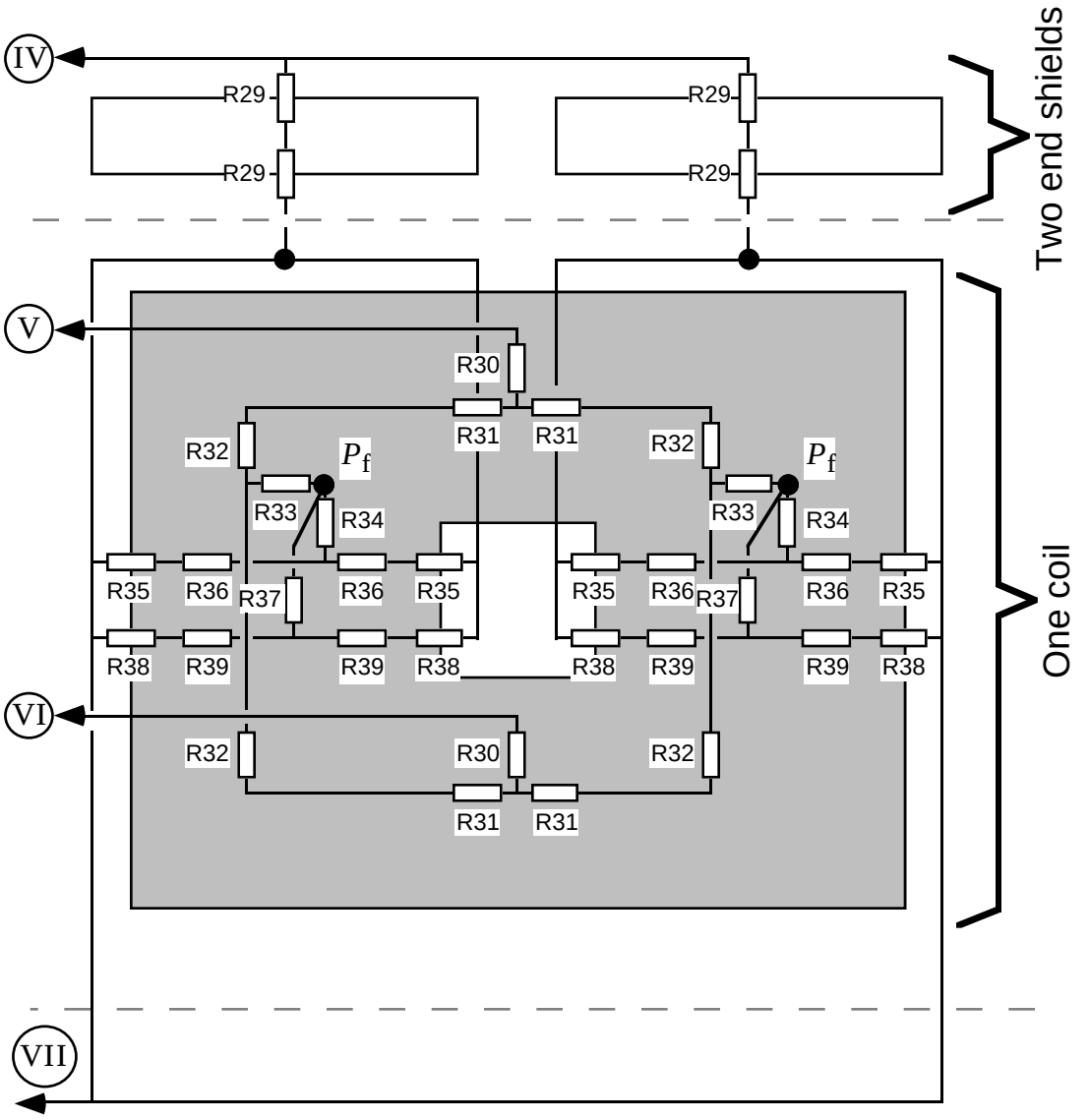

Figure B.4 The detailed model of the axial heat flow in the coil in the slots and the complete model of the end windings and the end shields.

The heat flow in the iron core is assumed to be two-dimensional. No heat flow in the axial direction is assumed because the thermal conductivity is about 30 times lower in that direction than along the laminations.

The heat flow in the coils is three-dimensional. The model of the slot pitch is connected to the model of a coil through the average temperatures (points V and VI) of the upper and lower coil sides.

The heat transfer coefficient α_1 at the outer surface of the stator yoke is estimated from data by Luke (1923). With a cooling air velocity of about 15 m/s, the value is assumed to be 60 W/(K m^2). The stator yoke is assumed to have cooling fins that increase the cooling surface to three times its own outer surface.

Table B.1 Definitions of thermal resistances in the detailed model.

$R0 = \frac{1}{q_{vc}\ \rho_c\ k_{thc}}$	$R21 = \frac{h_{s1} + h_{s2}}{l_u\ (0.5\ \tau\ +\ 0.5\ b_d)\ \lambda_{Fe}}$
$R1 = \frac{1}{3\ l\ b_d\ \alpha_1}$	$R22 = \frac{1}{l\ \ (\tau - b_{s1})\ \ \alpha_2}$
$R2 = \frac{1}{3\ l\ b_s\ \alpha_1}$	$R23 = \frac{1}{l\ \ b_m\ \ \alpha_2} + \frac{h_{m1}}{l\ \ b_m\ \ \lambda_{GRP}}$
$R3 = \frac{0.5\ h_{ys}}{l_u\ b_d\ \lambda_{Fe}}$	$R24 = \frac{0.5\ h_m}{l\ \ b_m\ \ \lambda_m}$
$R4 = \frac{0.5\ h_{ys}}{l_u\ b_s\ \lambda_{Fe}}$	$R25 = -\frac{1}{3}\ R24$
$R5 = \frac{0.5\ b_d}{l_u\ \ h_{ys}\ \ \lambda_{Fe}}$	$R26 = \frac{h_{m0}}{l\ \ b_m\ \ \lambda_{glue}}$
$R6 = \frac{0.5\ b_s}{l_u\ \ h_{ys}\ \ \lambda_{Fe}}$	$R27 = \frac{h_{yr}}{l\ \ \tau_p\ \ \lambda_{Fe}}$
$R7 = -\frac{1}{3}\ R5$	$R28 = \frac{1}{l\ \ \tau_p\ \ \alpha_5}$
$R8 = -\frac{1}{3}\ R6$	$R29 = \frac{1}{\pi\ (0.5\ d + h_s + h_{ys})^2\ \alpha_3}$
$R9 = -\frac{1}{3}\ R3$	$R30 = -\frac{1}{3}\ R31$
$R10 = -\frac{1}{3}\ R4$	$R31 = \frac{0.5\ l}{h_{Cu}\ \ b_{Cu}\ \ k_{Cu}\ \ \lambda_{Cu}}$
$R11 = \frac{h_i}{l\ \ b_{Cu}\ \ \lambda_i}$	$R32 = \frac{0.5\ l_b}{h_{Cu}\ \ b_{Cu}\ \ k_{Cu}\ \ \lambda_{Cu}}$
$R12 = \frac{0.5\ (h_{Cu} + 2\ h_i)}{l_u\ \ b_d\ \ \lambda_{Fe}}$	$R33 = -\frac{1}{3}\ R32$
$R13 = \frac{0.5\ h_{Cu}}{l\ \ b_{Cu}\ \lambda_{coil}}$	$R34 = -\frac{1}{3}\ R36$
$R14 = \frac{0.5\ b_d}{l_u\ \ (h_{Cu} + 2\ h_i)\ \lambda_{Fe}}$	$R35 = 2\ \frac{1}{l_b\ \ b_{Cu}\ \ \alpha_4}$
$R15 = \frac{h_i}{l\ \ \ h_{Cu}\ \ \lambda_i}$	$R36 = \frac{0.5\ h_{Cu}}{l_b\ \ b_{Cu}\ \ \lambda_{Coil}}$
$R16 = \frac{0.5\ b_{Cu}}{l\ \ h_{Cu}\ \lambda_{coil}}$	$R37 = -\frac{1}{3}\ R39$
$R17 = -\frac{1}{3}\ R14$	$R38 = 2\ \frac{1}{l_b\ \ h_{Cu}\ \ \alpha_4}$
$R18 = -\frac{1}{3}\ R16$	$R39 = \frac{0.5\ b_{Cu}}{l_b\ \ h_{Cu}\ \ \lambda_{Coil}}$
$R19 = -\frac{1}{3}\ R12$	
$R20 = -\frac{1}{3}\ R13$	

The heat transfer coefficient at the tooth tip α_2 is assumed to be lower than at the stator yoke back, because the rotor surface velocity is less than 15 m/s. The air flow in the air gap is assumed to be turbulent because of the rough rotor surface and, therefore, only the thermal resistances of the convective heat transfer at the tooth tip and at magnet surfaces are included in the model. The heat transfer coefficients at the end shields α_3, the end windings α_4 and the inner surface of the rotor yoke α_5 are all assumed to be equal.

The rotor pole model is simple and is mainly included to show that the temperature rise of the magnets should not be a problem. It includes losses in the magnets and cooling through the magnet and rotor yoke to the internal air of the generator. In addition, the thermal resistances of

Table B.2 The thermal constants used.

Heat transfer coefficient at the stator yoke back	$\alpha_1 = 60$ W/(K m^2)
Heat transfer coefficient in the air gap	$\alpha_2 = 40$ W/(K m^2)
Heat transfer coefficient at the end shields	$\alpha_3 = 25$ W/(K m^2)
Heat transfer coefficient at the end windings	$\alpha_4 = 25$ W/(K m^2)
Heat transfer coefficient at the rotor yoke back	$\alpha_5 = 25$ W/(K m^2)
Thermal conductivity of iron	$\lambda_{Fe} = 38$ W/(K m)
Thermal conductivity through the coil	$\lambda_{Coil} = 1.8$ W/(K m)
Thermal conductivity of copper, along the coil	$\lambda_{Cu} = 400$ W/(K m)
Thermal conductivity of insulation	$\lambda_i = 0.2$ W/(K m)
Thermal conductivity of NdFeB magnets	$\lambda_m = 9$ W/(K m)
Thermal conductivity of the magnet glue	$\lambda_{glue} = 0.7$ W/(K m)
Thermal conductivity of the GRP magnet protection	$\lambda_{GRP} = 0.2$ W/(K m)
Thickness of magnet glue	$h_{m0} = 0.1$ mm
Thickness of magnet reinforcement	$h_{m1} = 0.5$ mm
Coil insulation thickness	$h_i = 1$ mm

the magnet glue and the glass fibre reinforcement over the magnets are included. The thickness of the magnet glue is h_{m0} and of the glass fibre reinforcement h_{m1}.

The internal air in the generator is assumed to have a homogeneous temperature except in the air gap. The cooling is also assumed to be equally efficient at both end shields.

The value of the thermal resistance R21 is derived assuming that the tooth tip is rectangular instead of trapezoidal. It is assumed that the end windings overlap so that only half of their outer surface is used for cooling. Therefore, R35 and R38 include the factor 2.

The Simplified Model

From the detailed models for the different parts described above, a simplified thermal model of the complete generator can be derived. The simplified model is derived by connecting Q parallel models for a stator slot pitch, Q parallel models of a coil, 2 p parallel models of a rotor pole and the model for the internal air and the two end shields.

The thermal model is simplified by using symmetry to reduce the number of thermal resistances in the yoke, teeth, coil sides, end windings and end shields. The network is simplified as much as possible while keeping only the nodes that are necessary to model the temperature of the end windings and magnets accurately. Figures B.5 and B.6 illustrate how the simplified model is derived from the detailed models. The thermal resistances of the simplified model are defined in terms of the thermal resistances of the basic models and their definitions are shown in Table B.3.

The symmetry between the two end windings and end shields is used to reduce the model. Since the core losses are smaller than the copper losses and the temperature rise inside the stator iron is not so large, the core losses are moved in the thermal network to allow simplifications. The losses P1, P2, P3 and P9 are all moved to the other side of R9, R10, R19 and R19, respectively. By doing so, the number of nodes and thermal resistances can be decreased but the temperature rise of the iron core will be slightly overestimated. The same simplification is used for the magnet losses, thus, R25 is neglected. Since the aim of the model is only to show that the temperature in the magnets can be low enough, it is justified to overestimate the temperature rise of the magnets slightly. The thermal resistances ending at the slot wedge are excluded.

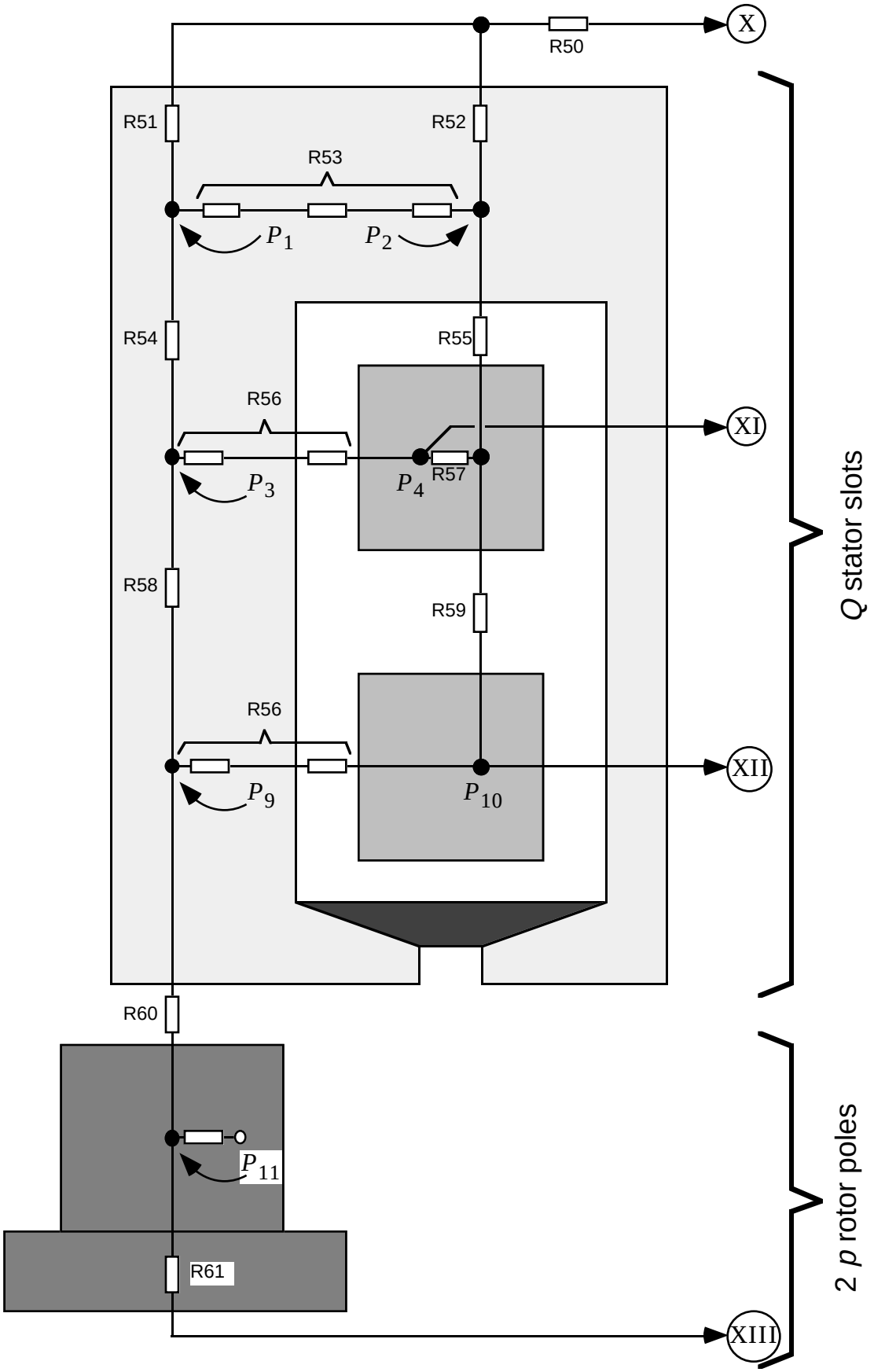

Figure B.5 Simplified thermal network for the stator and rotor.

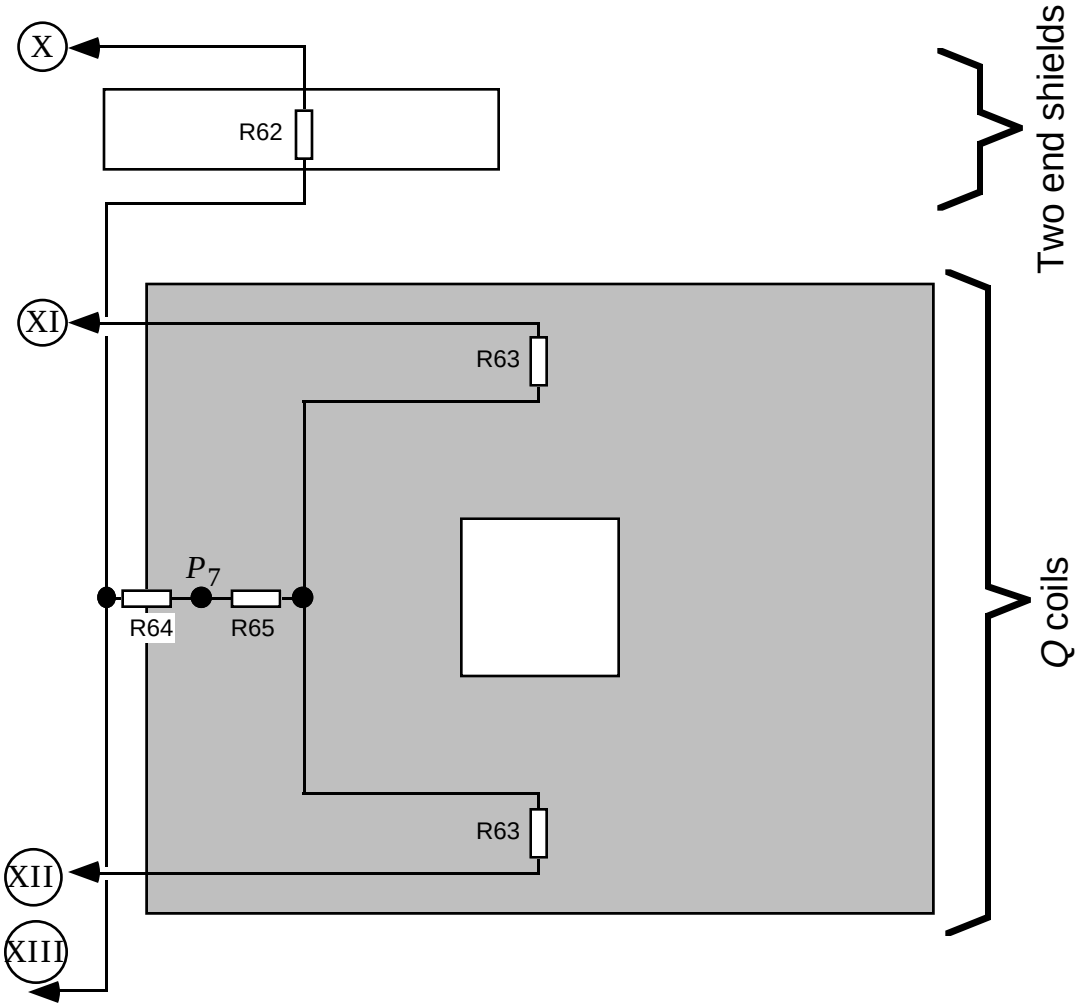

Figure B.6 Simplified thermal network for the end windings and end shields.

Table B.3 Thermal resistances of the simplified model.

$R50 = R0$	$R59 = \frac{2\,R13 + 2\,R11 + R20}{Q}$
$R51 = \frac{R1 + R3}{Q}$	$R60 = \frac{R12 + R21 + R22}{Q} + \frac{R23 + R24}{2\,p}$
$R52 = \frac{R2 + R4}{Q}$	$R61 = \frac{R24 + R26 + R27 + R28}{2\,p}$
$R53 = \frac{R7 + R8 + R9 + R10 + 0.5(R5 + R6)}{Q}$	$R62 = R29$
$R54 = \frac{R3 + R12}{Q}$	$R63 = \frac{R30 + 0.5(R31 + R32)}{Q}$
$R55 = \frac{R4 + R11 + R13}{Q}$	$R64 = R64a // R64b$ (in parallel)
$R56 = \frac{R19 + R17 + R18}{Q} + 0.5\,\frac{R14 + R15 + R16}{Q}$	$R64a = 0.5\,\frac{R34 + 0.5(R36 + R35)}{Q}$
$R57 = \frac{R20}{Q}$	$R64b = 0.5\,\frac{R37 + 0.5(R39 + R38)}{Q}$
$R58 = \frac{2\,R12}{Q}$	$R65 = \frac{0.5\,R33}{Q}$

Summary of the Thermal Model

The final thermal model is shown in Figure B.7 and the losses used in it are given in Table B.4. The thermal model has twelve nodes, plus the ambient temperature, and eighteen thermal resistances. The temperature rise problem is formulated as a matrix equation. The vector of temperature rises is evaluated by multiplying the loss vector by the inverse of the thermal conductance matrix.

References:

Luke G. E. 1923. "The Cooling of Electric Machines". Transactions of the AIEE 42, p. 636–652.

Perez I.J., Kassakian J.G., 1979. "A Stationary Thermal Model for Smooth Air-gap Rotating Electric Machines". Electric Machines and Electromechanics 3, 1979, p. 258-303.

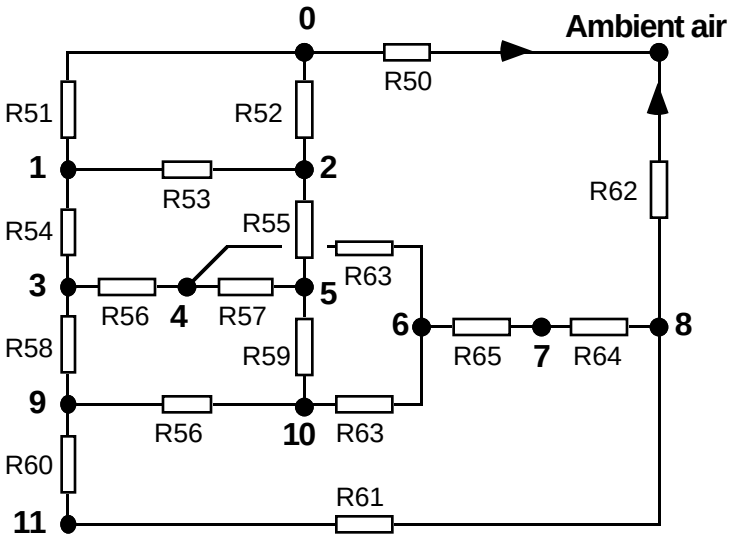

Figure B.7 The simplified thermal model.

Table B.4 The nodes and the losses of the simplified thermal model.

0: Stator cooling air (average temperature)	$P_0 = 0$
1: Temperature in the yoke above a tooth	$P_1 = \frac{b_d}{\tau} (P_{Hyys} + P_{Ftys})$
2: Temperature in the yoke above a slot	$P_2 = \frac{b_s}{\tau} (P_{Hyys} + P_{Ftys})$
3: Temperature in a tooth at the bottom coil side	$P_3 = 0.5 (P_{Hyd} + P_{Ftd})$
4 : Temperature in a bottom coil in a slot	$P_4 = 0.5 \frac{l}{l + l_b} P_{Cu}$
5: Fictitious model temperature	$P_5 = 0$
6: Fictitious model temperature	$P_6 = 0$
7: Temperature in an end winding	$P_7 = \frac{l_b}{l + l_b} P_{Cu}$
8: Temperature of the internal air	$P_8 = 0$
9: Temperature in a tooth at the top coil side	$P_9 = P_3 + P_{ad}$
10: Temperature in a top coil side in a slot	$P_{10} = P_4$
11: Temperature in the magnets	$P_{11} = P_{Ftm}$

Appendix C Average Efficiencies

In this appendix, the average efficiencies of a direct grid-connected induction generator and its gear are derived. In addition, the average efficiency of the frequency converters for the proposed direct-driven generators are derived.

The calculations are made in the same way as the average efficiency is calculated for the direct-driven generators, with average loss factors calculated with the wind speed probability density function. A medium wind speed site is assumed, with an average wind speed of 6.8 m/s and a capacity factor for the turbine power of 0.25.

Induction Generator Efficiency

The losses of a constant-speed induction generator can be divided into three types with different average loss factors:

- No-load losses which are independent of the load. (Includes stator core losses, friction and windage losses);
- Stator copper losses which are proportional to the square of the stator current;
- Rotor copper losses which are proportional to the square of the rotor current.

The additional losses are not neglected; they are included in the copper losses.

To calculate the average loss factors, the rotor and stator currents have to be expressed as functions of the wind speed. For this purpose, the following approximations are made. The rotor current is assumed to be proportional to the produced torque, and, thus, proportional to the active power. The stator current has been divided into one reactive part, which is assumed to be constant, and one active part which is assumed to be proportional to the active power. The reactive current, magnetizing current, is about 30 % of the rated current. With the function for the active power given as a function of wind speed, Equation (3.29), the average loss factors can be calculated. Note that the generator speed is constant for this generator system.

For the medium wind speed site, the average loss factor for the no-load losses is 0.77, for the stator copper losses 0.24, for the rotor copper losses 0.15 and the average factor for the active power is 0.25. The reason that the average loss factor for the no-load losses is less than 1 is that the wind energy converter is only operating 77 % of the year.

With these average loss factors and loss data for different machine sizes (ABB, 1991), the average efficiencies can be calculated. The losses and the average efficiencies are shown in Table C.1. Note that all the generators are standard induction generators. Recently, high-slip generators have been used in large wind energy converters, to limit turbine power peaks and damp power oscillations. The high slip generators have rotor copper losses of 2–3 % at rated load. Two-speed generators will also have lower efficiency than assumed here, in the order of 0.5–1 % lower at rated load.

Table C.1 The different losses of the induction generators and their efficiencies.

Rated power (kW)	No-load losses (p.u.)	Stator copper losses (p.u.)	Rotor copper losses (p.u.)	Efficiency at rated load (%)	Average losses (p.u.)	Average efficiency (%)
30	0.035	0.020	0.020	92.5	0.0348	86.1
500	0.020	0.009	0.007	96.4	0.0186	92.6
3000	0.018	0.010	0.007	96.5	0.0173	93.1

Gear Efficiency

The gear losses can be divided into (Shipley, 1991):

- No-load losses which are independent of load (Include friction and windage losses);
- Gear mesh losses, which are a constant percentage of the active power.

Since the gear mesh losses are a constant percentage of the power, their average factor will be equal to the average factor for the active power. The average factor for the gear mesh losses is 0.25 and for the no-load losses it is 0.77. In Table C.2, the losses and the average efficiencies of the different gear sizes are shown.

Table C.2 The different gear losses and the gear efficiencies.

Rated power (kW)	No-load losses (p.u.)	Gear mesh losses (p.u.)	Efficiency at rated load (%)	Average losses (p.u.)	Average efficiency (%)
30	0.010	0.020	97.0	0.0127	94.9
500	0.008	0.020	97.2	0.0112	95.5
3000	0.005	0.018	97.7	0.0084	96.7

Frequency Converter Efficiency

The losses in the frequency converter are calculated in a slightly simplified way, which overestimates them. The simplifications made are the following: the anti-parallel diodes of the converter valves are assumed to have the same voltage drop as the transistors; and the resistive losses, being rather small, are included in the voltage-drop losses. The frequency converters for the different rated powers are all assumed to have the same efficiency.

The frequency converter losses are, here, divided into:

- No-load losses which are constant (Include power to the cooling fans and the control circuits);
- Voltage drop losses which are proportional to the current (Include the semiconductor voltage drop and the switching losses).

For the rectifier, the current will be equal to the generator current and the average loss factor for the voltage drop losses is 0.26. For the inverter losses the average factor is different. The inverter is assumed to be controlled to keep the power factor at 1 and the grid voltage is constant, 1 p.u. This means that the current will be proportional to the active power and, consequently, the average loss factor for the voltage drop losses will be equal to the average factor for the power, 0.25.

The average factor for the no-load losses, of both the inverter and the rectifier, is 0.86. This average factor for the no-load losses differs from that of the direct grid-connected system because a variable speed turbine can operate in lower wind speeds and, therefore, it operates a larger part of the year.

The voltage drop losses of the inverter and rectifier were assumed to be 0.02 p.u. for each unit and the total no-load losses 0.001 p.u. The efficiency at rated load is, thus, 95.9 % and the average efficiency is 95.6 %.

References

ABB, 1991. Product Catalogue from ABB Motors, Sweden, 77 p.

Shipley E.E., 1991. "Loaded Gears in Action", In Dudley D.W. ed., Dudley's Gear Handbook, 2nd edition, New York, Townsend, 1991, p. 12.1–12.39.